NBER WORKING PAPER SERIES

WHY DOES THE FED MOVE MARKETS SO MUCH? A MODEL OF MONETARY POLICY AND TIME-VARYING RISK AVERSION

Carolin Pflueger
Gianluca Rinaldi

Working Paper 27856
http://www.nber.org/papers/w27856

NATIONAL BUREAU OF ECONOMIC RESEARCH
1050 Massachusetts Avenue
Cambridge, MA 02138
September 2020

We thank Adrien Auclert, Francesco Bianchi, John Campbell, Anna Cieslak, Rohan Kekre, Andreas Neuhierl, Adi Sunderam, Emil Siriwardane, Michael Weber, Luis Viceira, and seminar participants at the Dallas Federal Reserve, the University of Copenhagen, and the NBER SI Monetary Economics meeting 2020 for valuable comments. The paper was previously circulated under the title "A Finance-Integrated New Keynesian Model." The views expressed herein are those of the authors and do not necessarily reflect the views of the National Bureau of Economic Research.

Why Does the Fed Move Markets so Much? A Model of Monetary Policy and Time-Varying Risk Aversion

Carolin Pflueger and Gianluca Rinaldi

NBER Working Paper No. 27856
September 2020
JEL No. E43,E44,E52,G12

ABSTRACT

We build a new model integrating a work-horse New Keynesian model with investor risk aversion that moves with the business cycle. We show that the same habit preferences that explain the equity volatility puzzle in quarterly data also naturally explain the large high-frequency stock response to Federal Funds rate surprises. In the model, a surprise increase in the short-term interest rate lowers output and consumption relative to habit, thereby raising risk aversion and amplifying the fall in stocks. The model explains the positive correlation between changes in breakeven inflation and stock returns around monetary policy announcements with long-term inflation news.

Carolin Pflueger
University of Chicago
Harris School of Public Policy
1307 E 60th St
Chicago, IL 60637
and NBER
cpflueger@uchicago.edu

Gianluca Rinaldi
Harvard University
rinaldi@g.harvard.edu

1 Introduction

It is well understood that cyclical variation in investors' capacity to bear risk is essential to understanding the link between the macroeconomy and financial markets (see e.g. Cochrane (2017)). However, it is less clear how this time-varying link between the real economy and financial markets affects high-frequency stock and bond movements around monetary policy announcements, which are often used to assess the effectiveness of monetary policy for the real economy (Bernanke and Kuttner (2005)).

Our contribution is twofold. First, we integrate a small-scale New Keynesian model of monetary policy with the finance habit formation preferences of Campbell, Pflueger, and Viceira (2020), whereby investors become less willing to hold risky assets in times when output and consumption are low relative to a slowly-moving habit. These preferences have been shown to successfully reconcile the equity volatility puzzle of Shiller (1981), generate flight-to-safety in long-term Treasury bonds during the post-2001 period, and imply an exactly log-linear Euler equation typical of New Keynesian models. We fill a gap by departing from the reduced-form inflation and interest rate dynamics of Campbell, Pflueger, and Viceira (2020), and newly integrate finance habit preferences with a model of monetary policy.

Second, this new framework predicts how stocks and bonds should respond to monetary policy news, where news may be either about the short-term policy rate or long-term expected inflation. We show that our model, estimated to match quarterly macroeconomic moments, also matches the empirical high-frequency response of stock returns to monetary policy surprises around Federal Open Market Committee (FOMC) announcements. The model implies that time-varying risk premia are quantitatively important for stock responses to monetary policy, and especially so after declines in output.

We start by documenting empirically that stock returns around FOMC dates move differently with short-term interest rates and long-term breakeven inflation, building on an empirical literature that has documented that monetary policy announcements reveal information about long-term inflation and the economy (Romer and Romer (2000), Nakamura and Steinsson (2018)).[1] Figure 1, Panel A shows that a surprise decrease in the short-term Federal Funds rate around FOMC announcements is typically accompanied by a large increase in stock returns in the same time interval. This well-known result of Bernanke and Kuttner (2005) has been interpreted as evidence that the Fed can effectively stimulate the economy by temporarily lowering interest rates. Panel B shows

[1]Figure 1, Panel A uses intraday changes in the Federal Funds rate from Gorodnichenko and Weber (2016) and in the S&P from TAQ. Panel B uses one-day changes in 10-year breakeven computed as the difference between Gürkaynak, Sack, and Wright (2007) nominal and Gürkaynak, Sack, and Wright (2010) Treasury Inflation-Protected Securities (TIPS) bond yields and one-day value-weighted stock returns from CRSP. For a detailed description of the empirical results see Section 4.5.

that an increase in long-term breakeven, which is defined as the difference between 10-year nominal and real bond yields and often interpreted as a proxy of long-term inflation expectations, has the opposite correlation with stock returns on FOMC announcement dates, as recently documented by Jarociński and Karadi (2020) and Andrade and Ferroni (2020). This finding is often interpreted as evidence of a "Fed information effect", whereby the Federal Reserve announcements reveal correlated news about long-term inflation and economic activity. The comovement shown in Panel B zeros in on FOMC dates and hence differs from the unconditional stock market beta of nominal bonds studied in Campbell, Pflueger, and Viceira (2020).[2]

We derive log-linear macroeconomic dynamics from consumers' intertemporal Euler equation and firms' profit optimization, and combine them with a log-linear Taylor-type rule for short-term interest rates. We assume a representative consumer with finance habit preferences, whereby utility is determined by consumption in excess of a slowly moving habit, and surplus consumption dynamics take precisely the form needed to generate an exact log-linear consumption Euler equation. Different from Campbell, Pflueger, and Viceira (2020) we link the household and firm problems by integrating leisure into these preferences. Assuming that leisure is valued for its value in home production as in the classic model of Greenwood, Hercowitz, and Huffman (1988) separates wages from the intratemporal consumption-savings decision, thereby sidestepping the counterfactual labor implications that have previously affected models of asset pricing habits within production economies (Lettau and Uhlig (2000)).

We derive a standard log-linearized Phillips curve, assuming that firms set prices optimally subject to Calvo (1983) staggered price setting with backwards indexation. Productivity features learning-by-doing (Lucas (1988)) to generate an endogenous stochastic output trend, and predictable productivity growth. Euler equation and Phillips curve shocks arise from shocks to habit and markups. All fundamental shocks are assumed to be conditionally homoskedastic, so time varying risk premia arise endogenously from preferences, rather than from auxiliary assumptions about time-varying quantities of risk.

We model monetary policy via a Taylor (1993)-type interest rate rule suited to study variation in short-term interest rates and breakeven around FOMC dates. The rule has two different types of shocks to match the multivariate stock return pattern documented

[2]Relatedly, Hanson and Stein (2015), and Nakamura and Steinsson (2018) have documented that long-term real bond yields co-move with short-term interest rates on FOMC dates, and Nakamura and Steinsson (2018) have linked this finding to news about economic growth. The empirical variation that we emphasize is complementary and largely orthogonal, as most variation in breakeven changes on FOMC days is uncorrelated with Federal Funds rate news over our sample period. While our model matches the empirical comovement between nominal short-term and real long-term interest rates (Appendix F.2), we emphasize the breakeven-stock comovement because of our focus on time-varying risk premia, which are more important for stocks than for long-term real bonds.

in Figure 1. The first shock is a traditional short-term monetary policy shock that raises the the Federal Funds rate this quarter and lowers output and consumption through the Euler equation. The second shock captures long-term economic news and is modeled via a shock to trend inflation. A decline in long-term inflation expectations acts like a costly disinflation similarly to Ball (1994) and Gürkaynak, Sack, and Swanson (2005), moving the output gap and consumption expectations in the same direction as expected inflation. These effects are in line with the effects of permanent interest rate shocks in Cochrane (2018), Uribe (2018), and Schmitt-Grohé and Uribe (2018).

We model high-frequency stock returns and bond yield changes around FOMC dates by decomposing the quarterly shock into pre-FOMC and FOMC components, and solving for pre-FOMC asset prices at the expected state vector conditional on the pre-FOMC shock. Our solution for asset prices preserves their full nonlinearity, following the best practices numerical solution of Wachter (2005). Nonlinear asset prices imply that after a sequence of bad shocks, when consumption is close to habit, required compensation for holding risky assets – such as stocks – is high and required compensation for holding safe asses – such as nominal Treasury bonds – is low or even negative. The highly nonlinear nature of risk premia generates high and volatile stock returns and ensures that the consumption Euler equation is log-linear. The main approximation we use in solving the model is a standard log-linearization for the Phillips curve.[3] By solving for log-linear macroeconomic dynamics, we keep the asset pricing solution tractable and focus on nonlinearities where they are most salient, namely in asset prices.

We estimate the model in two steps. We first calibrate the preference parameters, the parameters governing the firms' problem, and the monetary policy rule to standard values in the literature. In a second step, we use simulated method of moments (SMM) to estimate the volatilities of shocks. Our estimation targets reduced-form macroeconomic impulse responses for output, inflation, and the Federal Funds rate, and the volatility of quarterly changes in long-term breakeven, thereby matching basic volatilities and comovements in macroeconomic data. Despite the significant additional structure, our model is similarly successful in generating a low volatility of the output gap with a much higher volatility of stock returns as in Campbell and Cochrane (1999), and a negative stock market beta of long-term nominal Treasuries as in Campbell, Pflueger, and Viceira (2020). We obtain an equity Sharpe ratio of 0.50, an annualized equity premium of 6.82% and annualized equity return volatility of 13.55%. The model generates volatile excess returns for 10-year real bonds and breakeven, defined as the difference between nominal and real bond returns, though they are not as volatile in the data. Our model does not

[3]Because we preserve the full nonlinearity of asset prices, and the Euler equation and monetary policy rule are already exactly log-linear, we do not mix different orders of approximation.

match the average risk premium in long-term nominal or real bonds, which is however hard to estimate reliably over a short sample of 20 years.

The model naturally explains the empirical evidence in Figure 1, Panel A, but only if the stock return response is amplified by countercyclical risk aversion. In the model, a positive shock to the short-term nominal rate leads to declines in output and consumption. These model responses are hump-shaped, consistent with the data and the role of habits in macroeconomic models.[4] As consumption declines towards habit, risk aversion and the return consumers require to hold risky stocks increase. Stock prices hence fall more than expected dividends, and our model attributes about one-half of the decline in stock prices to the higher required compensation for holding risk, in line with the empirical decomposition in Bernanke and Kuttner (2005).

The model ascribes the empirical evidence on breakeven inflation in Figure 1, Panel B, to information about long-term inflation being revealed on FOMC dates. In the model, downward revisions to long-term inflation expectations tend to go along with lower expected output, as a permanent decline in inflation acts as a costly disinflation. The long-term monetary policy shock hence induces breakeven inflation and stock prices to rise and fall together, matching the positive empirical comovement on FOMC dates. Risk premia again amplify the model decline in stock prices as consumption falls towards habit.

Our model generates the unique prediction that when times are bad, stock markets react more strongly to monetary policy even if the real economy does not. This finding suggests that during crises, such as the ongoing Covid-19 crisis, dramatic stock market responses to monetary policy need not indicate equally dramatic effectiveness for the real economy. This prediction arises naturally in our model from endogenous variation in risk bearing capacity implied by finance habit preferences. When consumption is close to habit, households' marginal utility is particularly sensitive to consumption, so a monetary policy action that lifts the economy has an especially strong calming effect on household risk aversion, amplifying the risk premium effect on stocks that is present in normal times. Consistent with this prediction, we find that stock return volatility around FOMC announcements was amplified during the financial crisis of 2008-09.

This paper is complementary to recent innovations in understanding heterogeneous consumer responses to monetary policy and their implications for macroeconomic outcomes (Kaplan, Moll, and Violante (2018), McKay, Nakamura, and Steinsson (2016), Auclert, Rognlie, and Straub (2020)) and financial asset prices (Drechsler, Savov, and Schnabl (2018), Kekre and Lenel (2020)). We keep the representative agent assumption,

[4] Fuhrer (2000) include habits within a macroeconomic model, while Boldrin, Christiano, and Fisher (2001) use habits that resolve the equity premium but not the smooth risk-free rate puzzle.

but instead assume finance habit formation. The advantage of finance habits is that their quantitative implications for asset prices are well-understood. We thereby provide a parsimonious model that jointly explains a number of empirical findings: high-frequency stock return responses to both Federal Funds rate innovations and long-term inflation news, volatile aggregate stock returns and a smooth risk-free rate, and hump-shaped macroeconomic impulse responses. Finance habits and heterogeneous agents would likely lead to interesting interactions and amplify each other, though modeling these interactions is beyond the scope of this paper. We similarly view our model as complementary to the liquidity-based model of stock responses to Federal Funds rate innovations of Lagos and Zhang (2020).

We also contribute to a growing literature jointly modeling financial asset prices with endogenous macroeconomic dynamics, by allowing finance habit formation preferences to be integrated into a standard small-scaled New Keynesian model. Prior work has used ambiguity aversion (Bianchi, Ilut, and Schneider (2018)), disaster risks (Gourio (2012), Kilic and Wachter (2018)) and long-run risks (e.g. Kung (2015), Gourio and Ngo (2020)) to understand asset pricing implications within models of the macroeconomy. While these papers usually require an exogenously assumed link between the quantity of risk and other state variables, our endogenous link between the level of monetary policy shocks and risk premia in financial markets generates new predictions about the state-dependence of stock return responses to monetary policy. Prior research, including Uhlig (2007), Dew-Becker (2014), Rudebusch and Swanson (2008), Lopez (2014), Stavrakeva and Tang (2019), and Bretscher, Hsu, and Tamoni (2019) has embedded simplified finance habit preferences into a New Keynesian model. Following Campbell, Pflueger, and Viceira (2020), we preserve the full non-linearity of Campbell and Cochrane (1999)'s consumption-based habit formation preferences, and thereby retain their favorable asset pricing properties generating volatile stock returns and stable short-term interest rates.

The paper is organized as follows. Section 2 presents the model. Section 3 solves the model. Section 4 estimates the model and assesses its macroeconomic and asset pricing implications. Section 5 concludes.

2 Model

2.1 Summary

The model is specified such that households' and firms' first-order conditions imply the smallest scale New Keynesian work-horse model, i.e. a log-linear consumption Euler

equation and Phillips curve:

$$x_t = f^x E_t x_{t+1} + \rho^x x_{t-1} - \psi\left(r_t - r_t^a\right) + v_{x,t}, \tag{1}$$

$$\pi_t = f^\pi E_t \pi_{t+1} + \rho^\pi \pi_{t-1} + \kappa x_t + v_{\pi,t}, \tag{2}$$

while nesting the asset pricing habit preferences of Campbell, Pflueger, and Viceira (2020), which, in turn, build on a long-standing literature of habits in finance (Constantinides (1990), Campbell and Cochrane (1999), Wachter (2006)).

Here, r_t denotes the log real risk-free interest rate that can be earned from time t to time $t+1$, the output gap, x_t, equals log real output minus log potential output at the hypothetical equilibrium without price–setting frictions (Woodford (2003), p.245), and π_t is log quarterly inflation. The rate r_t^a is the frictionless real rate related to expected productivity growth. The demand and Phillips curve shocks $v_{x,t}$ and $v_{\pi,t}$, and the positive coefficients f^x, ρ^x, ψ, f^π, ρ^π, κ arise from consumer preferences and the firm's problem. The consumption Euler equation is exact, and the Phillips curve is derived from the usual log-linearization. Both equations are specified up to a constant. We use lower-case letters to denote log variables throughout.

2.2 Preferences

2.2.1 Finance habit

There is a representative agent whose utility depends on the difference between consumption C_t and external habit H_t:

$$U_t = \frac{(C_t - H_t)^{1-\gamma} - 1}{1-\gamma} = \frac{(S_t C_t)^{1-\gamma} - 1}{1-\gamma}. \tag{3}$$

Here C_t is the quantity of market goods available for consumption, H_t is consumers' habit level for market-produced goods, and γ is a curvature parameter. The surplus consumption ratio

$$S_t = \frac{C_t - H_t}{C_t} \tag{4}$$

is the fraction of market consumption that is available to generate utility. Relative risk aversion varies inversely with the surplus consumption ratio: $-U_{CC}C/U_C = \gamma/S_t$.

The consumer first-order condition implies that the gross one-period real return $(1 + R_{t+1})$ on any asset satisfies

$$1 = \mathrm{E}_t\left[M_{t+1}\left(1 + R_{t+1}\right)\right], \tag{5}$$

where the stochastic discount factor is related to the log surplus consumption ratio s_{t+1}

and log consumption c_{t+1} by

$$M_{t+1} = \frac{\beta U'_{t+1}}{U'_t} = \beta \exp\left(-\gamma(\Delta s_{t+1} + \Delta c_{t+1})\right). \tag{6}$$

2.2.2 Surplus consumption dynamics

We model implicitly how habit adjusts to the history of consumption through the dynamics for log surplus consumption:

$$\begin{aligned} s_{t+1} &= (1-\theta_0)\bar{s} + \theta_0 s_t + \theta_1 x_t + \theta_2 x_{t-1} + \varepsilon_{s,t} + \lambda(s_t)\varepsilon_{c,t+1}, & (7)\\ \varepsilon_{c,t+1} &= c_{t+1} - \mathrm{E}_t c_{t+1}. & (8) \end{aligned}$$

Here, $\bar{s}$ is steady-state log surplus consumption and $\varepsilon_{s,t}$ is a serially uncorrelated homoskedastic habit shock. The consumption shock $\varepsilon_{c,t}$ will be derived as a function of fundamental shocks in equilibrium. For now, we note that it is conditionally homoskedastic and serially uncorrelated with standard deviation σ_c. The sensitivity function $\lambda(s_t)$ takes the form:

$$\begin{aligned} \lambda(s_t) &= \begin{cases} \frac{1}{\bar{S}}\sqrt{1-2(s_t-\bar{s})} - 1 & s_t \le s_{max} \\ 0 & s_t > s_{max} \end{cases}, & (9)\\ \bar{S} &= \sigma_c \sqrt{\frac{\gamma}{1-\theta_0}}, & (10)\\ \bar{s} &= \log(\bar{S}), & (11)\\ s_{max} &= \bar{s} + 0.5(1-\bar{S}^2). & (12) \end{aligned}$$

The downward-sloping relation between $\lambda(s_t)$ and s_t has the intuitive implication that marginal consumption utility is particularly sensitive to consumption innovations when investors are close to their habit consumption level, as would be the case after a sequence of bad shocks. The particular non-linear form of $\lambda(s_t)$ implies that s_t drops out of the asset pricing Euler equation for the real risk-free rate, because the associated intertemporal substitution and precautionary savings terms cancel exactly. The terms $\theta_1 x_t$ and $\theta_2 x_{t-1}$ make habit depend on the output gap. Our model has no real investment, so it is intuitive to interpret the x_t terms as consumption relative to a frictionless level entering into habit. If $\theta_1 > 0$ and $\theta_2 < 0$, as in our empirical specification, the dependence of habit on the most recent consumption lag increases relative to simple geometric weights, see Appendix A. The habit shock $\varepsilon_{s,t}$ captures independent fluctuations in habit and leads to a shock in the consumption Euler equation. A positive $\varepsilon_{s,t}$ lowers future expected habit and

increases future expected surplus consumption, reducing risk aversion.[5]

2.2.3 Labor-leisure trade-off

Before describing the firm's problem we need to specify households' intratemporal labor-leisure trade-off, which is at the heart of wage determination. To achieve a standard functional form for the Phillips curve, we choose a labor disutility specification that ensures surplus consumption does not enter into the intratemporal labor-leisure trade-off. Following the classic model of Greenwood, Hercowitz, and Huffman (1988), we assume that the representative household's total consumption, C_t^{tot}, is the sum of market consumption, C_t, and home production C_t^{home}:

$$C_t^{tot} = C_t + C_t^{home}, \tag{13}$$

$$C_t^{home} = A_t N_t \frac{\int_0^1 (1 - L_{i,t})^{1-\chi} \, di}{1 - \chi}. \tag{14}$$

Here, $L_{i,t}$ denotes the differentiated labor used for production by firm i and $(1 - L_{i,t})$ is labor used for home production. Home production has decreasing returns to scale, as in Campbell and Ludvigson (2001), and the parameter χ determines the elasticity of market labor supply. The differentiated labor assumption follows Woodford (2003, Chapter 3) and generates real rigidities from labor immobility across sectors (Ball and Romer (1990)).

The utility function (3) is specified in terms of market consumption C_t and habit H_t, which allows us to fit the model to data on market goods output. However, this utility function is clearly equivalent to a power utility function over the difference between total consumption and total habit, with total habit given by $H_t^{tot} = H_t + C_t^{home}$. Intuitively, home consumption drives up total habit one-for-one, and does not generate time-varying risk aversion over market goods consumption.

2.3 Firm Problem

2.3.1 Demand

Demand for the differentiated good i is downward-sloping in its product price $P_{i,t}$:

$$Y_{i,t} = Y_t \left(\frac{P_{i,t}}{P_t} \right)^{-\theta_t}. \tag{15}$$

[5] A similar intuition is captured by the reduced-form "moody investor" model of Bekaert, Engstrom, and Grenadier (2010) and Bekaert, Engstrom, and Xu (2019). We go beyond this prior literature by integrating preferences with typical New Keynesian microfoundations, and we separate habit shocks from heteroskedasticity in fundamentals.

Here, $P_t = \left[\int_0^1 P_{i,t}^{-(\theta_t-1)} di\right]^{-\frac{1}{\theta_t-1}}$ is the aggregate price level. The time-varying elasticity of substitution θ_t is assumed to be log-normally distributed around steady-state θ. Shocks to $\log \theta_t$ are denoted $\varepsilon_{\theta,t}$ and assumed to be serially uncorrelated and homoskedastic. Aggregate output and labor are Dixit-Stiglitz aggregates of differentiated goods $Y_{i,t}$ and labor $L_{i,t}$

$$Y_t \equiv \left[\int_0^1 Y_{i,t}^{\frac{\theta_t-1}{\theta_t}} di\right]^{\frac{\theta_t}{\theta_t-1}}, \; L_t \equiv \left[\int_0^1 L_{i,t}^{\frac{(\theta_t-1)(1-\tau)}{\theta_t}} di\right]^{\frac{\theta_t}{(\theta_t-1)(1-\tau)}}. \tag{16}$$

Because there is no time-varying real investment, consumption equals output $C_t = Y_t$.[6]

2.3.2 Production

Firm i produces according to a Cobb-Douglas production function with capital share τ:

$$Y_{i,t} = A_t N_t L_{i,t}^{1-\tau}. \tag{17}$$

Productivity is the product of technology, A_t, and human capital, N_t. Following Lucas (1988), human capital depends on the average skill acquired by all agents, so agents do not internalize the effect of acquiring skills on aggregate production. We assume that for some constants $0 \leq \phi \leq 1$ and $\nu > 0$, changes in log human capital are driven by past market labor, l_{t-1}:

$$n_t = \nu + n_{t-1} + (1-\phi)(1-\tau) l_{t-1}. \tag{18}$$

Alternatively, the process (18) can be interpreted as a simple endogenous capital stock, similarly to Woodford (2003) (Chapter 5), if a fixed proportion of employment each period is used as an input to produce investment goods. If real investment comes out of labor, this interpretation would leave the relationship between consumption and output unchanged and only the constants in the home production function (14) would change. The purpose of n_t is simply to detrend the output gap, so the specific interpretation is not central for us.

We incorporate predictable productivity growth in the simplest possible manner, assuming that A_t is predictable one period ahead, i.e. that the change in log technology Δa_{t+1} is known at time t. To economize on state variables, we assume that productivity growth is perfectly predictable and is a linear function of existing state variables, and in

[6] We do not include real investment in order to present the simplest possible model of monetary policy and finance habits. Our analysis is therefore complementary to the classic paper of Jermann (1998), which studies a real business cycle model with habit formation preferences.

particular the real risk-free rate deviation from the frictionless steady-state

$$\Delta a_{t+1} = \rho^a (r_t - \bar{r}) \tag{19}$$

This relationship captures the intuition that the central bank may try to set the real risk-free rate following variation in the natural rate due to variation in expected growth rates (Nakamura and Steinsson (2018)). We use the notation

$$r_t^a = \gamma \Delta a_{t+1} \tag{20}$$

for the natural real rate due to expected productivity growth.[7]

2.3.3 Price setting

When a firm can update its product price, it maximizes the discounted sum of current and future expected profits discounted at the stochastic discount factor while the price remains in place. Firm profits equal output minus the cost of labor, subject to the production function (17), demand for differentiated goods (15), and taking wages from consumers' labor-leisure trade-off as given.

Firms face price-setting frictions in the manner of Calvo (1983), where fraction $1-\alpha$ of firms can change prices every period with equal probabilities across firms. When firms cannot update, their prices are indexed to lagged inflation (**?**Christiano, Eichenbaum, and Evans, 2005). A firm that last reset its price at time t to $\tilde{P}_t$, charges a nominal time $t+j$ price $\tilde{P}_t \left(\frac{P_{t-1+j}}{P_{t-1}} \right)$.

2.4 Monetary Policy

Motivated by the empirical evidence in Figure 1, we choose the simplest Taylor-type rule with a two factor shock structure (ignoring constants):

$$i_t = \rho^i i_{t-1} + \left(1 - \rho^i\right) i_t^* + v_{ST,t}, \tag{21}$$

$$v_t^* = v_{t-1}^* + v_{LT,t} \tag{22}$$

$$i_t^* = \gamma^x x_t + \gamma^\pi \pi_t + (1 - \gamma^\pi)\, v_t^* \tag{23}$$

The first shock, $v_{ST,t}$, is a short-term monetary policy shock and represents a standard

[7] Our main model results for high-frequency stock returns against innovations in the Federal Funds rate and breakeven are robust to setting $\rho^a = 0$, see Appendix F.1. The purpose of time-varying expected productivity growth is simply to generate volatility in real bonds, and to drive down the real bond return correlation with output and stock returns. Note that the frictionless real rate, more broadly defined, would encompass both r_t^a and shocks to preferences (Woodford (2003)).

innovation to the short-term nominal interest rate. The second shock, v^*_{LT}, is a long-term monetary policy shock and shifts the random walk component of inflation expectations, v^*_t, thereby moving the entire term structure of nominal interest rates.[8] We assume that short-term and long-term monetary policy shocks are uncorrelated, motivated by the empirical correlation between Fed Funds rate and breakeven innovations on FOMC dates in our sample being close to zero. Here, i^*_t denotes the central bank's interest rate target, to which it adjusts slowly with a smoothing coefficient ρ^i.

To keep the macroeconomic dynamics tractable and log-linear we use the common log-linear approximation for the nominal log short-term interest rate

$$i_t \quad = \quad r_t + E_t\pi_{t+1}. \tag{24}$$

The approximation error stemming from (24) in our estimated model is small and within the range of measurement error of bond yields. We do not approximate longer-term bond prices, instead solving for time-varying risk premia numerically.

2.5 Stocks

We model stocks as a levered claim on consumption, as in Abel (1990) and Campbell (2003), while preserving the cointegration of consumption and dividends. Let P^c_t denote the price of a claim to the entire future consumption stream C_{t+1}, C_{t+2},... At time t the aggregate firm buys P^c_t and sells equity worth δP^c_t, with the remainder of the firm's position financed by one-period risk-free debt worth $(1-\delta)P^c_t$. Stocks in our model should therefore simply be interpreted as a financial asset with pro-cyclical dividends, rather than a financial claim tied specifically to firm cash flows.[9]

3 Model Solution and Discussion

3.1 Steady-State and Output Gap

We log-linearize output, consumption, and labor around the steady-state with $\bar{Y}_t = A_t\bar{L}^{1-\tau}$, where $\bar{L}$ is the labor supply consistent with flexible prices and steady-state

[8] We do not explicitly model the zero-lower-bound (ZLB) for simplicity, leaving this application for future research. One simple way to incorporate the ZLB explicitly into the model would be through a Markov regime switching model, which would preserve the tractability of the model.

[9] Alternatively, one could models stocks as a claim on firm profits rather than consumption. However, this would require modeling infrequent wage setting to match the cyclical behavior of dividends (Favilukis and Lin (2016)). Since our goal is to understand the implications of a time-varying price of risk in response to monetary policy more generally, it is not crucial for us whether stocks represent a claim on profits.

markups. We use hats to denote log deviations from this steady-state. In a flexible-price equilibrium, each firm wishes to charge a markup $\frac{\theta_t}{\theta_t - 1}$ over real marginal cost.

The log output gap x_t is the deviation of log output from the flexible-price equilibrium (up to a constant):

$$x_t \quad = \quad y_t - n_t - a_t = c_t - (1-\phi)\sum_{j=0}^{\infty}\phi^j c_{t-1-j} - \sum_{j=0}^{\infty}\phi^j \Delta a_{t-j}. \tag{25}$$

Here, we have used the resource constraint $y_t = c_t$ and the process for human capital (18). Equation (25) has the appealing feature that the empirical output gap from the Bureau of Economic Analysis closely resembles stochastically detrended consumption (Campbell, Pflueger, and Viceira (2020)). Inverting equation (25) gives an intuitive expression for consumption growth in terms of the output gap and productivity growth:

$$\Delta c_{t+1} \quad = \quad x_{t+1} - \phi x_t + \Delta a_{t+1}. \tag{26}$$

3.2 Euler Equation

We obtain the *exact* log-linear Euler equation (1) in terms of preference parameters:

$$x_t = \underbrace{\frac{1}{\phi - \theta_1}}_{f^x}\mathrm{E}_t x_{t+1} + \underbrace{\frac{\theta_2}{\phi - \theta_1}}_{\rho^x} x_{t-1} - \underbrace{\frac{1}{\gamma(\phi - \theta_1)}}_{\psi}(r_t - r_t^a) + \underbrace{\frac{1}{\phi - \theta_1}}_{v_{x,t}}\varepsilon_{s,t}. \tag{27}$$

This expression is the no-arbitrage condition (5) for the one-period real risk-free bond, substituting in the stochastic discount factor (6), log surplus consumption dynamics (7), and the updating equation for consumption growth (26). The log-linear Euler equation (27) does not depend on the specific microfoundations for consumption and output, provided that consumption is homoskedastic and satisfies the updating equation (26).

Our modeling choices simplify the no-arbitrage condition for the one-period real risk-free bond, and ensure that it takes exactly the form of a New-Keynesian consumption Euler equation. The specific nonlinear form of the sensitivity function $\lambda(s_t)$ has the unique advantage that the precautionary savings and intertemporal substitution terms from s_t cancel, and s_t is not a state variable for macroeconomic dynamics. Surplus consumption dynamics are of course linked to the consumption Euler equation (27) through consumption and habit shocks.

The Euler equation (27) shows that $\theta_2 > 0$ generates a lagged output gap term. As a lagged output gap term is known to be crucial for matching hump-shaped output gap responses to monetary policy shocks (Boldrin, Christiano, and Fisher (2001) and Fuhrer (2000)), this parameter is essential for linking the finance and monetary policy sides of

our model. In our estimation, we constrain the parameter θ_1 so that the forward- and backward-looking terms in the consumption Euler equation sum to one.

The habit shock microfounds risk-centric demand shocks in the Euler equation, and shows that shocks to risk-bearing capacity enter into macroeconomic dynamics in line with a growing literature including Christiano, Motto, and Rostagno (2014), Caballero and Simsek (2020), Pflueger, Siriwardane, and Sunderam (2020), and Kekre and Lenel (2020). Demand shocks from other microfoundations, such as a gap between interest earned by consumers relative to the interest rate controlled by the central bank (Smets and Wouters (2007)), or a shock to the rate of time preference (e.g. Justiniano and Primiceri (2008), Albuquerque, Eichenbaum, Luo, and Rebelo (2016)), would lead to similar macroeconomic dynamics but different asset pricing implications. Demand shocks microfounded from habit allow us to use a single stochastic discount factor to price all assets, and drive real bonds and stocks in opposite directions similarly to the data.

3.3 Phillips Curve

Combining the labor-leisure choice (14) with external habit preferences (3) and log-linearizing around a steady-state with $\bar{L}_{i,t} = \bar{L}$ gives a standard expression for the log-linearized real wage in terms of labor supply (up to a constant):

$$\hat{w}_{i,t} = \underbrace{\left(\chi \frac{\bar{L}}{1-\bar{L}}\right)}_{\text{Inverse Frisch } \eta} \hat{l}_{i,t}. \tag{28}$$

Equation (28) makes clear that the log-linearized real wage takes a standard form independent of habit, thereby sidestepping the issue noted by Lettau and Uhlig (2000) that habit may affect labor supply decisions in a production economy. Comparing to standard New Keynesian models (e.g. Galí (2008)) our log real wage is even somewhat simpler because it does not depend on aggregate consumption.[10] When consumption is close to habit the marginal utility from both market and home consumption is high, leaving the wage unaffected. In practice, this might capture that after an adverse shock consumers shift from eating out to cooking at home, as documented in Aguiar, Hurst, and Karabarbounis (2013). The assumption that home production increases with aggregate productivity, $A_t N_t$, ensures that the labor-leisure trade-off does not become irrelevant over time (Kehoe, Lopez, Midrigan, and Pastorino (2019)), consistent with empirical evidence (Chodorow-Reich and Karabarbounis (2016)).

We then proceed with standard log-linearization of the firms' price-setting problem

[10] Because labor supply and consumption are linked in equilibrium, this has no effect on the qualitative nature of the log-linearized Phillips curve and a negligible quantitative effect.

around the random walk component v_t^* (Cogley and Sbordone (2008)) to obtain the log-linearized Phillips curve:

$$\pi_t = \underbrace{\frac{\beta_g}{1+\beta_g}}_{f^\pi} E_t \pi_{t+1} + \underbrace{\frac{1}{1+\beta_g}}_{\rho^\pi} \pi_{t-1} + \kappa x_t + \underbrace{\left(-\frac{\kappa}{\omega(\theta-1)}\right)}_{v_{\pi,t}} \varepsilon_{\theta,t}. \tag{29}$$

Here, $\beta_g = \beta exp\left(-(\gamma-1)g\right)$ is the growth-adjusted time discount rate, and the slope of the Phillips curve equals $\kappa = \frac{1-\alpha}{\alpha}\frac{1-\beta_g\alpha}{1+\beta_g}\frac{\omega}{1+\omega\theta}$. The parameter $\omega = (\tau+\eta)/(1-\tau)$ captures the steady-state elasticity of real marginal cost vs. own-firm output.

A complementary approach to separate wages from consumption habit would be to introduce separate habits for consumption and leisure combined with labor market frictions, though matching asset pricing moments can be challenging in such a setup (Uhlig (2007), Rudebusch and Swanson (2008), Lopez (2014)). Our formulation is more parsimonious and requires only one parameter, closely related to the Frisch elasticity of labor supply, to describe preferences over leisure (χ). Because of this parsimony we consider our model a useful template to study the interaction between labor market frictions and habits in future research.

3.4 Macroeconomic Equilibrium Dynamics

We first solve for log-linear macroeconomic dynamics, and second for highly nonlinear asset prices. The tractability of this two step solution method is achieved because the surplus consumption ratio does not appear directly in the Euler equation or the Phillips curve, though finance and macroeconomics are connected through habit and consumption shocks. Equilibrium macroeconomic dynamics are determined by the real rate Euler equation (27), the log-linearized Phillips curve (29), and the monetary policy rule (21) through (23). The macroeconomic state vector is:

$$Y_t = [x_t, \pi_t - v_t^*, i_t - v_t^*]', \tag{30}$$

and the vector of structural shocks is

$$v_t = [v_{x,t}, v_{\pi,t}, v_{ST,t}, v_{LT,t}]'. \tag{31}$$

The vector of shocks v_t is assumed to be homoskedastic with a time-invariant diagonal variance-covariance matrix. Further, v_t is assumed to be serially uncorrelated and multivariate normal. We denote the standard deviations σ_x, σ_π, σ_{ST}, and σ_{LT}. We solve for a

minimum state variable equilibrium of the form:

$$Y_t = BY_{t-1} + \Sigma v_t, \tag{32}$$

where B and Σ are [3×3] and [3×4] matrices, respectively. We solve for the matrix B using Uhlig (1999) formulation of the Blanchard and Kahn (1980) method. For our estimation, we choose a monetary policy rule that raises real rates in response to an increase in inflation ($\gamma^{\pi} > 1$), so there exists a unique equilibrium of the form (32) in which all eigenvalues of B are less than one in absolute value. However, New Keynesian models are subject to well-known equilibrium multiplicity issues and equilibria with additional state variables or sunspots may exist (Cochrane (2011)), and resolving these issues is beyond this paper.

3.5 Solving for Asset Prices

We use numerical best practices to preserve the full nonlinearity of asset prices (Wachter (2005)). We use the following recursion to solve for the price-consumption ratio of an n-period zero-coupon consumption claim:

$$\frac{P^c_{nt}}{C_t} = \mathrm{E}_t\left[M_{t+1}\frac{C_{t+1}}{C_t}\frac{P^c_{n-1,t+1}}{C_{t+1}}\right]. \tag{33}$$

The price-consumption ratio for a claim to aggregate consumption is equal to the infinite sum of zero-coupon consumption claims:

$$\frac{P^c_t}{C_t} = \sum_{n=1}^{\infty}\frac{P^c_{nt}}{C_t}. \tag{34}$$

The price of the levered equity claim equals $P^{\delta}_t = \delta P^c_t$. Leverage hence scales stock returns roughly proportionally, increasing stock return volatility but leaving the Sharpe ratio unchanged. We initialize the recursions for real and nominal zero coupon bond prices:

$$P_{1,t} = \exp\left(-r_t\right), \; P^{\$}_{1,t} = \exp(-i_t). \tag{35}$$

The n-period zero coupon prices follow the recursions:

$$P_{n,t} = \mathrm{E}_t\left[M_{t+1}P_{n-1,t+1}\right], \tag{36}$$

$$P^{\$}_{n,t} = \mathrm{E}_t\left[M_{t+1}\exp(-\pi_{t+1})P^{\$}_{n-1,t+1}\right]. \tag{37}$$

Log bond yields for real and nominal zero coupon bonds with maturity n are defined by $y_{n,t} = -\log(P_{n,t})/n$ and $y^{\$}_{n,t} = -\log\left(P^{\$}_{n,t}\right)/n$.

The model generates an intuitive flight-to-safety effect, driving up safe asset prices and decreasing risky asset prices when surplus consumption is low. To gain intuition, we solve analytically for the risk premium of a one-period consumption claim. This claim pays aggregate consumption in period $t+1$ and pays nothing in all other periods, thereby sharing the cyclical properties of stocks but having a shorter horizon. We denote the log return on the one-period consumption claim by $r^c_{1,t+1}$. The risk premium, adjusted for a standard Jensen's inequality term, equals the conditional covariance between the negative log SDF and and log output:

$$E_t\left[r^c_{1,t+1} - r_t\right] + \frac{1}{2}Var\left(r^c_{1,t+1}\right) = \text{Cov}_t\left(-m_{t+1}, x_{t+1}\right) = \gamma\left(1+\lambda\left(s_t\right)\right)\sigma_c^2. \tag{38}$$

Equation (38) shows that risk premia are time-varying and increase with the sensitivity function $\lambda(s_t)$. Investors require a higher expected return for holding risky assets when surplus consumption is highly sensitive to consumption, as is the case when surplus consumption is low. The relationship between risk premia and surplus consumption has the reverse sign for safe assets that comove positively with SDF.

We solve for asset prices numerically on a four-dimensional grid consisting of the macroeconomic state vector $\hat{Y}_t$ and the surplus consumption ratio s_t. Iterating along a grid, as opposed to local approximation or global solution methods, is the best practice for this type of numerical problem because it imposes the least structure (Wachter (2005)). By contrast, approximation with polynomials would miss the particularly strong non-linearity of the sensitivity function as the log surplus consumption ratio becomes small, distorting numerical asset prices even around the steady-state. Grid iteration is facilitated in our framework because macroeconomic dynamics are log-linear. For details of the numerical solution see the Appendix.

3.6 Modeling High-Frequency Asset Prices around Monetary Policy Announcements

We make the simplifying assumption that FOMC dates occur at the end of the quarter, so post-FOMC asset prices correspond to end-of-quarter asset prices.[11] In order to model the discrete arrival of news on FOMC dates, we assume that the quarterly fundamental

[11] Given that our results are robust to varying the volatility of news released on FOMC dates (Appendix C.7), modeling FOMC dates as occurring every six weeks is unlikely to change our findings.

shock vector v_t consists of independent pre-FOMC v_t^{pre} and FOMC v_T^{FOMC} components

$$v_t \quad = \quad v_t^{pre} + v_t^{FOMC}.$$

The vector of FOMC shocks v_t^{FOMC} is assumed to have a diagonal variance-covariance matrix with standard deviations $\sigma_x^{FOMC} = 0$, $\sigma_\pi^{FOMC} = 0$, $\sigma_{ST}^{FOMC} < \sigma_{ST}$, and $\sigma_{LT}^{FOMC} < \sigma_{LT}$.

Pre-FOMC asset prices in our model differ from quarter $t-1$ asset prices because they also reflect information encoded in v_t^{pre}, which in our application is assumed to include the full habit and Phillips curve shocks realized in quarter t as well as substantial portions of the quarter t short-term and long-term monetary policy shocks. We compute quarter t pre-FOMC asset prices at the expected quarter t state vector conditional on information available at the end of period $t-1$ and v_t^{pre}. We model FOMC announcements as occurring instantaneously, so no dividends are paid and the aggregate price level is constant during the short FOMC interval. The model high-frequency log stock return around monetary policy news then simply equals the post- minus the pre-FOMC log price for the levered consumption claim. The model high-frequency change in breakeven around monetary policy news equals post- minus pre-FOMC log 10-year breakeven. For details of model high-frequency asset price changes see Appendix C.7.

4 Estimated Model

We estimate the model in two steps. In a first step, we set preference parameters, firm parameters, and monetary policy parameters to standard values from the literature. In a second step, we use a Simulated Method of Moments (SMM) procedure to estimate the standard deviations of shocks.

4.1 Calibrated Parameters

Table 1, Panel A lists the calibrated parameters. The consumption growth rate, utility curvature, steady-state real risk free rate, persistence of surplus consumption, and the learning-by-doing parameter ϕ responsible for detrending output are taken from Campbell, Pflueger, and Viceira (2020). We choose the preference parameters θ_1 and θ_2 to match the macroeconomics literature. We choose $\theta_2 = 0.6$ in line with the habit parameters in Fuhrer (2000), Smets and Wouters (2007), Christiano, Eichenbaum, and Evans (2005). The parameter θ_1 is set to ensure that the forward- and backward-looking parameters in the real rate Euler equation sum to one.

On the firm side, we follow Galí (2008). We set the price-stickiness parameter to

0.67, meaning that the average price duration is three-quarters. The capital share of production is set to a standard value of $\tau = 1/3$. The cross-goods substitutability is set to $\theta = 6$, implying a steady-state markup of 20%. The steady-state Frisch elasticity of labor supply, which in our model equals $\left(\chi \frac{\bar{L}}{1-\bar{L}}\right)^{-1}$, is set to one. We set the leverage parameter to 0.4. We interpret this leverage parameter broadly, to include operational leverage. The main purpose of this parameter is to match the volatility of equity returns, while leaving the equity Sharpe ratio unchanged.

We also choose conventional monetary policy parameters. The reaction coefficients for inflation and output fluctuations are from Taylor (1993) and equal $\gamma_x = 0.5$ and $\gamma_\pi = 1.5$. We set the monetary policy smoothing parameter to $\rho^i = 0.9$ to match the larger root in interest rates, and $\rho^a = 0.34 = 0.68/\gamma$ to match the relationship between the frictionless real rate embedded in growth expectations and the actual real rate from Nakamura and Steinsson (2018).

4.2 SMM Estimation

Having calibrated this initial set of parameters, we estimate the vector of standard deviations $\sigma = [\sigma_x, \sigma_\pi, \sigma_{ST}, \sigma_{LT}]$ by minimizing the objective function

$$J(\sigma) = (\Psi(\sigma) - \hat{\Psi})' \hat{W} (\Psi(\sigma) - \hat{\Psi}). \tag{39}$$

Following Christiano, Eichenbaum, and Evans (2005), the vector $\hat{\Psi}$ collects empirical macroeconomic impulse responses, and we weight the moments by a diagonal matrix $\hat{W}$ with the inverses of the bootstrapped variances along the diagonal. Our sample begins in 2001Q2, when the relationship between inflation and empirical output gap measures displays a structural change (Campbell, Pflueger, and Viceira, 2020), and ends in 2019Q2. The vector $\Psi(\sigma)$ collects the corresponding model moments, obtained by applying the same procedure to simulated data of the same length. Our moments are from a one lag VAR in the log output gap, the one-quarter change in inflation, and the difference between the nominal Federal Funds rate and inflation, thereby respecting the joint unit root in inflation and nominal interest rates in the model.[12] Impulse responses are orthogonalized so shocks to the Fed Funds rate do not contemporaneously affect inflation or output, and inflation innovations do not enter into the same period output. This orthogonalization

[12] Quarterly real GDP, real potential GDP, and the GDP deflator in 2012 chained dollars are from the FRED database at the St. Louis Federal Reserve. Since output, unlike asset prices, is a flow over a quarter, it can be treated either as occurring at the beginning or end of a quarter. We follow Campbell (2003) and align output reported for quarter t with interest rates and stock prices measured at the end of quarter $t-1$. The log output gap is in percent units. We use the Federal Funds rate averaged over the last week of the quarter from the Federal Reserve's H.15 publication. Interest rates and inflation are in annualized percent.

does not directly identify the structural shocks in our model, and merely defines a unique set of empirical macroeconomic moments that are comparable to the literature. We target the output gap, inflation, and Fed Funds rate responses in periods 0, 1, 2 , 4, 8, and 12 quarters after the initial shock. Since σ_{LT} is not well identified from the reduced-form macroeconomic impulse responses, we additionally target the standard deviation of quarterly changes in inflation swap rates for 10-year inflation starting 10 years from now, which we estimate to equal 0.26% over our sample.[13] For details of the SMM procedure see Appendix E.

The estimated standard deviations of shocks are shown in Table 1, Panel B. The Phillips curve shock is somewhat more volatile than the demand and short-term monetary policy shocks. The long-term monetary policy shock is the least volatile, and its volatility of 0.22% closely matches the standard deviation of quarterly changes in 10 on 10-year breakeven inflation in the model, which equals 0.26% just like in the data.

4.3 Model Fit

4.3.1 Macroeconomic Dynamics

Figure 2 shows that the model matches the empirical volatilities of the output gap, inflation, and Fed Funds rate, their persistence over time, and their comovements. It is important to keep in mind that the impulse responses shown in Figure 2 are not structural, only a statistical decomposition, and that each innovation reflects a combination of the underlying structural shocks. We turn to structural impulse responses in Section 4.4.1.

Both in the model and in the data the output gap, inflation, and the Federal Funds rate tend to move together in response to all innovations, with the exception of the interest rate innovation. The interest rate innovation has a negative but quantitatively small output gap response both in the model and in the data. The overall positive inflation-output gap comovement in Figure 2 is consistent with prior literature, which documents that the output gap-inflation correlation is positive and long-term nominal bonds are hedges for the post-2001 period (Baele, Bekaert, and Inghelbrecht (2010), Campbell, Sunderam, Viceira, et al. (2017), Song (2017), Campbell, Pflueger, and Viceira (2020), Gourio and Ngo (2020)).

4.3.2 Asset Prices

Table 2 shows that our model also generates volatile stock returns with an empirically plausible equity Sharpe ratio of 0.50, an equity premium of 6.82%, and annualized equity

[13] Inflation swap rates, in annualized percent, are from Bloomberg.

return volatility of 13.55%. This high stock return volatility is achieved through time-varying risk premia of the form (38).[14] The model fits the negative breakeven beta with respect to the stock market, which Campbell, Pflueger, and Viceira (2020) argue is important to generate endogenous flight-to-safety towards nominal bonds when equity risk premia rise. The real bond-stock beta in the model is slightly positive, compared to a slightly negative real bond beta in the data. Breakeven excess returns are volatile at 4.76% similarly to the data, and real bond excess returns in the model have substantial volatility at 1.56%. The empirical volatility of 10-year TIPS excess returns exceeds the real bond return volatility in the model at 6.82%. However, this empirical volatility is likely overestimated because TIPS contain large and time-varying liquidity premium (Gürkaynak, Sack, and Wright (2010), Fleckenstein, Longstaff, and Lustig (2014)).

While the model matches the data well along many dimensions, it misses realized excess bond returns over our sample period. We face a choice between fitting betas or term premia and we prefer to fit second moments, which are measured more precisely over short samples. The fundamental tension between matching a positive term premium and a negative bond beta is not specific to our model and arises for most single-factor models. For example, the seminal contribution of Wachter (2005) obtains a positive term premium from a positive bond-stock beta, which however has turned negative in our more recent sample. Regime switches in monetary policy can potentially resolve this tension (Song (2017)), and although exploring them is beyond this current paper the convenient log-linear macroeconomic dynamics would make our model a tractable building block for such an analysis.

4.4 Model Drivers

To better understand the model mechanisms, we show impulse responses to the structural innovations $v_{x,t}$, $v_{\pi,t}$, $v_{ST,t}$ and $v_{LT,t}$.

4.4.1 Structural Macroeconomic Responses

Figure 3 confirms that the macroeconomic side of our model behaves like a standard three-equation New Keynesian model. A habit shock acts as a demand shock and leads

[14] To compute the empirical asset pricing moments, we use value-weighted combined NYSE/AMEX/-Nasdaq stock returns including dividends from CRSP. The dividend-price ratio is constructed using data for real S&P 500 dividends and the S&P 500 real price from Robert Shiller's website. For both bonds and stocks, we consider log returns in excess of the log T-bill rate, where the end-of-quarter three-month T-bill is from the CRSP monthly Treasury risk-free rate file. Log bond returns are derived from changes in yields in the data. End-of-quarter bond yields for both nominal Treasuries and TIPS are from the daily zero coupon curves of Gürkaynak, Sack, and Swanson (2005) and Gürkaynak, Sack, and Wright (2010). All yields and returns are continuously compounded.

to a temporary increase in output, and a smaller temporary increase in inflation. A positive Phillips curve shock, due to an increase in markups, leads to a decline in output and an increase in inflation. A short-term increase in the short-term interest rate causes a decline in output through consumers' consumption-savings decision, and lower inflation through the Phillips curve. Finally, a negative long-term monetary policy shock leads to a costly disinflation, lowering inflation expectations ahead of nominal interest rates, and thereby raising the real rate and contracting output. The backward-looking component in the consumption Euler equation ensures a hump-shaped output gap responses as in Fuhrer (2000) and Boldrin, Christiano, and Fisher (2001).

4.4.2 Structural Asset Price Responses

Figure 4 shows that the structural impulse responses for stocks and bonds follow naturally from the macroeconomic impulse responses. The first row shows cumulative equity returns in excess of the steady-state return, and the subsequent rows show yields on 10-year nominal and real bonds. Because bond yields are inversely related to prices, an increase in the 10-year yield implies a decrease in the corresponding bond price.

Comparing the first rows across Figures 3 and 4 shows that stock prices move in the same direction as output gap responses, with the overall stock response quantitatively dominated by time-varying risk premia.[15] The second row of Figure 4 shows that long-term nominal bond yields respond in the same direction as the Federal Funds rate in Figure 3. The third row of Figure 4 shows that 10-year real bond yields respond in the same direction as the short-term real rate and are almost exclusively driven by the risk-neutral component.

The first column of Figure 4 helps understand the habit shock, and shows that it affects asset prices through both intertemporal substitution and risk aversion. The expected increase in surplus consumption generates an incentive for intertemporal substitution, driving down risk-neutral prices of both real bonds and stocks. Because bond yields move inversely with prices, risk-neutral long-term real bond yields increase. Higher expected surplus consumption also affects risk premia, because it leads to higher consumption today through the consumption Euler equation, raising surplus consumption and driving up stock prices. The risk premium effect dominates the stock price response, whereas the risk-neutral component dominates the real bond yield response. The demand shock therefore has the unique ability to drive down the real bond-stock beta towards zero.

[15]The risk neutral response for all asset prices is computed as if assets were priced by a risk neutral agent, holding macroeconomic dynamic fixed. The risk premium component is the difference between the total and the risk neutral responses.

4.5 Stock Returns around Monetary Policy News

Having seen that time-varying risk premia amplify stock return responses to macroeconomic shocks, we now turn to the implications for high-frequency stock price changes around monetary policy news. In this section, we first expand on the motivating evidence reported in Figure 1 and then show how the model can account for these empirical patterns. Appendix F.2 shows that the model matches the comovement between the short-term policy rate and long-term real bond yields documented by Hanson and Stein (2015) and Nakamura and Steinsson (2018), in part because the natural real rate moves together with expected growth through (19) in our model.

4.5.1 Empirical Stocks Returns around Monetary Policy News

In Table 3, we formally establish the empirical relationships described in Figure 1. Column (1) corresponds to the left panel of Figure 1, and replicates the classic result of Bernanke and Kuttner (2005). We find that a 25 bps surprise increase in the Federal Funds rate leads to a one percentage point drop in the stock price on average. Column (2) mirrors the right panel of Figure 1 and shows that breakeven changes on FOMC dates have a statistically significant and economically meaningful positive relationship with stock returns around FOMC announcements. In contrast to column (1), a 25 bps surprise increase in 10-year breakeven tends to be associated with a 1.5 percentage point increase in stock returns.[16] To establish that FOMC dates reveal separate information about short-term interest rates and long-term inflation expectations, we report multivariate regression results in column (3). Both coefficients are statistically significant and quantitatively similar to the univariate regressions in columns (1) and (2). Column (4) further shows that changes in 10-year breakeven, as a proxy for long-term inflation expectations, are uncorrelated with Federal Funds rate surprises around FOMC announcements over our sample period.

4.5.2 Model Stock Returns around Monetary Policy News

Table 4 shows the corresponding model regressions. We compute high-frequency model stock returns, short-term interest rate changes, and 10-year breakeven changes using post-

[16] We collect the release date of FOMC statements from January 1st 2001 until Dec 31st 2019 from the Federal Reserve's website. To construct an empirical counterpart to the short-term monetary policy shock in our model, we collect one-hour changes in Federal Funds rate around scheduled FOMC announcements from the updated data of Gorodnichenko and Weber (2016), while for the long-term monetary shock we use one-day changes in zero coupon nominal Treasury yields and TIPS yields are from Gürkaynak, Sack, and Swanson (2005) and Gürkaynak, Sack, and Wright (2010). We are unable to construct higher frequency proxies for this shock due to data availability for long-term bond yields. The equity return outcome variable is measured using S&P 500 returns in the same one-hour windows around FOMC announcement constructed from Trade and Quote data, accessed through WRDS.

minus pre-FOMC asset prices to compute, where we split aggregate quarterly shocks into pre-FOMC and FOMC components as described in Section 3.6. As in the data, we assume that FOMC date monetary policy shocks represent only a portion of the quarterly volatility of monetary policy shocks. To match the volatilities of Federal Funds and 10-year breakeven changes around FOMC dates and their lack of a significant relationship in our sample, we assume that the FOMC date short-term monetary policy shock has a standard deviation of $\sigma_{ST}^{FOMC} = 4.3$ bps, the FOMC date long-term monetary policy shock has a standard deviation of $\sigma_{LT}^{FOMC} = 3.3$ bps, and the two shocks on FOMC dates are uncorrelated.[17]

Table 4, column (2) shows that the model matches the baseline empirical regression in Table 3, column (3). Table 4, column (3) replaces the change in 10-year breakeven by its risk-neutral counterpart. Both regression coefficients remain unchanged, showing that 10-year breakeven changes proxy for a shock to long-term inflation expectations in these regressions, and therefore capture long-term monetary policy shocks in the model.

In column (4) we highlight the amplification effect from countercyclical risk-aversion, showing that the model attributes roughly half of the stock market's response to both monetary policy shocks to time-varying risk premia. This large risk premium component for the stock market response to monetary policy news is quantitatively in line with the empirical decomposition into cash flow news versus discount rate news by Bernanke and Kuttner (2005).

Why do stock returns move so much in response to short-term monetary policy news? The macroeconomic and asset pricing responses to a short-term interest rate increase in Figures 3 and 4 show that such a shock leads to a hump-shaped decrease in output and consumption. As surplus consumption declines towards habit, investors require higher compensation for holding risky stocks. The fall in stocks due to lower expected consumption is therefore compounded by risk premia. Because time-varying risk premia in our model are quantitatively important in equilibrium, they are similarly quantitatively important around monetary policy news events, helping to explain why stock returns decrease so much in response to a surprise increase in the Federal Funds rate in the data.

To understand the relationship between high-frequency changes in 10-year breakeven and stock returns around the FOMC shock in the model, note that Figures 3 and 4 show that long-term monetary policy shocks move long-term inflation expectations and the output gap in the same direction, but have little immediate impact on short-term interest rates. The long-term monetary policy shock therefore has the potential to move stock returns in the same direction as 10-year breakeven around monetary policy news

[17] We show in Appendix Figure A1 that the model regression slope coefficients are not sensitive to varying the volatilities of monetary policy news on FOMC dates.

events, independently of movements in the short-term nominal rate. As output and consumption decline, investors become more risk averse, amplifying the fall in stocks in response to a negative long-term monetary policy shock. In contrast to stocks, the risk premium component in breakeven is smaller because breakeven returns have a stock market beta that is much smaller than one in magnitude, and changes in breakeven are hence closely correlated with long-term monetary policy shocks.[18] Appendix Table A1 shows that the results in Table 4 are robust to switching off various model components.

The average model monetary policy effects in Table 4 conceal substantial state-dependence with respect to the level of surplus consumption. In Figure 5 we estimate the model high-frequency stock response to monetary policy news separately in ten different sub-samples, one for each decile of the pre-FOMC surplus consumption ratio. The figure shows that the overall effect (solid lines) of both long- and short-term monetary policy shocks increases in magnitude when surplus consumption is low, as would be the case after a sequence of output declines. Since the macroeconomic consequences of the shocks reported in Figure 3 are invariant to the level of surplus consumption, the risk neutral component (dashed lines) is flat. The variation in stock return responses to long- and short-term monetary policy shocks is driven by more volatile risk premia (dotted lines) when consumption is low relative to habit. In line with this model prediction, we confirm that during the height of the financial crisis (defined as October 2008 through December 2009), stock returns on FOMC dates were fifty percent more volatile than in the rest of our sample even though Federal Funds rate surprises and breakeven changes were no more volatile.[19] The model prediction of greater stock return sensitivity to announcements during recessions is also consistent with the empirical evidence from macroeconomic announcements by Law, Song, and Yaron (2019).

5 Conclusion

We integrate a small-scale New Keynesian model of monetary policy with countercyclical risk premia using the habit formation preferences of Campbell and Cochrane (1999) and Campbell, Pflueger, and Viceira (2020), and apply it to understand asset price movements around monetary policy announcements. The model easily matches the large

[18] While our results support the notion that FOMC dates reveal news about long-term inflation, we cannot speak to whether specific tools and or communications move investors' long-term inflation expectations, which may very well be time-varying (Goodfriend and King (2005)), context-specific (Coibion, Gorodnichenko, and Weber (2020)), and depend on behavioral channels (Orphanides and Williams (2004), Gabaix (2019)).

[19] In Appendix G, we find that the point estimates from our benchmark regression in Table 3 also increase in magnitude for this crisis subsample, though the coefficients are not statistically significant due the small number of observations.

stock return response to traditional monetary policy shocks, but only if stock responses are amplified by time-varying compensation for risk. Our model attributes the large and positive empirical relationship between breakeven inflation innovations and stock returns around monetary policy announcements to correlated news about long-term inflation and output, supporting the notion that monetary policy announcements reveal news about the economy in a "Fed information effect".

Taken together, our analysis suggests that volatile stock returns in lower frequency data and quantitatively large stock return responses to monetary policy announcements are internally consistent and two sides of the same coin. This has important implications for interpreting asset price reactions to monetary policy. Our model suggests that policy makers, economists, and market observers need to be careful to not extrapolate from average relationships during crises, as risk bearing capacity and stock markets may react a lot even to monetary policy announcements with modest real effects.

Our framework is tractable and portable towards broader macroeconomic models. We anticipate that our framework will be useful to interpret macroeconomic drivers of asset price fluctuations beyond the channels considered in this basic macroeconomic model, such as wage rigidities or heterogeneity in price-setting frictions (Weber (2015)). We also believe that the framework will be useful to understand the role of time-varying risk premia in other empirical puzzles, such as the empirical finding that equity returns are typically high prior to FOMC dates (Lucca and Moench (2015), Cieslak, Morse, and Vissing-Jorgensen (2019), Cieslak and Pang (2019), Laarits (2019)).

References

Abel, Andrew B, 1990, Asset Prices under Habit Formation and Catching up with the Joneses, *American Economic Review* pp. 38–42.

Aguiar, Mark, Erik Hurst, and Loukas Karabarbounis, 2013, Time use during the great recession, *American Economic Review* 103, 1664–96.

Albuquerque, Rui, Martin Eichenbaum, Victor Xi Luo, and Sergio Rebelo, 2016, Valuation risk and asset pricing, *Journal of Finance* 71, 2861–2904.

Andrade, Philippe, and Filippo Ferroni, 2020, Delphic and Odyssean monetary policy shocks: Evidence from the euro area, *Journal of Monetary Economics*.

Auclert, Adrien, Matthew Rognlie, and Ludwig Straub, 2020, Micro jumps, macro humps: Monetary policy and business cycles in an estimated hank model, National Bureau of Economic Research Working Paper wp26647.

Baele, Lieven, Geert Bekaert, and Koen Inghelbrecht, 2010, The determinants of stock and bond return comovements, *Review of Financial Studies* 23, 2374–2428.

Ball, Laurence, 1994, Credible disinflation with staggered price-setting, *American Economic Review* 84, 282–289.

Ball, Laurence, and David Romer, 1990, Real rigidities and the non-neutrality of money, *Review of Economic Studies* 57, 183–203.

Bekaert, Geert, Eric Engstrom, and Steven R Grenadier, 2010, Stock and bond returns with moody investors, *Journal of Empirical Finance* 17, 867–894.

Bekaert, Geert, Eric C Engstrom, and Nancy R Xu, 2019, The time variation in risk appetite and uncertainty, .

Bernanke, Ben S, and Kenneth N Kuttner, 2005, What explains the stock market's reaction to federal reserve policy? *Journal of Finance* 60, 1221–1257.

Bianchi, Francesco, Cosmin L Ilut, and Martin Schneider, 2018, Uncertainty shocks, asset supply and pricing over the business cycle, *Review of Economic Studies* 85, 810–854.

Blanchard, Olivier Jean, and Charles M Kahn, 1980, The solution of linear difference models under rational expectations, *Econometrica* pp. 1305–1311.

Boldrin, Michele, Lawrence J Christiano, and Jonas DM Fisher, 2001, Habit persistence, asset returns, and the business cycle, *American Economic Review* 91, 149–166.

Bretscher, Lorenzo, Alex Hsu, and Andrea Tamoni, 2019, The real response to uncertainty shocks: The risk premium channel, *Working Paper, London Business School, Rutgers, and Georgia Tech*.

Caballero, Ricardo J, and Alp Simsek, 2020, A risk-centric model of demand recessions and macroprudential policy, *Quarterly Journal of Economics* forthcoming.

Calvo, Guillermo A, 1983, Staggered Prices in a Utility-Maximizing Framework, *Journal of Monetary Economics* 12, 383–398.

Campbell, John Y, 2003, Consumption-Based Asset Pricing, *Handbook of the Economics of Finance* 1, 803–887.

Campbell, John Y, and John H Cochrane, 1999, By force of habit: A consumption-based explanation of aggregate stock market behavior, *Journal of Political Economy* 107, 205–251.

Campbell, John Y, and Sydney Ludvigson, 2001, Elasticities of substitution in real business cycle models with home production, *Journal of Money, Credit and Banking* 33, 847–875.

Campbell, John Y, Carolin Pflueger, and Luis M Viceira, 2020, Macroeconomic drivers of bond and equity risks, *Journal of Political Economy* 128, 3148–3185.

Campbell, John Y, Adi Sunderam, Luis M Viceira, et al., 2017, Inflation Bets or Deflation Hedges? The Changing Risks of Nominal Bonds, *Critical Finance Review* 6, 263–301.

Chodorow-Reich, Gabriel, and Loukas Karabarbounis, 2016, The cyclicality of the opportunity cost of employment, *Journal of Political Economy* 124, 1563–1618.

Christiano, Lawrence H., Martin Eichenbaum, and Charles L. Evans, 2005, Nominal rigidities and the dynamic effects of a shock to monetary policy, *Journal of Political Economy* 113, 1–45.

Christiano, Lawrence J, Roberto Motto, and Massimo Rostagno, 2014, Risk shocks, *American Economic Review* 104, 27–65.

Cieslak, Anna, Adair Morse, and Annette Vissing-Jorgensen, 2019, Stock returns over the FOMC cycle, *Journal of Finance* 74, 2201–2248.

Cieslak, Anna, and Hao Pang, 2019, Common shocks in stocks and bonds, *Duke University, Working Paper*.

Cochrane, John H, 2011, Determinacy and Identification with Taylor Rules, *Journal of Political Economy* 119, 565–615.

Cochrane, John H., 2017, Macro-Finance, *Review of Finance*.

Cochrane, John H, 2018, Michelson-Morley, Fisher, and Occam: The Radical Implications of Stable Quiet Inflation at the Zero Bound, *NBER Macroeconomics Annual* 32, 113–226.

Cogley, Timothy, and Argia M. Sbordone, 2008, The time-varying volatility of macroeconomic fluctuations, *American Economic Review* 98, 2101–2126.

Coibion, Olivier, Yuriy Gorodnichenko, and Michael Weber, 2020, Monetary policy communications and their effects on household inflation expectations, *NBER WP 26778*.

Constantinides, George M, 1990, Habit formation: A resolution of the equity premium puzzle, *Journal of Political Economy* 98, 519–543.

Dew-Becker, Ian, 2014, Bond pricing with a time-varying price of risk in an estimated medium-scale Bayesian DSGE model, *Journal of Money, Credit and Banking* 46, 837–888.

Drechsler, Itamar, Alexi Savov, and Philipp Schnabl, 2018, A model of monetary policy and risk premia, *Journal of Finance* 73, 317–373.

Favilukis, Jack, and Xiaoji Lin, 2016, Wage rigidity: A quantitative solution to several asset pricing puzzles, *Review of Financial Studies* 29, 148–192.

Fleckenstein, Matthias, Francis A Longstaff, and Hanno Lustig, 2014, The TIPS-Treasury bond puzzle, *the Journal of Finance* 69, 2151–2197.

Fuhrer, Jeffrey C, 2000, Habit formation in consumption and its implications for monetary-policy models, *American Economic Review* 90, 367–390.

Gabaix, Xavier, 2019, A behavioral New Keynesian model, *Harvard University Working Paper*.

Galí, Jordi, 2008, *Monetary Policy, Inflation, and the Business Cycle* (Princeton University Press).

Goodfriend, Marvin, and Robert G King, 2005, The incredible volcker disinflation, *Journal of Monetary Economics* 52, 981–1015.

Gorodnichenko, Yuriy, and Michael Weber, 2016, Are sticky prices costly? evidence from the stock market, *American Economic Review* 106, 165–99.

Gourio, Francois, 2012, Disaster risk and business cycles, *American Economic Review* 102, 2734–66.

Gourio, François, and Phuong Ngo, 2020, Risk Premia at the ZLB: A Macroeconomic Interpretation, *Federal Reserve Bank of Chicago*.

Greenwood, Jeremy, Zvi Hercowitz, and Gregory W Huffman, 1988, Investment, capacity utilization, and the real business cycle, *American Economic Review* pp. 402–417.

Gürkaynak, Refet S, Brian Sack, and Eric Swanson, 2005, The sensitivity of long-term interest rates to economic news: Evidence and implications for macroeconomic models, *American Economic Review* 95, 425–436.

Gürkaynak, Refet S, Brian Sack, and Jonathan H Wright, 2007, The US treasury yield curve: 1961 to the present, *Journal of Monetary Economics* 54, 2291–2304.

Gürkaynak, Refet S, Brian Sack, and Jonathan H Wright, 2010, The TIPS yield curve and inflation compensation, *American Economic Journal: Macroeconomics* 2, 70–92.

Hanson, Samuel G, and Jeremy C Stein, 2015, Monetary policy and long-term real rates, *Journal of Financial Economics* 115, 429–448.

Jarociński, Marek, and Peter Karadi, 2020, Deconstructing monetary policy surprises—The role of information shocks, *American Economic Journal: Macroeconomics* 12, 1–43.

Jermann, Urban J., 1998, Asset pricing in production economies, *Journal of Moentary Economics* 41, 257–275.

Justiniano, Alejandro, and Giorgio E. Primiceri, 2008, Trend inflation, indexation, and inflation persistence in the New Keynesian Phillips Curve, *American Economic Review* 98, 604–641.

Kaplan, Greg, Benjamin Moll, and Giovanni L Violante, 2018, Monetary policy according to hank, *American Economic Review* 108, 697–743.

Kehoe, Patrick J, Pierlauro Lopez, Virgiliu Midrigan, and Elena Pastorino, 2019, Asset prices and unemployment fluctuations, Discussion paper, National Bureau of Economic Research.

Kekre, Rohan, and Moritz Lenel, 2020, Monetary policy, redistribution, and risk premia, *Working Paper, University of Chicago and Princeton University*.

Kilic, Mete, and Jessica A Wachter, 2018, Risk, unemployment, and the stock market: A rare-event-based explanation of labor market volatility, *Review of Financial Studies* 31, 4762–4814.

Kung, Howard, 2015, Macroeconomic linkages between monetary policy and the term structure of interest rates, *Journal of Financial Economics* 115, 42–57.

Laarits, Toomas, 2019, Pre-announcement risk, Working Paper, NYU Stern.

Lagos, Ricardo, and Shengxing Zhang, 2020, Turnover liquidity and the transmission of monetary policy, *American Economic Review, forthcoming*.

Law, Tzuo Hann, Dongho Song, and Amir Yaron, 2019, Fearing the Fed: How Wall Street reads Main Street, Working Paper, Boston College, Johns Hopkins University, and Wharton.

Lettau, Martin, and Harald Uhlig, 2000, Can habit formation be reconciled with business cycle facts? *Review of Economic Dynamics* 3, 79–99.

Lopez, Pierlauro, J. David, 2014, Macro- finance separation by force of habit, *unpublished paper, Federal Reserve Board and Banque de France*.

Lucas, Robert E. Jr., 1988, On the mechanics of economic development, *Journal of*

Monetary Economics 22, 3–42.

Lucca, David O, and Emanuel Moench, 2015, The pre-FOMC announcement drift, *Journal of Finance* 70, 329–371.

McKay, Alisdair, Emi Nakamura, and Jón Steinsson, 2016, The power of forward guidance revisited, *American Economic Review* 106, 3133–58.

Nakamura, Emi, and Jón Steinsson, 2018, High-frequency identification of monetary non-neutrality: the information effect, *Quarterly Journal of Economics* 133, 1283–1330.

Orphanides, Athanasios, and John Williams, 2004, Imperfect Knowledge, Inflation Expectations, and Monetary Policy, in Ben S. Bernanke, and Michael Woodford, eds.: *The Inflation-Targeting Debate* . pp. 201–246 (University of Chicago Press).

Pflueger, Carolin, Emil Siriwardane, and Adi Sunderam, 2020, Financial market risk perceptions and the macroeconomy, *Quarterly Journal of Economics* 135, 1443–1491.

Romer, Christina D, and David H Romer, 2000, Federal reserve information and the behavior of interest rates, *American Economic Review* 90, 429–457.

Rudebusch, Glenn D, and Eric T Swanson, 2008, Examining the bond premium puzzle with a dsge model, *Journal of Monetary Economics* 55, S111–S126.

Schmitt-Grohé, Stephanie, and Martín Uribe, 2018, Exchange rates and uncovered interest differentials: The role of permanent monetary shocks, Discussion paper, National Bureau of Economic Research.

Shiller, Robert J, 1981, Do stock prices move too much to be justified by subsequent changes in dividends? *American Economic Review* 71, 421–436.

Smets, Frank, and Rafael Wouters, 2007, Shocks and frictions in us business cycles: A Bayesian DSGE approach, *American Economic Review* pp. 586–606.

Song, Dongho, 2017, Bond Market Exposures to Macroeconomic and Monetary Policy Risks, *Review of Financial Studies* 30, 2761–2817.

Stavrakeva, Vania, and Jenny Tang, 2019, The dollar during the great recession: US monetary policy signaling and the flight to safety, Working Paper, London Business School and Boston Federal Reserve.

Taylor, John B, 1993, Discretion versus policy rules in practice, in *Carnegie-Rochester conference series on public policy* vol. 39 pp. 195–214. Elsevier.

Uhlig, Harald, 1999, A Toolkit for Analysing Nonlinear Dynamic Stochastic Models Easily, in Ramon Marimon, and Andrew Scott, eds.: *Computational Methods for the Study of Dynamic Economics* . pp. 30–61 (Oxford University Press).

Uhlig, Harald, 2007, Explaining asset prices with external habits and wage rigidities in a DSGE model, *American Economic Review* 97, 239–243.

Uribe, Martín, 2018, The neo-Fisher effect: Econometric evidence from empirical and optimizing models, Discussion paper, National Bureau of Economic Research.

Wachter, Jessica A., 2005, Solving models with external habit, *Finance Research Letters* 2, 210–226.

Wachter, Jessica A, 2006, A consumption-based model of the term structure of interest rates, *Journal of Financial Economics* 79, 365–399.

Weber, Michael, 2015, Nominal rigidities and asset pricing, *Working Paper, University of Chicago.*

Woodford, Michael, 2003, *Interest and Prices* (Princeton University Press).

Table 1: Model Parameters

Panel A: Calibrated Parameters		
Consumption Growth Rate	g	1.89
Utility Curvature	γ	2.00
Steady-State Riskfree Rate	$\bar{r}$	0.94
Persistence Surplus Consumption Ratio	θ_0	0.87
Dependence Output Gap	θ_1	-0.67
Dependence Lagged Output Gap	θ_2	0.60
Capital Share of Production	τ	0.33
Learning-by-Doing	ϕ	0.93
Frisch Elasticity	$\chi\frac{\bar{L}}{1-\bar{L}}$	1.00
Price Stickiness	α	0.67
Cross-Goods Substitutability	θ	6.00
Productivity Growth - Real Rate	ρ^a	0.34
Leverage	δ	0.40
MP Coefficient Output	γ^x	0.50
MP Coefficient Inflation	γ^π	1.50
MP Persistence	ρ^i	0.90
Panel B: Estimated Parameters		
Std. Demand Shock (%)	σ_x	0.37
Std. PC Shock (%)	σ_π	0.49
Std. Short-Term MP (%)	σ_{ST}	0.37
Std. Long-Term MP (%)	σ_{LT}	0.22
Panel C: Implied Parameters		
Discount Rate	β	0.90
Steady-State Surplus Consumption Ratio	$\bar{S}$	0.04
Maximum Surplus Consumption Ratio	S^{max}	0.07
Euler Equation Lag Coefficient	ρ^x	0.37
Euler Equation Forward Coefficient	f^x	0.63
Euler Equation Real Rate Slope	ψ	0.08
Phillips Curve Lag Coefficient	ρ^π	0.51
Phillips Curve Forward Coefficient	f^π	0.49
Phillips Curve Slope	κ	0.06

Note: Panel A shows the parameters we calibrate following previous literature, as detailed in Section 4.1. Panel B displays the parameters we estimate by matching the empirical impulse response functions and the volatility of long-term breakeven as described in Section 4.2. Panel C reports moments implied by the other parameters listed above. Consumption growth and the steady-state risk-free rate are in annualized percent. The discount rate and the persistence of surplus consumption are annualized. The monetary policy coefficients and the Phillips curve slope are reported in units corresponding to our empirical variables, i.e. the log output gap is in percent, and inflation, the Fed Funds rate are in annualized percent. The implied Euler equation real rate slope is hence reported as $\frac{1}{4}\psi$ and the implied Phillips curve slope is reported as 4κ. We report quarterly standard deviations of shocks to percent output gap, annualized percent inflation, the annualized percent Fed Funds rate, and the annualized percent long-term monetary policy target.

Table 2: Asset Prices

		Model	Data
Stocks			
	Volatility	13.55	16.96
	Equity Premium	6.82	7.41
	Sharpe Ratio	0.50	0.44
10Y Breakeven			
	Volatility	4.76	7.01
	Breakeven-Stock Beta	-0.13	-0.23
	Excess Returns	-0.67	0.55
	Sharpe Ratio	-0.14	0.08
10Y Real Bonds			
	Volatility	1.56	6.83
	Real Bond-Stock Beta	0.03	-0.08
	Excess Returns	0.07	3.76
	Sharpe Ratio	0.05	0.55

Note: This table reports the unconditional asset pricing moments both empirically and in model simulated data. The equity premium is computed as the quarterly log return on the value-weighted combined NYSE/AMEX/Nasdaq stock return including dividends from CRSP in excess of the log 3-month Treasury bill plus one-half times the log excess return variance to adjust for Jensen's inequality. Breakeven excess returns are defined as nominal minus real bond excess returns. Real bond excess returns are quarterly log returns on 10-year real Treasury bonds in excess of the log nominal 3-month Treasury bill return. We compute empirical log returns on the 10-year nominal Treasury bond and inflation-indexed bond (TIPS) from log bond yields: $r^{\$}_{n,t} = -(n-1)y^{\$}_{n-1,t} + ny^{\$}_{n,t}$ and $r^{TIPS}_{n,t} = -(n-1)y^{TIPS}_{n-1,t} + ny^{TIPS}_{n,t} + \pi_t$. We obtain continuously compounded 10-year zero-coupon yields from Gürkaynak, Sack, and Wright (2007, 2010). We report average excess real bond and breakeven log returns plus one-half times the log excess return variance. Excess returns and volatilities are in annualized percent. Our sample period is from 2001Q2 until 2019Q2, except for TIPS data which begins in 2003Q1. Model moments follows the same procedures as above on simulated data and are averaged over 2 simulations of length 10000.

Table 3: Empirical High-Frequency Stock Returns on FOMC Dates

	Dependent variable:			
	S&P 500 Return			10Y Breakeven
	(1)	(2)	(3)	(4)
FF Shock	-4.89^{***}		-4.11^{***}	-0.15
	(1.64)		(1.50)	(0.11)
10Y Breakeven		5.90^{**}	5.05^{*}	
		(2.54)	(2.60)	
Constant	0.07	0.06	0.05	0.004
	(0.05)	(0.06)	(0.06)	(0.003)
Observations	146	146	146	146
R^2	0.08	0.09	0.14	0.03
Adjusted R^2	0.07	0.08	0.13	0.03

Note: Columns (1) to (3) show regressions of the form: $r_t^{\delta,FOMC} = b_0 + b_1\Delta^{FOMC}i_t + b_2\Delta^{FOMC}b_{10,t} + \varepsilon_t$. $\Delta^{FOMC}i_{n,t}$ is the change in the Federal Funds rate in the one hour around FOMC announcements and $\Delta^{FOMC}b_{10,t}$ is the daily change in the 10-year breakeven rate, defined as the difference between 10-year nominal and 10-year real bond yields. We include these variables separately in columns (1) and (2), and jointly in column (3). The data on Federal Fund rate surprises is from Gorodnichenko and Weber (2016), breakeven rate changes are constructed using the data of Gürkaynak, Sack, and Wright (2007) and Gürkaynak, Sack, and Wright (2010), and one hour S&P 500 returns are from TAQ data. Column (4) reports a regression of the form $\Delta^{FOMC}b_{10,t} = b_0 + b_1\Delta^{FOMC}b_{n,t} + \varepsilon_t$. Our sample consists of scheduled FOMC days from January 2001 up to March 2019. Heteroskedasticity adjusted standard errors are reported in parentheses below the estimates. *p<0.1; **p<0.05; ***p<0.01

Table 4: Model High-Frequency Stock Returns around Monetary Policy News

	Dependent variable:				
	S&P 500 Return				
	Data	Overall		Risk Premium	
	(1)	(2)	(3)	(4)	(5)
FF Shock	-4.11^{***}	-5.27	-5.35	-2.54	-2.58
	(1.50)				
10Y Breakeven	5.05^{*}	5.89		2.70	
	(2.50)				
10Y Breakeven RN			5.96		2.73

Note: This table compares the asset price reactions around monetary policy news in the model and in the data. Column (1) repeats the empirical estimates from Table 3, column (3). Column (2) estimates the analogous regression on model simulated data, assuming that FOMC dates are subject to uncorrelated long-term and short-term monetary policy shocks. The standard deviations of the ST and LT monetary policy shocks on FOMC dates are set to $\sigma_{ST}^{FOMC} = 4.3bps$ and $\sigma_{LT}^{FOMC} = 3.3bps$ to match the volatilities of one-hour Fed Funds surprises and daily breakeven changes on FOMC dates in the data. Column (3) uses the risk neutral component of the 10-year breakeven change on the right-hand-side instead. Columns (4) and (5) report model regressions, with the component of stock returns due to time-varying risk premia as the left-hand-side variable. For details of model FOMC asset prices see Section 3.6. Risk neutral asset prices are the asset prices that would obtain under a risk neutral investor taking macroeconomic dynamics as given. The risk premium component of stock returns is the difference between the overall return minus the risk neutral return. Heteroskedasticity adjusted standard errors are reported in parentheses below the empirical estimates. *p<0.1; **p<0.05; ***p<0.01

Figure 1: Stocks and Bonds on FOMC Dates

Panel A: Stocks and the Federal Funds Rate

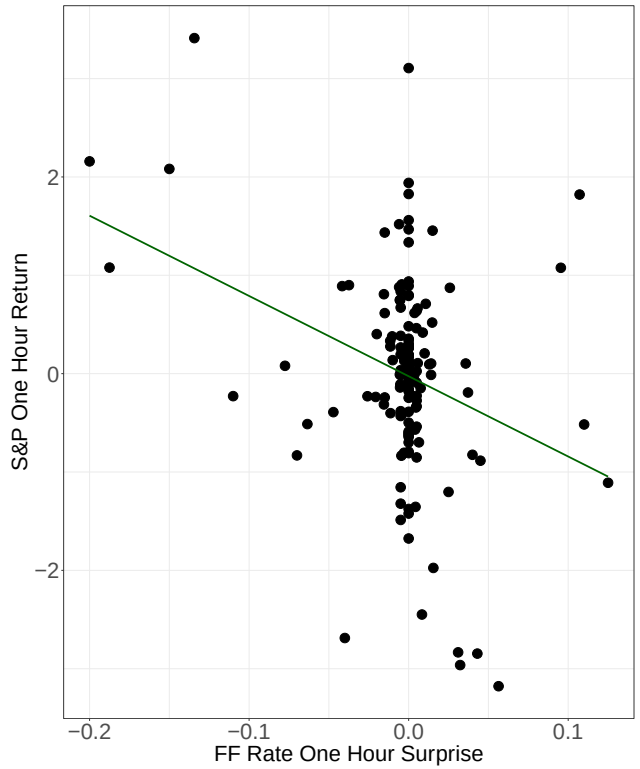

Panel B: Stocks and Breakeven Inflation

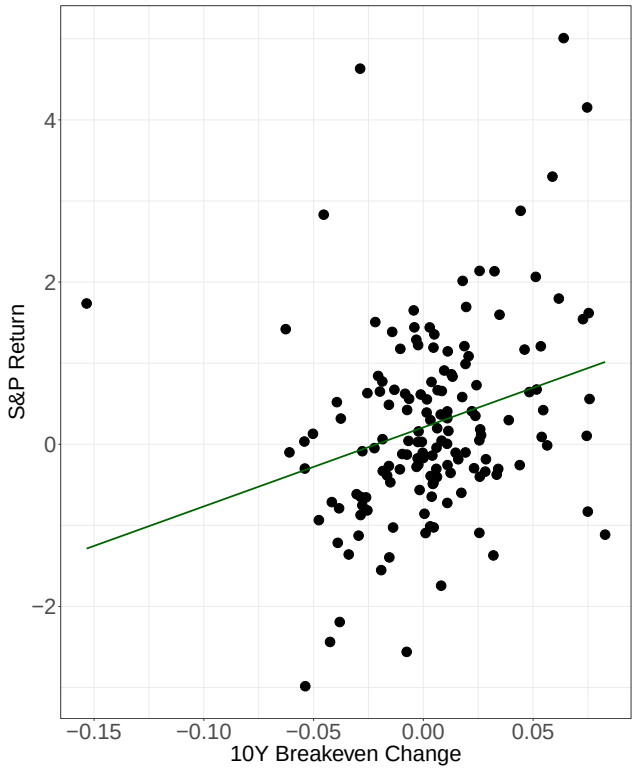

Note: Panel A shows the relationship of Federal Funds rates surprises in an hourly window around FOMC announcements from Gorodnichenko and Weber (2016) and S&P 500 returns in the same window constructed from TAQ data, where each data point corresponds to a FOMC meeting. Panel B shows the relationship of the daily change in 10-year breakeven inflation rates and daily S&P 500 returns where again each data point corresponds to a FOMC meeting. The breakeven rate is the difference between the 10-year nominal Treasury yield and 10-year TIPS yield from Gürkaynak, Sack, and Wright (2007, 2010). The green lines are linear regression best fit lines. The sample of scheduled FOMC days is from the start of 2001 until end of 2019. For Panels B and C, the data begins from the start of 2003 since this is when the TIPS data start.

Figure 2: Reduced Form Macro Impulse Responses

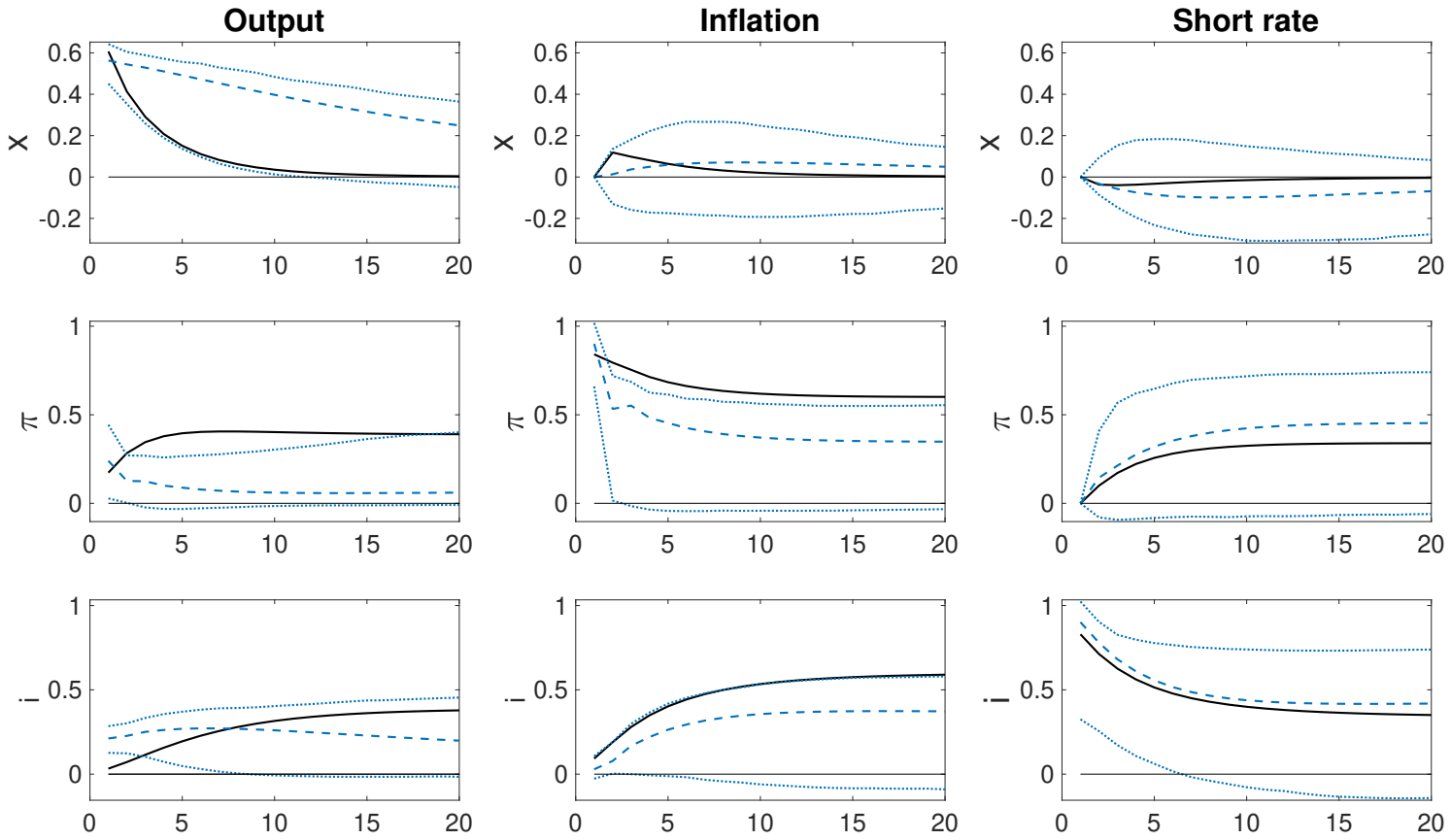

Note: This figure shows macroeconomic impulse responses to reduced-form output gap, inflation, and Federal Funds rate innovations in the model and in the data. The estimation of impulse responses is identical on actual and simulated data and is described in detail in Section 4.2. All impulses are one-standard deviation shocks and are orthogonalized so innovations to the Fed Funds rate do not contemporaneously affect inflation or the output gap, and inflation innovations do not enter into the same period output gap. The first row shows the response of output in percent, the second row shows the response of inflation in annualized percent. The third row shows the response of the Federal Funds rate in annualized percent. The horizontal axis of each panel shows the number of quarters after the shock.

Figure 3: Structural Macro Impulse Responses

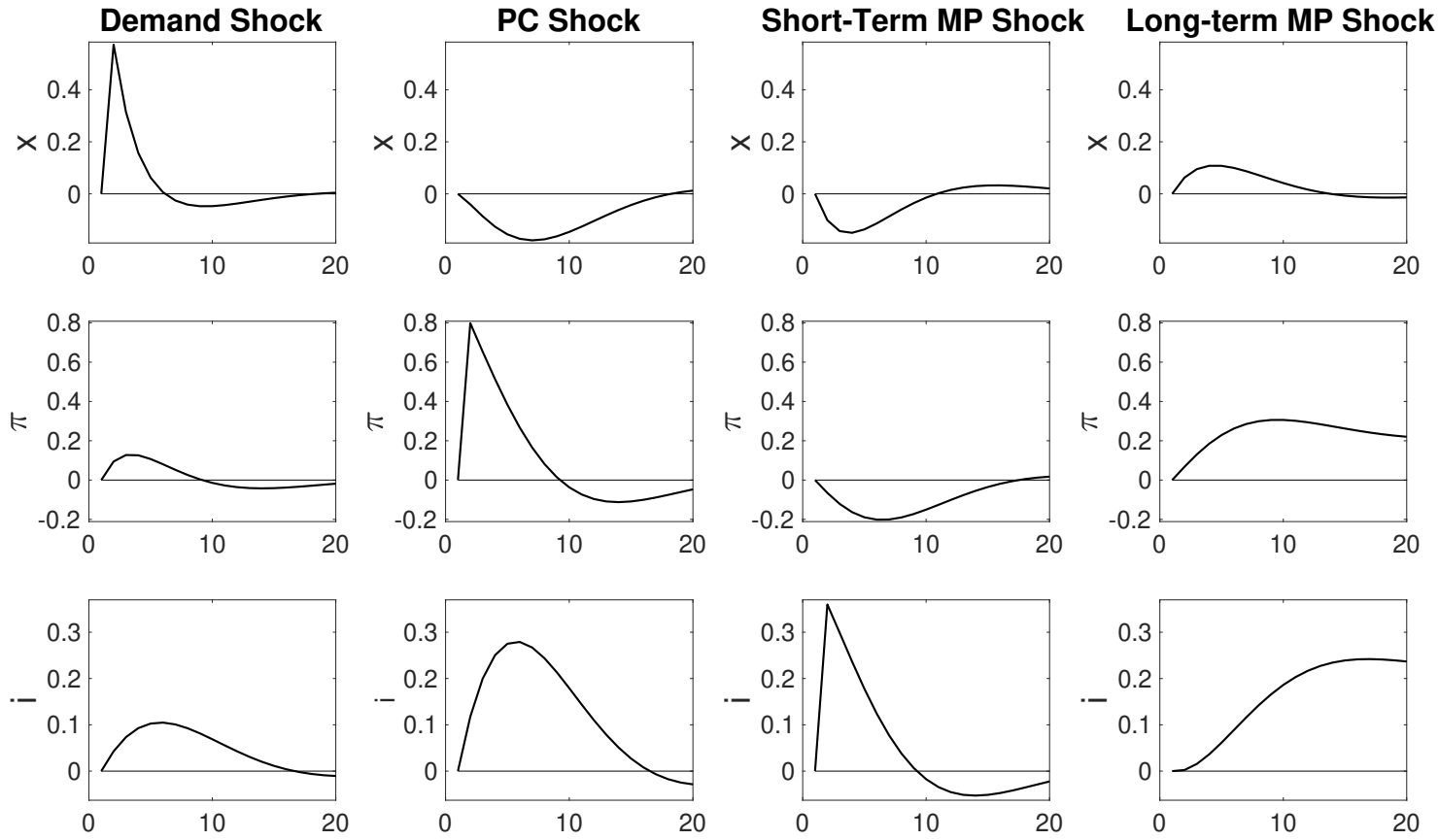

Note: Each column of this figure shows the macroeconomic impulse responses to one of the structural shocks, namely the demand shock, the Phillips Curve (PC) shock, the short-term monetary policy shock, and the long-term monetary policy shock. All impulses are one-standard deviation shocks. The first row shows the response of the output gap in percent, the second row shows the response of inflation in annualized percent. The third row shows the response of the Federal Funds rate in annualized percent. The horizontal axis of each panel shows the number of quarters after the shock.

Figure 4: Structural Asset Price Impulse Responses

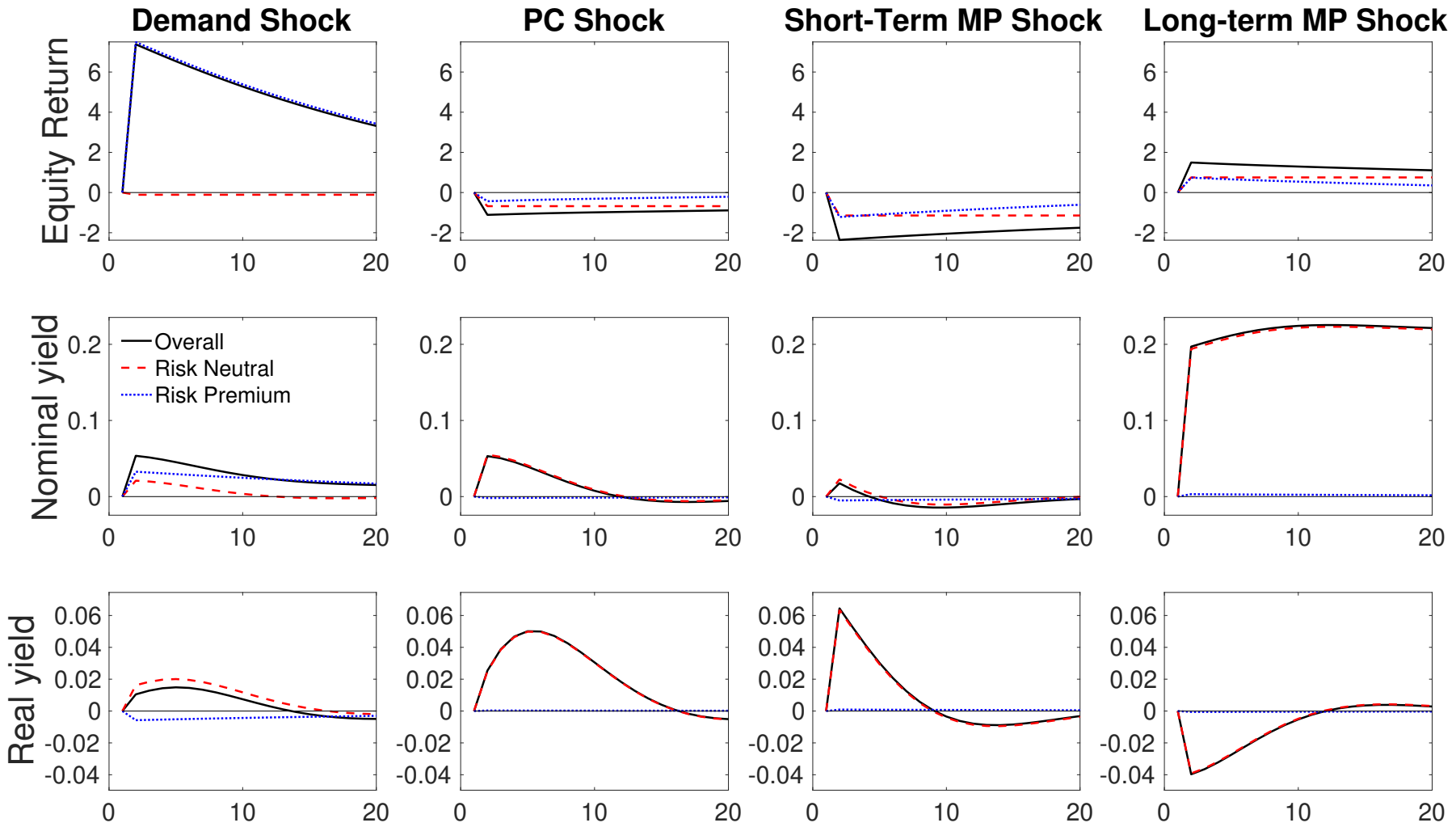

Note: Each column of this figure shows the impulse responses of asset prices to one of the structural shocks, namely the demand shock, the Phillips Curve (PC) shock, the short-term monetary policy shock, and the long-term monetary policy shock. All impulses are one-standard deviation shocks. The first row shows the response of unexpected equity returns in percent, the second row shows the response of nominal yield in annualized percent. The third row shows the response of the real yield in annualized percent. The horizontal axis of each panel shows the number of quarters after the shock. Responses are decomposed into the risk neutral component, which is computed as if assets were priced by a risk neutral agent, and the risk premium component. The risk neutral and risk premium components add up to the total response. Unexpected equity returns are computed subtracting from each quarter's return the steady state equity return in the absence of shocks.

Figure 5: State-Dependence of Model High-Frequency Stock Returns

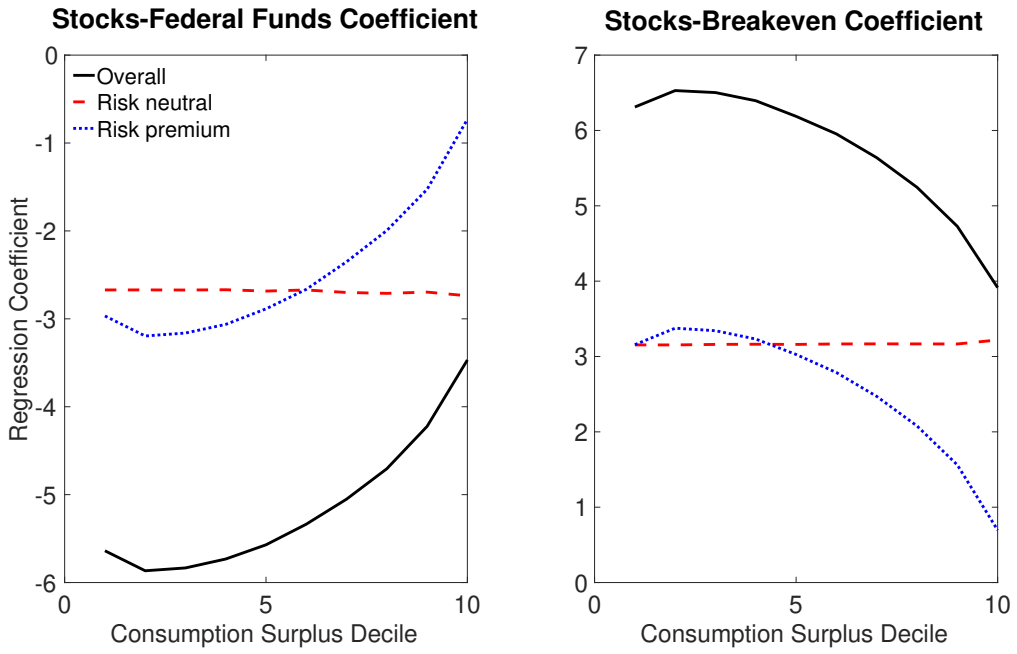

Note: This figure shows model regressions of the same form as in Tables 3 and 4 conditional on the model surplus consumption ratio: $r_t^{\delta,FOMC} = b_0 + b_1 \Delta^{FOMC} i_t + b_2 \Delta^{FOMC} b_{10,t} + \varepsilon_t$. The left panel plots the coefficient b_1 on the y-axis against surplus consumption deciles on the x-axis. The right panel plots the coefficient b_2 against surplus consumption deciles on the x-axis. Δ^{FOMC} is the change in the short term interest rate around the FOMC date, $\Delta^{FOMC} b_{10,t}$ is the change in the breakeven rate around in the same time period and $r_t^{\delta,FOMC}$ is the equity return. The simulated data is split into ten sub samples according to the deciles of the surplus consumption ration $\hat{s}$ so a lower decile corresponds higher effective risk aversion. We plot the coefficients obtained by running the regression separately within each of these ten subsamples. Solid lines use overall equity returns as the left-hand-side variable, dashed lines use risk neutral stock returns, and dotted lines use the risk premium component of stock returns. Risk neutral and risk premium coefficients add up to the overall coefficient. For details of model FOMC asset prices see Section 3.6 and for details of the decomposition into risk neutral and risk premium returns see Table 4. The results are obtained by averaging over 5 model simulations of length 30000.

APPENDIX - FOR ONLINE PUBLICATION

Why Does the Fed Move Markets so Much? A Model of Monetary Policy and Time-Varying Risk Aversion

Carolin Pflueger and Gianluca Rinaldi[1]

September 2020

[1]Pflueger: University of Chicago, Harris School of Public Policy, NBER, and CEPR. Email cpflueger@uchicago.edu. Rinaldi: Harvard University. Email rinaldi@g.harvard.edu.

A Loglinear habit dynamics around steady state

This section derives the loglinear dynamics of the habit stock using a first order approximation around the steady state $S_t = \bar{S}$. We write log habit h_t as a distributed lag of moments of consumption, the habit shock $\varepsilon_{s,t}$, and the output gap, which also equals the deviation of log consumption from the frictionless level. This loglinear expansion therefore implies that we can broadly view habit as a function of (lags of) consumption moments, and the shock $\varepsilon_{s,t}$, which for this reason we refer to as a "habit shock".

In the paper, we model how habit adjusts to consumption implicitly by modeling the evolution of the log surplus consumption ratio. In order to solve for log habit we need an approximate relation between log habit, log consumption, and the log surplus consumption ratio. Defining $\hat{s}_t = s_t - \bar{s}$, we develop a first-order Taylor expansion of $\hat{s}_t$ in terms of $c_t - h_t$. We take the first derivative of $\hat{s}_t$ with respect to $c_t - h_t$:

$$\frac{d\hat{s}_t}{d(c_t - h_t)} = \frac{d}{d(c_t - h_t)} \left(\log \left(\frac{1 - exp(-(c_t - h_t))}{\bar{S}} \right) \right), \tag{A1}$$

$$= \frac{\bar{S}}{1 - exp(-(c_t - h_t))} \frac{exp(-(c_t - h_t))}{\bar{S}}, \tag{A2}$$

$$= -\left(1 - \frac{1}{S_t}\right), \tag{A3}$$

so at the steady state this first derivative equals:

$$\left.\frac{d\hat{s}_t}{d(c_t - h_t)}\right|_{S_t = \bar{S}} = -\left(1 - \frac{1}{\bar{S}}\right). \tag{A4}$$

The first order Taylor expansion for $\hat{s}_t$ in terms of $c_t - h_t$ around the steady-state therefore equals (up to constant):

$$\hat{s}_t \approx \left(1 - \frac{1}{\bar{S}}\right)(h_t - c_t), \tag{A5}$$

or

$$h_t \approx c_t + \frac{\hat{s}_t}{1 - \frac{1}{\bar{S}}}. \tag{A6}$$

The relation (A6) is approximate rather than exact because we ignore second- and higher-order terms in $(c_t - h_t)$. Further approximating $\lambda(s_t) \approx \lambda(\bar{s}) = \frac{1}{\bar{S}} - 1$, the approximate dynamics for $\hat{s}_t$ near the steady state are given by:

$$\hat{s}_{t+1} \approx \theta_0 \hat{s}_t + \theta_1 x_t + \theta_2 x_{t-1} + \varepsilon_{s,t} + \left(\frac{1}{\bar{S}} - 1\right) \varepsilon_{c,t+1}. \tag{A7}$$

Combining (A6) with (A7) gives the approximate dynamics for log habit:

$$h_{t+1} \approx c_{t+1} + \frac{1}{1-\frac{1}{\bar{S}}}\hat{s}_{t+1}, \tag{A8}$$

$$\approx c_{t+1} + \frac{1}{1-\frac{1}{\bar{S}}}\left(\theta_0\hat{s}_t + \theta_1 x_t + \theta_2 x_{t-1} + \varepsilon_{s,t} + \left(\frac{1}{\bar{S}} - 1\right)\varepsilon_{c,t+1}\right), \tag{A9}$$

$$\approx c_{t+1} - \varepsilon_{c,t+1} + \theta_0\left(h_t - c_t\right) - \frac{\theta_1}{\frac{1}{\bar{S}}-1}x_t - \frac{\theta_2}{\frac{1}{\bar{S}}-1}x_{t-1} - \frac{1}{\frac{1}{\bar{S}}-1}\varepsilon_{s,t}, \tag{A10}$$

$$\approx \theta_0 h_t + (1-\theta_0)c_t + E_t\Delta c_{t+1} - \frac{\theta_1 x_t + \theta_2 x_{t-1}}{\frac{1}{\bar{S}}-1} - \frac{1}{\frac{1}{\bar{S}}-1}\varepsilon_{s,t}, \tag{A11}$$

where we use $\Delta c_{t+1} = c_{t+1} - c_t$ to denote the change in log consumption from time t to time $t+1$. We now iterate (A11) to obtain:

$$h_{t+1} \approx \sum_{j=0}^{\infty}\theta_0^j\left((1-\theta_0)c_{t-j} + E_{t-j}\Delta c_{t-j+1} - \frac{1}{\frac{1}{\bar{S}}-1}\varepsilon_{s,t-j} - \frac{\theta_1 x_{t-j} + \theta_2 x_{t-j-1}}{\frac{1}{\bar{S}}-1}\right), \tag{A12}$$

$$\approx (1-\theta_0)\sum_{j=0}^{\infty}\theta_0^j c_{t-j} + \sum_{j=0}^{\infty}\theta_0^j E_{t-j}\Delta c_{t-j+1} - \frac{1}{\frac{1}{\bar{S}}-1}\sum_{j=0}^{\infty}\theta_0^j\varepsilon_{s,t-j} - \frac{\theta_1}{\frac{1}{\bar{S}}-1}x_t \tag{A13}$$

$$-\frac{\theta_0\theta_1 + \theta_2}{\frac{1}{\bar{S}}-1}\sum_{j=0}^{\infty}\theta_0^j x_{t-j-1}. \tag{A14}$$

The expansion (A14) shows that approximate log habit depends on lagged moments of consumption, the output gap, and the habit shock. The resource constraint implies that output equals consumption, so the output gap equals the deviation of log consumption relative to a frictionless level.

In order to understand the compounded dependence of habit on the first and second lags of consumption, we substitute in for x_t from equation (25) in the main paper:

$$h_{t+1} \approx (1-\theta_0)\sum_{j=0}^{\infty}\theta_0^j c_{t-j} + \sum_{j=0}^{\infty}\theta_0^j E_{t-j}\Delta c_{t-j+1} - \frac{1}{\frac{1}{\bar{S}}-1}\sum_{j=0}^{\infty}\theta_0^j\varepsilon_{s,t-j} \tag{A15}$$

$$-\frac{\theta_1}{\frac{1}{\bar{S}}-1}\left(c_t - (1-\phi)\sum_{i=0}^{\infty}\phi^i c_{t-1-i} - \sum_{i=0}^{\infty}\phi^i\Delta a_{t-i}\right) \tag{A16}$$

$$-\frac{\theta_0\theta_1 + \theta_2}{\frac{1}{\bar{S}}-1}\sum_{j=0}^{\infty}\theta_0^j\left(c_{t-j-1} - (1-\phi)\sum_{i=0}^{\infty}\phi^i c_{t-j-2-i} - \sum_{i=0}^{\infty}\phi^i\Delta a_{t-i-1}\right). \tag{A17}$$

The Campbell and Cochrane (1999) case corresponds to $\theta_1 = \theta_2 = 0$ and constant expected consumption growth. In that case, expression (A17) shows that log habit is approximately an exponentially-weighted moving average of lagged log consumption with exponential parameter θ_0.

Our estimated model has $\theta_1 < 0$ and $\theta_2 > 0$, which allows us to generate hump-shaped output responses to monetary policy shocks that have been documented in macroeconomic data. Because $\frac{1}{\frac{1}{\bar{S}}-1} > 0$ and $1-\phi$ is close to zero, a negative value for θ_1 raises the sensitivity of habit to the first two lags of consumption, while a positive value for θ_2 lowers the sensitivity of habit with respect to the second lag of consumption. Our model

uses $-\theta_1 > 0$, and $\theta_1(1-\phi) - (\theta_0\theta_1 + \theta_2) = 0$ (which is the condition ensuring that the forward- and backward-looking coefficients in the log-linear macro Euler equation sum to one). Equation (A17) then implies that habit loads more on the first lag of consumption than in the Campbell-Cochrane case, but the loading onto the second consumption lag is unchanged.

B Proof of Phillips Curve

The derivation of the log-linearized Phillips curve is tedious, but almost all the steps in our derivation are standard. Our asset pricing habit preferences potentially enter in two places. This section shows that the log-linearized Phillips curve is invariant to both of these channels for the following two reasons:

1. Firms' real marginal cost depends on the real wage, which depends on preferences. The log-linearized Phillips curve is invariant to this channel, because we separate the intertemporal consumption-savings decision and the intratemporal labor-leisure choice as in Greenwood, Hercowitz, and Huffman (1988). We therefore obtain a standard functional form for log-linearized real marginal cost that does not depend on habit or surplus consumption.

2. The SDF enters into firms' first-order condition for the optimal price-setting decision. The log-linearized Phillips curve is invariant to this channel, because up to first-order our SDF is standard and second-order terms drop out of the log-linearized first-order condition, leading to a standard log-linearized Phillips curve.

We log linearize inflation around its random walk component v_t^* and output and labor around the steady-state with $\bar{Y}_t = A_t \bar{L}^{1-\tau}$ and $\bar{L}$ the labor supply consistent with steady-state markups when prices are flexible. We use bars to denote steady-state values and hats to denote log deviations from this steady-state. We use lower-case letters to denote logs.

B.1 Marginal Cost of Production and Steady-State

The New Keynesian Phillips curve links inflation to the marginal cost of production. By linking the marginal cost of production to the output gap, one then obtains a relationship between inflation and output. It is therefore important to check that our asset pricing preferences give rise to a standard log-linearized expression for the *real marginal cost* of producing another unit of output. In this section, we show that log deviation of marginal cost from steady-state takes the form:

$$\hat{mc}_{i,t} \quad = \quad a_0 \hat{y}_t - a_1 \left(p_{i,t} - p_t \right), \tag{A18}$$

i.e. it increases in the log deviation of output from the steady state, and decreases in the log own-firm price deviation from the log aggregate price level where both a_0 and a_1 are positive constants.

The labor-leisure trade-off implies that the real wage paid by firms producing good i equals:

$$W_{i,t} = \left(\frac{dU}{dC_t}\right) / \left(\frac{dU}{dL_{i,t}}\right) = A_t \left(1 - L_{i,t}\right)^{-\chi}. \tag{A19}$$

The total cost of producing a quantity $Y_{i,t}$ of good i equals:

$$Cost(Y_{i,t}) = W_{i,t} \left(\frac{Y_{i,t}}{A_t}\right)^{1/(1-\tau)} \tag{A20}$$

Taking the derivative with respect to $Y_{i,t}$ gives the marginal cost of supplying good i:

$$MC(Y_{i,t}) = \frac{1}{1-\tau} \frac{W_{i,t}}{A_t} \left(\frac{Y_{i,t}}{A_t}\right)^{\frac{\tau}{1-\tau}}, \tag{A21}$$

$$= \frac{1}{1-\tau} \left(1 - \left(\frac{Y_{i,t}}{A_t}\right)^{1/(1-\tau)}\right)^{-\chi} \left(\frac{Y_{i,t}}{A_t}\right)^{\frac{\tau}{1-\tau}}. \tag{A22}$$

Note that here we have assumed that the producer is a wage taker following Woodford (2003, p.148). We define the steady-state labor supply $\bar{L}$ to be the amount of labor supplied if markups are equal to the steady-state value $\bar{\mu} = \frac{\theta}{1-\theta}$, and all firms charge the same price. From (A22), we see that $\bar{L}$ must be the solution to

$$\bar{\mu}^{-1} = \frac{1}{1-\tau} \left(1 - \bar{L}\right)^{-\chi} \bar{L}^{\frac{\tau}{1-\tau}}. \tag{A23}$$

We log-linearize around the steady-state output:

$$\bar{Y}_t = A_t \bar{L}^{1-\tau}. \tag{A24}$$

Log-linearizing the real wage around the flexible-wage steady-state gives:

$$\hat{w}_{i,t} = \chi \frac{\bar{L}}{1-\bar{L}} \hat{l}_{i,t}, \tag{A25}$$

$$= \eta \hat{l}_{i,t}, \tag{A26}$$

where $\eta \equiv \chi \frac{\bar{L}}{1-\bar{L}}$ is the inverse of the steady-state Frisch elasticity of labor supply.

The elasticity of real marginal cost with respect to own-firm output near the steady-state equals:

$$\frac{dMC_{i,t}}{dY_{i,t}} \frac{Y_{i,t}}{MC_{i,t}} = \frac{\tau}{1-\tau} + \frac{\eta}{1-\tau}, \tag{A27}$$

$$\equiv \omega. \tag{A28}$$

Using θ to denote the steady-state value of θ_t, we then approximate firm i's deviation of

marginal cost from $\bar{\mu}^{-1}$ log-linearly:

$$\begin{aligned}\widehat{mc}_{i,t} &= \log\left(MC_{i,t}\right) - \log\left(\bar{\mu}^{-1}\right), \\ &= \omega\hat{y}_{i,t}, \qquad \text{(A29)} \\ &= \omega\hat{y}_t - \omega\theta(p_{i,t} - p_t), \qquad \text{(A30)}\end{aligned}$$

In the last step, we have used the demand function (15), log-linearized around the steady-state elasticity of substitution θ, to substitute $\hat{y}_{i,t} - \hat{y}_t = \theta\left(p_{i,t} - p_t\right)$. We hence obtain the functional form (A18) with $a_0 = \omega$ and $a_1 = \omega\theta$.

We can compare (A30) to the log real marginal cost obtained with standard preferences (e.g. Woodford, 2003), where the real wage is given by

$$W_t = \frac{L_{i,t}^{\eta}}{C_t^{-\gamma}}, \qquad \text{(A31)}$$

where η is the inverse of the Frisch elasticity of labor supply and γ is risk aversion. This expression is log-linearized to

$$\hat{w}_{i,t} = \gamma\hat{y}_t + \eta\hat{l}_{i,t}. \qquad \text{(A32)}$$

If instead, the log-linearized real wage took the form (A32), we would obtain the following log-linearized expression for the real marginal cost:

$$\widehat{mc}_{i,t} = \left(\omega + \gamma\right)\hat{y}_t - \omega\theta(p_{i,t} - p_t), \qquad \text{(A33)}$$

i.e. $a_0 = \omega + \gamma$ and $a_1 = \omega\theta$. Comparing expressions (A30) and (A33) shows that the log-linearized real wage in our model takes the same functional form as under standard preferences, which is why the log-linearized Phillips curve will also take the same form.

B.2 Discount Factor for Phillips Curve

We now derive the first-order approximation of the stochastic discount factor, which is needed for the derivation of the log-linearized Phillips curve. We show that because the first-order approximation of our stochastic discount factor is standard, our asset pricing preferences do not affect the log-linearized Phillips curve. In the steady-state, log consumption grows at rate g and s_t is constant at $\bar{s}$. The steady-state SDF for discounting time $t+j$ real cash flows at time t takes the standard form:

$$\bar{M}_{t,t+j} = \beta^j exp(-\gamma g j). \qquad \text{(A34)}$$

We denote log deviation of the SDF from this steady-state:

$$\hat{m}_{t,t+j} = \log\left(M_{t,t+j}/\bar{M}_{t,t+j}\right). \qquad \text{(A35)}$$

We will see that $\hat{m}_{t,t+j}$ drops out of the log-linearized price-setting first-order condition, which is why we can apply all the standard tools for deriving the log-linearized Phillips curve.

B.3 Price Level Law of Motion

The price level law of motion is standard. Because we have a unit root in inflation, we are careful to follow Cogley and Sbordone (2008) in log-linearizing inflation around its random-walk trend v_t^*. Log deviations in inflation from steady-state are defined as

$$\hat{\pi}_t \quad = \quad \pi_t - v_t^* \tag{A36}$$

and we log-linearize around $\hat{\pi}_t = 0$.

Since the probability of being able to adjust the price-level is independent and equal across firms, each firm that has the chance to re-set its price at time t chooses the same price $\tilde{P}_t$. The law of motion for the price level is

$$P_t^{-(\theta_t - 1)} \quad = \quad \alpha \left(P_{t-1} \frac{P_{t-1}}{P_{t-2}} \right)^{-(\theta_t - 1)} + (1 - \alpha) \tilde{P}_t^{-(\theta_t - 1)}. \tag{A37}$$

Dividing (A37) by $P_t^{-(\theta_t - 1)}$ gives

$$1 \quad = \quad \alpha exp\left((\theta_t - 1) \left(\hat{\pi}_t - \hat{\pi}_{t-1} + v_{LT,t} \right) \right) + (1 - \alpha) \left(\frac{\tilde{P}_t}{P_t} \right)^{-(\theta_t - 1)}. \tag{A38}$$

Using $\tilde{p}_t$ to denote log deviations of $\frac{\tilde{P}_t}{P}$ from one, the log-linearized law of motion becomes:

$$\tilde{p}_t \quad = \quad \frac{\alpha}{1 - \alpha} \left(\hat{\pi}_t - \hat{\pi}_{t-1} + v_{LT,t} \right). \tag{A39}$$

B.4 Price-Setting First-Order Condition

The firm's first-order condition for optimal price-setting is standard and follows Walsh (2017) while adding markup shocks and price indexing as in Cogley and Sbordone (2008) and Smets and Wouters (2007). A firm that re-sets its price at time t and does not get to re-set again during the next j periods indexes its price to the aggregate price increase from time $t-1$ to $t-1+j$ as in Smets and Wouters (2007). This means that such a firm has time $t+j$ price:

$$\tilde{P}_t \left(P_{t-1+j} / P_{t-1} \right). \tag{A40}$$

A firm that has the opportunity to re-set prices at time t chooses $\tilde{P}_t$ to maximize expected discounted profits conditional on the price still being in place:

$$\underset{\tilde{P}_t}{max} E_t \sum_{j=0}^{\infty} \alpha^j M_{t,t+j} Y_{t+j} \left(\left(\frac{\tilde{P}_t}{P_t} \frac{P_{t-1+j} / P_{t-1}}{P_{t+j} / P_t} \right)^{1 - \theta_{t+j}} - \frac{Cost\left(Y_{i,t+j} \right)}{Y_{t+j}} \right) \tag{A41}$$

the first-order condition:

$$\begin{aligned}
&\frac{\tilde{P}_t}{P_t} E_t \sum_{j=0}^{\infty} \alpha^j M_{t,t+j} Y_{t+j} (\theta_{t+j} - 1) \left(\frac{P_{t-1+j}/P_{t-1}}{P_{t+j}/P_t} \right)^{1-\theta_{t+j}} \\
= \; & E_t \sum_{j=0}^{\infty} \alpha^j M_{t,t+j} Y_{t+j} \theta_{t+j} \left(\frac{P_{t-1+j}/P_{t-1}}{P_{t+j}/P_t} \right)^{-\theta_{t+j}} MC_{i,t+j}. \qquad \text{(A42)}
\end{aligned}$$

B.5 Log-Linearization

We now log-linearize the first-order condition (A42) following the steps outlined in Walsh (2017), Chapter 8.7. In the flexible-price equilibrium with θ_t at its steady-state value θ, all firms charge the same price so $\overline{MC} = \bar{\mu}^{-1} = \frac{\theta-1}{\theta}$. Denoting the log of steady-state output by $\bar{y}_t \equiv \log \bar{Y}_t$ we have that

$$\begin{aligned}
\bar{y}_{t+1} - \bar{y}_t &= n_{t+1} - n_t + \Delta a_{t+1}, && \text{(A43)} \\
&= \nu + (1-\phi)(1-\tau) l_t + \Delta a_{t+1}, && \text{(A44)} \\
&= g + (1-\phi)\hat{y}_t + \Delta a_{t+1}, && \text{(A45)}
\end{aligned}$$

where the relationship between the steady-state growth rate g, ν, and ϕ is given by

$$g = \nu + (1-\phi)(1-\tau)\bar{l}. \qquad \text{(A46)}$$

To save on notation, we define:

$$\beta_g = \beta exp(-(\gamma - 1)g) \qquad \text{(A47)}$$

and

$$\tilde{p}_t = \log\left(\tilde{P}_t / P_t\right). \qquad \text{(A48)}$$

The log-linear expansion for the left-hand-side of (A42) conditional on $\bar{Y}_t$ becomes:

$$\begin{aligned}
&(1 + \tilde{p}_t) E_t \sum_{j=0}^{\infty} \Big[(\beta_g \alpha)^j \bar{Y}_t (1 + \hat{y}_{t+j})(1 + (\bar{y}_{t+j} - \bar{y}_t - g)) (1 + \hat{m}_{t,t+j}) \left(\theta(1 + \hat{\theta}_{t+j}) - 1 \right) \times \\
&\left(1 + (1 - \theta(1 + \hat{\theta}_{t+j})) \left(\hat{\pi}_t - \hat{\pi}_{t+j} + (v_{t+1}^{LT} + ... + v_{t+j}^{LT}) \right) \right) \Big]. \qquad \text{(A49)}
\end{aligned}$$

Dropping second-order terms and collecting terms that are independent of j gives

$$\begin{aligned}
&\frac{\bar{Y}_t(\theta - 1)}{1 - \beta_g \alpha} + \frac{\bar{Y}_t \tilde{p}_t (\theta - 1)}{1 - \beta_g \alpha} \\
&+ \bar{Y}_t(\theta - 1) E_t \sum_{j=0}^{\infty} (\beta_g \alpha)^j \left(\hat{y}_{t+j} + (\bar{y}_{t+j} - \bar{y}_t - g) + \hat{m}_{t,t+j} + \bar{\mu} \hat{\theta}_{t+j} + (1 - \theta)(\hat{\pi}_t - \hat{\pi}_{t+j}) \right). \qquad \text{(A50)}
\end{aligned}$$

Next, we approximate the right-hand-side of (A42) log-linearly. This gives

$$E_t \sum_{j=0}^{\infty} \Big[(\beta_g \alpha)^j \bar{Y}_t (1+\hat{y}_{t+j})(1+(\bar{y}_{t+j}-\bar{y}_t-g))\,(1+\hat{m}_{t,t+j})\,\theta(1+\hat{\theta}_{t+j})\times$$
$$\left(1-\theta(1+\hat{\theta}_{t+j})\left(\hat{\pi}_t-\hat{\pi}_{t+j}+(v_{t+1}^{LT}+...+v_{t+j}^{LT})\right)\right)\overline{MC}(1+\widehat{mc}_{t+j})\Big]. \tag{A51}$$

Next, we use $\theta\overline{MC}=\theta-1$, note that $E_t v_{t+k}^{LT}=0$ for $k>0$, substitute in (A30), and drop second-order terms:

$$\frac{\bar{Y}_t(\theta-1)}{1-\beta_g\alpha}+\bar{Y}_t(\theta-1)E_t\sum_{j=0}^{\infty}(\beta_g\alpha)^j\left(\hat{y}_{t+j}+(\bar{y}_{t+j}-\bar{y}_t-g)+\hat{m}_{t,t+j}+\hat{\theta}_{t+j}\right)$$
$$+\bar{Y}_t(\theta-1)E_t\sum_{j=0}^{\infty}(\beta_g\alpha)^j\left(-\theta\left(\hat{\pi}_t-\hat{\pi}_{t+j}\right)+\widehat{mc}_{t+j}\right), \tag{A52}$$
$$=\frac{\bar{Y}_t(\theta-1)}{1-\beta_g\alpha}+\bar{Y}_t(\theta-1)E_t\sum_{j=0}^{\infty}(\beta_g\alpha)^j\left(\hat{y}_{t+j}+(\bar{y}_{t+j}-\bar{y}_t-g)+\hat{m}_{t,t+j}+\hat{\theta}_{t+j}\right)$$
$$+\bar{Y}_t(\theta-1)E_t\sum_{j=0}^{\infty}(\beta_g\alpha)^j\left(-\theta\left(\hat{\pi}_t-\hat{\pi}_{t+j}\right)+a_0\hat{y}_{t+j}\right)$$
$$-a_1\left(\frac{\bar{Y}_t(\theta-1)\tilde{p}_t}{1-\beta_g\alpha}+\bar{Y}_t(\theta-1)E_t\sum_{j=0}^{\infty}(\beta_g\alpha)^j\left(\hat{\pi}_t-\hat{\pi}_{t+j}\right)\right). \tag{A53}$$

Equating (A50) and (A53), cancelling common terms, and dividing by $\bar{Y}_t(\theta-1)$ gives

$$(1+a_1)\left(\frac{\tilde{p}_t}{1-\beta_g\alpha}+\frac{\hat{\pi}_t}{1-\beta_g\alpha}-E_t\sum_{j=0}^{\infty}(\beta_g\alpha)^j\hat{\pi}_{t+j}\right)$$
$$=E_t\sum_{j=0}^{\infty}(\beta_g\alpha)^j\left(a_0\hat{y}_{t+j}+\hat{\mu}_{t+j}\right), \tag{A54}$$

where the log deviation of the markup from steady-state is given by

$$\hat{\mu}_{t+j}=\frac{d\mu_{t+j}}{d\theta_{t+j}}\frac{\mu_{t+j}}{\theta_{t+j}}\hat{\theta}_{t+j}=\frac{1}{\theta-1}\hat{\theta}_{t+j}=(1-\bar{\mu})\,\hat{\theta}_{t+j}. \tag{A55}$$

Note in particular that $\hat{m}_{t,t+j}$ drops out of (A54). Because this is the main place where we differ from the standard New Keynesian model, this makes clear that our asset pricing preferences drop out of the log-linearized optimal price-setting decision.

B.6 Substituting out $\tilde{p}_t$

Next, we follow a number of standard steps (e.g. Walsh (2017)) to solve for $\hat{\pi}_t$. From equation (A54) we have:

$$\begin{aligned}
\tilde{p}_t + \hat{\pi}_t &= (1-\beta_g\alpha)E_t\sum_{j=0}^{\infty}(\beta_g\alpha)^j\left(\frac{a_0\hat{y}_{t+j}+\hat{\mu}_{t+j}}{1+a_1}+\hat{\pi}_{t+j}\right), && \text{(A56)}\\
&= \frac{1-\beta_g\alpha}{1+a_1}(a_0\hat{y}_t+\hat{\mu}_t)+(1-\beta_g\alpha)\hat{\pi}_t \\
&\quad +\beta_g\alpha(1-\beta_g\alpha)E_t\sum_{j=0}^{\infty}(\beta_g\alpha)^j\left(\frac{a_0\hat{y}_{t+1+j}+\hat{\mu}_{t+1+j}}{1+a_1}+\hat{\pi}_{t+1+j}\right), \\
&= \frac{1-\beta_g\alpha}{1+a_1}(a_0\hat{y}_t+\hat{\mu}_t)+(1-\beta_g\alpha)\hat{\pi}_t+\beta_g\alpha E_t\left(\tilde{p}_{t+1}+\hat{\pi}_{t+1}\right) && \text{(A57)}
\end{aligned}$$

This equation relates the optimal relative price to the current-period marginal cost, current-period optimal markup, and the next-period expected optimal relative price. Subtracting $\hat{\pi}_t$ from both sides gives

$$\tilde{p}_t = \frac{1-\beta_g\alpha}{1+a_1}(a_0\hat{y}_t+\hat{\mu}_t)-\beta_g\alpha\hat{\pi}_t+\beta_g\alpha E_t\hat{\pi}_{t+1}+\beta_g\alpha E_t\tilde{p}_{t+1}. \quad \text{(A58)}$$

Substituting in the log-linearized law of motion for inflation (A39) and multiplying by $\frac{1-\alpha}{\alpha}$ gives

$$\left(\hat{\pi}_t-\hat{\pi}_{t-1}+v_t^{LT}\right) = \frac{1-\alpha}{\alpha}\frac{1-\beta_g\alpha}{1+a_1}(a_0\hat{y}_t+\hat{\mu}_t)-\beta_g\hat{\pi}_t+\beta_g E_t\hat{\pi}_{t+1} \quad \text{(A59)}$$

Solving for $\hat{\pi}_t$ gives the New Keynesian Phillips Curve (ignoring constants)

$$\hat{\pi}_t = \frac{\beta_g}{1+\beta_g}E_t\hat{\pi}_{t+1}+\frac{1}{1+\beta_g}\hat{\pi}_{t-1}+\kappa\hat{y}_t+\frac{\kappa}{a_0}\hat{\mu}_t-\frac{1}{1+\beta_g}v_t^{LT}, \quad \text{(A60)}$$

where the Phillips curve slope coefficient on $\hat{y}_t$ equals

$$\kappa = \frac{1}{1+\beta_g}\frac{1-\alpha}{\alpha}(1-\beta_g\alpha)\frac{a_0}{1+a_1}. \quad \text{(A61)}$$

Finally, we use that (up to a constant)

$$\begin{aligned}
\hat{\mu}_t &= \frac{1}{1-\theta}\varepsilon_{\theta,t} && \text{(A62)}\\
x_t &= \hat{y}_t, && \text{(A63)}\\
a_0 &= \omega, && \text{(A64)}\\
a_1 &= \omega\theta, && \text{(A65)}
\end{aligned}$$

and add the unit root component v_t^* to both sides of (A60) to obtain the log-linearized New Keynesian Phillips curve (29) in the main paper.

Note that the Phillips curve slope κ is identical to Woodford(1999, p.342) with three

exceptions. First, β is replaced by β_g because we have equilibrium growth in our model. Second, the factor $\frac{1}{1+\beta_g}$ is new. This is due to indexing. Third, $a_0 = \omega$, whereas in Woodford (2003) the sensitivity of marginal cost with respect to aggregate log output is $\omega + \gamma$. This is due to our separation between the intertemporal consumption-savings trade-off and the intratemporal labor-leisure trade-off as in Greenwood, Hercowitz, and Huffman (1988). However, (Woodford (2003, p.341)) estimates a very small value for the curvature parameter from macroeconomic data of $\gamma = 0.16$, so the log-linearized Phillips curve in our model is not only qualitatively but also quantitatively in line with this prior work.

C Model Solution

C.1 Output gap and consumption relationships

With the assumption on the evolution of human capital (18), we can iterate to obtain

$$\begin{aligned} n_t &= \nu + n_{t-1} + (1-\phi)(1-\tau)l_{t-1}, && \text{(A66)} \\ &= \nu + n_{t-1} + (1-\phi)(y_{t-1} - a_{t-1}), && \text{(A67)} \\ &= \frac{\nu}{1-\phi} + (1-\phi)\sum_{j=0}^{\infty}\phi^j\left(y_{t-1-j} - a_{t-1-j}\right). && \text{(A68)} \end{aligned}$$

The deviation of output from the flexible-price equilibrium then equals (up to a constant):

$$\begin{aligned} x_t &= y_t - n_t - a_t, && \text{(A69)} \\ &= y_t - (1-\phi)\sum_{j=0}^{\infty}\phi^j\left(y_{t-1-j} - a_{t-1-j}\right) - a_t, && \text{(A70)} \\ &= c_t - (1-\phi)\sum_{j=0}^{\infty}\phi^j c_{t-1-j} - \sum_{j=0}^{\infty}\phi^j\Delta a_{t-j}, && \text{(A71)} \end{aligned}$$

i.e. equation (25) in the main paper. Because Δa_t is stationary and the geometric series ϕ^j has a finite sum, the deviation between the output gap x_t and stochastically detrended consumption is stationary. Consumption growth then takes the following simple form (up to a constant):

$$\begin{aligned} \Delta c_{t+1} &= (x_{t+1} + \sum_{j=0}^{\infty}\phi^j\Delta a_{t+1-j}) - \phi(x_t - \sum_{j=0}^{\infty}\phi^j\Delta a_{t-j}), && \text{(A72)} \\ &= x_{t+1} - \phi x_t + \Delta a_{t+1}, && \text{(A73)} \end{aligned}$$

i.e. equation (26) in the main paper.

C.2 Deriving the macro Euler equation

With the updating equation for log consumption growth (A73), the asset pricing Euler equation for the one-period real risk-free rate is given by:

$$\begin{aligned} r_t &= \gamma E_t \Delta c_{t+1} + \gamma E_t \Delta \hat{s}_{t+1} - \frac{\gamma^2}{2}\left(1+\lambda(s_t)\right)^2 \sigma_c^2, && \text{(A74)} \\ &= \gamma E_t \Delta c_{t+1} + \gamma(\theta_0 - 1)\hat{s}_t + \gamma\theta_1 x_t + \gamma\theta_2 x_{t-1} + \gamma\varepsilon_{s,t} - \frac{\gamma^2}{2}\left(1+\lambda(s_t)\right)^2 \sigma_c^2, && \text{(A75)} \\ &= \gamma \Delta a_{t+1} + \gamma E_t x_{t+1} - \gamma\phi x_t + \gamma(\theta_0 - 1)\hat{s}_t + \gamma\theta_1 x_t + \gamma\theta_2 x_{t-1} + \gamma\varepsilon_{s,t} - \frac{\gamma^2}{2}\left(1+\lambda(s_t)\right)^2 \sigma_c^2 \end{aligned}$$

The sensitivity function has just the right form so that surplus consumption $\hat{s}_t$ drops out and (up to a constant):

$$r_t = \gamma \Delta a_{t+1} + \gamma E_t x_{t+1} - \gamma\phi x_t + \gamma\theta_1 x_t + \gamma\theta_2 x_{t-1} + \gamma\varepsilon_{s,t} \quad \text{(A76)}$$

Rearranging and continuing to ignore constants gives:

$$x_t = \frac{1}{\phi - \theta_1} E_t x_{t+1} + \frac{\theta_2}{\phi - \theta_1} x_{t-1} - \frac{1}{\gamma(\phi - \theta_1)}\left(r_t - \gamma \Delta a_{t+1}\right) + \frac{1}{\phi - \theta_1}\varepsilon_{s,t}. \quad \text{(A77)}$$

With the definition of the growth frictionless rate (20), this gives the log-linear Euler equation (27) in the main paper. Note that we have not made any approximations in the derivation of (27).

C.3 Solving for macroeconomic dynamics

We want to find a solution of the form

$$Y_t = BY_{t-1} + \Sigma v_t, \quad \text{(A78)}$$

where the matrix B is $[3 \times 3]$, the matrix Σ is $[3 \times 4]$, and the state vector Y_t is defined in equation (30) in the main paper. Throughout, we use Σ_v to denote the (diagonal) variance-covariance matrix of the vector of shocks, v_t. Substituting in for predictable productivity growth from equation (19) in main paper into (A77), We collect the log-linear equations describing the macroeconomic equilibrium dynamics:

$$\begin{aligned} x_t &= f^x E_t x_{t+1} + \rho^x x_{t-1} - \psi\left(r_t - \gamma\rho^a r_t - \gamma\varepsilon_{s,t}\right), && \text{(A79)} \\ \pi_t &= f^\pi E_t \pi_{t+1} + \rho^\pi \pi_{t-1} + \kappa x_t + v_{\pi,t}, && \text{(A80)} \\ i^* &= \gamma^x x_t + \gamma^\pi \pi_t + (1-\gamma^\pi) v_t^*, && \text{(A81)} \\ i_t &= \rho^i i_{t-1} + (1-\rho^i) i_t^* + v_{ST,t}, && \text{(A82)} \\ v_t^* &= v_{t-1}^* + v_{LT,t} && \text{(A83)} \end{aligned}$$

Writing this in terms of the elements of Y_t and using that $v_{x,t} = \gamma\psi\varepsilon_{s,t}$ gives

$$\begin{aligned}
Y_{1,t} &= f^x E_t Y_{1,t+1} + \rho^x Y_{1,t-1} - \psi(1-\gamma\rho^a)\left(Y_{3,t} - E_t Y_{2,t+1}\right) + v_{x,t}, && \text{(A84)}\\
Y_{2,t} &= f^\pi E_t Y_{2,t+1} + \rho^\pi Y_{2,t-1} + \kappa Y_{1,t} + v_{\pi,t} - \rho^\pi v_{LT,t}, && \text{(A85)}\\
Y_{3,t} &= \rho^i Y_{3,t-1} + (1-\rho^i)\left(\gamma^x Y_{1,t} + \gamma^\pi Y_{2,t}\right) + v_{ST,t} - \rho^i v_{LT,t}, && \text{(A86)}\\
v_t^* &= v_{t-1}^* + v_{LT,t}. && \text{(A87)}
\end{aligned}$$

The same thing in matrix form:

$$0 = FE_tY_{t+1} + GY_t + HY_{t-1} + Mv_t,$$

where the matrices F, G and H are given by

$$\begin{aligned}
F &= \begin{bmatrix} f^x & \psi(1-\gamma\rho^a) & 0 \\ 0 & f^\pi & 0 \\ 0 & 0 & 0 \end{bmatrix},\\
G &= \begin{bmatrix} -1 & 0 & -\psi(1-\gamma\rho^a) \\ \kappa & -1 & 0 \\ (1-\rho^i)\gamma^x & (1-\rho^i)\gamma^\pi & -1 \end{bmatrix},\\
H &= \begin{bmatrix} \rho^x & 0 & 0 \\ 0 & \rho^\pi & 0 \\ 0 & 0 & \rho^i \end{bmatrix}.
\end{aligned}$$

The matrix M is $[3 \times 4]$ and equals:

$$M = \begin{bmatrix} 1 & 0 & 0 & 0 \\ 0 & 1 & 0 & -\rho^\pi \\ 0 & 0 & 1 & -\rho^i \end{bmatrix} \qquad \text{(A88)}$$

Following Uhlig (1999), we solve for the generalized eigenvectors and eigenvalues of the matrix Ξ with respect to the matrix Δ, where

$$\Xi = \begin{bmatrix} -G & -H \\ I_3 & 0_3 \end{bmatrix}, \qquad \text{(A89)}$$

$$\Delta = \begin{bmatrix} F & 0_3 \\ 0_3 & I_3 \end{bmatrix} \qquad \text{(A90)}$$

To obtain a solution, we then pick three generalized eigenvalues $\lambda_1, \lambda_2, \lambda_3$ with generalized eigenvectors $[\lambda z_1', z_1']'$, $[\lambda_2 z_2', z_2]'$, and $[\lambda_3 z_3', z_3']'$. We denote the diagonal matrix of these eigenvalues by $\Lambda = diag\left(\lambda_1, \lambda_2, \lambda_3\right)$, and the matrix of the lower $[3 \times 1]$ portion of the eigenvectors by $\Omega = [z_1, z_2, z_3]$. The corresponding solutions for B and Σ are then given by:

$$\begin{aligned}
B &= \Omega\Lambda\Omega^{-1}, && \text{(A91)}\\
\Sigma &= \left[FB + G\right]^{-1} M. && \text{(A92)}
\end{aligned}$$

In our empirical application, there exist exactly three generalized eigenvalues with absolute value less than one, and we pick the non-explosive solution corresponding to these three eigenvalues.

C.4 Rotated state vector

Our state space for solving for asset prices is five-dimensional: It consists of $\tilde{Z}_t$, which a scaled version of Y_t, the surplus consumption ratio relative to steady-state $\hat{s}_t$, and the lagged output gap x_{t-1}. The lagged output gap x_{t-1} is not actually needed as a state variable and we have verified that our numerical solutions for asset prices do not vary with x_{t-1}. Our code includes x_{t-1} as a state variable for legacy reasons.

We next describe the definition of $\tilde{Z}_t$. To simplify the numerical implementation of the asset pricing recursions, we require that shocks to the scaled state vector $\tilde{Z}_t$ are independent standard normal and that the first dimension of the scaled state vector is perfectly correlated with output gap innovations. This rotation facilitates the numerical analysis, because it is easier to integrate over independent random variables. Aligning the first dimension of the scaled state vector with output gap innovations (and hence surplus consumption innovations) helps, because it allows us to use a finer grid to integrate numerically over this crucial dimension over which asset prices are most non-linear.

If the scaled state vector equals $\tilde{Z}_t = AY_t$ for some invertible matrix A, the dynamics of $\tilde{Z}_t$ are given by:

$$\begin{aligned} \tilde{Z}_t &= AY_t, && \text{(A93)} \\ \tilde{Z}_{t+1} &= \underbrace{ABA^{-1}}_{\tilde{B}}\tilde{Z}_t + \underbrace{A\Sigma v_{t+1}}_{\epsilon_{t+1}}. && \text{(A94)} \end{aligned}$$

We hence want a matrix, A, such that

$$\begin{aligned} Var\left(\epsilon_{t+1}\right) &= A\Sigma\Sigma_v\Sigma' A', && \text{(A95)} \\ &= \begin{bmatrix} 1 & 0 & 0 \\ 0 & 1 & 0 \\ 0 & 0 & 1 \end{bmatrix}. && \text{(A96)} \end{aligned}$$

Finding such a matrix A should in general be possible, because the matrix M and therefore $\Sigma\Sigma_v\Sigma'$ hence generally have rank three. We require that the first dimension of ϵ_{t+1} is perfectly correlated with the consumption shock. We can therefore find the three rows of A using the following steps:

1. Set $A_1 = \frac{e_1}{\sqrt{e_1\Sigma\Sigma_v\Sigma' e_1'}}$.

2. We use the MATLAB function *null* to compute the null space of $A_1\Sigma\Sigma_v\Sigma'$. Let n_2 denote the first vector in $null\left(A_1\Sigma\Sigma_v\Sigma'\right)$. We then define the second row of A as the normalized version of n_2:

$$A_2 = \frac{n_2}{\sqrt{n_2\Sigma\Sigma_v\Sigma' n_2'}}. \quad \text{(A97)}$$

3. Let n_3 denote the first vector in $null\left(A_1\Sigma\Sigma_v\Sigma', A_2\Sigma\Sigma_v\Sigma'\right)$. We then define the third row of A as the normalized version of n_3:

$$A_3 = \frac{n_3}{\sqrt{n_3\Sigma\Sigma_v\Sigma' n_3'}}. \tag{A98}$$

It is then straightforward to verify that equation (A96) holds for

$$A = \begin{bmatrix} A_1 \\ A_2 \\ A_3 \end{bmatrix}. \tag{A99}$$

C.5 Asset pricing recursions

Before deriving the recursions for the numerical asset pricing computations, we derive a convenient form for the dynamics of the log surplus consumption ratio. We use e_i to denote a row vector with 1 in position i and zeros elsewhere. The matrix

$$\Sigma_M = e_1\Sigma \tag{A100}$$

denotes the loading of consumption innovations onto the vector of shocks v_t, where e_1 is a basis vector with a one in the first position and zeros everywhere else. The volatility of consumption surprises equals:

$$\sigma_c^2 = \Sigma_M\Sigma_v\Sigma_M'. \tag{A101}$$

To simplify notation, we define $\hat{s}_t$ as the log deviation of surplus consumption from its steady state. The dynamics of $\hat{s}_t$ are:

$$\hat{s}_t = s_t - \bar{s}, \tag{A102}$$
$$\hat{s}_t = \theta_0\hat{s}_{t-1} + \theta_1 x_{t-1} + \theta_2 x_{t-2} + \varepsilon_{s,t-1} + \lambda(\hat{s}_{t-1})\varepsilon_{c,t}, \tag{A103}$$

where with an abuse of notation we write:

$$\lambda(\hat{s}_t) = \lambda_0\sqrt{1-2\hat{s}_t} - 1, \hat{s}_t \leq s_{max} - \bar{s}, \tag{A104}$$
$$\lambda(\hat{s}_t) = 0, \hat{s}_t \geq s_{max} - \bar{s}. \tag{A105}$$

The steady-state surplus consumption sensitivity equals:

$$\lambda_0 = \frac{1}{\bar{S}}. \tag{A106}$$

In our calculations of asset prices, we repeatedly substitute out expected log SDF growth, which equals:

$$E_t\left[m_{t+1}\right] = \log\beta - \gamma E_t\Delta\hat{s}_{t+1} - \gamma E_t\Delta c_{t+1}, \tag{A107}$$
$$= -r_t - \frac{\gamma}{2}(1-\theta_0)(1-2\hat{s}_t). \tag{A108}$$

We often combine this with $r_t = \bar{r} + (e_3 - e_2 B) Z_t$ and $\hat{r}_t = (e_3 - e_2 B) Z_t$.

Including the constant, consumption growth is given by:

$$\begin{aligned} \Delta c_{t+1} &= g + x_{t+1} - \phi x_t + \Delta a_{t+1}, && \text{(A109)} \\ &= g + x_{t+1} - \phi x_t + \rho^a \hat{r}_t. && \text{(A110)} \end{aligned}$$

The steady state real short-term interest rate at $x_t = 0$ and $s_t = \bar{s}$ is the same as in Campbell and Cochrane (1999):

$$\bar{r} = \gamma g - \frac{1}{2}\gamma^2 \sigma_c^2 / \bar{S}^2 - log(\beta). \quad \text{(A111)}$$

The updating rule for the log surplus consumption ratio can then be written in terms of the state variables as:

$$\begin{aligned} \hat{s}_{t+1} &= \hat{s}_t + E_t \Delta \hat{s}_{t+1} + \lambda(\hat{s}_t)\varepsilon_{c,t+1}, && \text{(A112)} \\ &= \hat{s}_t - E_t \Delta \hat{c}_{t+1} + \frac{1}{\gamma}\left(\log\beta + \hat{r}_t + \bar{r} + \frac{\gamma}{2}(1-\theta_0)(1-2\hat{s}_t)\right) + \lambda(\hat{s}_t)\varepsilon_{c,t+1}, && \text{(A113)} \\ &= \theta_0 \hat{s}_t + \frac{1}{\gamma}(e_3 - e_2 B) A^{-1} \tilde{Z}_t - e_1 [B - \phi I] A^{-1} \tilde{Z}_t - \rho^a \hat{r}_t + \lambda(\hat{s}_t)\varepsilon_{c,t+1}, && \text{(A114)} \\ &= \theta_0 \hat{s}_t + \frac{1}{\gamma}(1 - \gamma\rho^a)(e_3 - e_2 B) A^{-1} \tilde{Z}_t - e_1 [B - \phi I] A^{-1} \tilde{Z}_t + \lambda(\hat{s}_t)\varepsilon_{c,t+1}, && \text{(A115)} \end{aligned}$$

C.5.1 Recursion for zero-coupon consumption claims

We now derive the recursion for zero-coupon consumption claims in terms of state variables $\tilde{Z}_t$, $\hat{s}_t$ and x_{t-1}. Let P^c_{nt}/C_t denote the price-dividend ratio of a zero-coupon claim on consumption at time $t+n$. The outline of our strategy here is that we first derive an analytic expression for the price-dividend ratio for P^c_{1t}/C_t. For $n \geq 1$ we guess and verify recursively that there exists a function $F_n(\tilde{Z}_t, \hat{s}_t, x_{t-1})$, such that

$$\frac{P^c_{nt}}{C_t} = F_n\left(\tilde{Z}_t, \hat{s}_t, x_{t-1}\right). \quad \text{(A116)}$$

The ex-dividend price-consumption ratio for a claim to all future consumption is then given by

$$\frac{P_t}{C_t} = F\left(\tilde{Z}_t, \hat{s}_t, x_{t-1}\right), \quad \text{(A117)}$$

where we define

$$F\left(\tilde{Z}_t, \hat{s}_t, x_{t-1}\right) = \sum_{n=1}^{\infty} F_n\left(\tilde{Z}_t, \hat{s}_t, x_{t-1}\right). \quad \text{(A118)}$$

We now derive the recursion of zero-coupon consumption claims in terms of state variables $\tilde{Z}_t$ and $\hat{s}_t$. The one-period zero coupon price-consumption ratio solves:

$$\frac{P^c_{1,t}}{C_t} = E_t\left[\frac{M_{t+1} C_{t+1}}{C_t}\right] \quad \text{(A119)}$$

We simplify

$$\frac{M_{t+1}C_{t+1}}{C_t} = \beta exp\left(E_t m_{t+1} + E_t \Delta c_{t+1} - \gamma(\hat{s}_{t+1} - E_t s_{t+1}) - (\gamma-1)(c_{t+1} - E_t c_{t+1})\right).$$

Using the notation $f_n = \log(F_n)$, this gives the log one-period price-consumption ratio as:

$$\begin{aligned} f_1\left(\tilde{Z}_t, \hat{s}_t, x_{t-1}\right) &= -r_t - \frac{\gamma}{2}(1-\theta_0)(1-2\hat{s}_t) + g + \Delta a_{t+1} + E_t x_{t+1} - \phi x_t \\ &\quad + \frac{1}{2}\left(\gamma\lambda(\hat{s}_t) + (\gamma-1)\right)^2 \sigma_c^2, \qquad \text{(A120)} \\ &= g + e_1\left[B - \phi I\right] A^{-1}\tilde{Z}_t + \frac{1}{2}\left(\gamma\lambda(\hat{s}_t) + (\gamma-1)\right)^2 \sigma_c^2 \\ &\quad - \bar{r} - (1-\rho^a)\left(e_3 - e_2 B\right) A^{-1}\tilde{Z}_t - \frac{\gamma}{2}(1-\theta_0)(1-2\hat{s}_t) \qquad \text{(A121)} \end{aligned}$$

Next, we solve for f_n, $n \geq 2$ iteratively. Note that:

$$\frac{P^c_{nt}}{C_t} = \mathbb{E}_t\left[\frac{M_{t+1}C_{t+1}}{C_t}\frac{P^c_{n-1,t+1}}{C_{t+1}}\right] = \mathbb{E}_t\left[\frac{M_{t+1}C_{t+1}}{C_t}F_{n-1}\left(\tilde{Z}_{t+1}, \hat{s}_{t+1}, x_t\right)\right] \qquad \text{(A122)}$$

This gives the following expression for f_n:

$$\begin{aligned} f_n(\tilde{Z}_t, \hat{s}_t, \hat{r}_{t-1}) &= \log\Big[\mathbb{E}_t\Big[\exp\Big(g + e_1[B-\phi I]A^{-1}\tilde{Z}_t \\ &\quad -\bar{r} - (1-\rho^a)(e_3 - e_2 B)A^{-1}\tilde{Z}_t - \frac{\gamma}{2}(1-\theta_0)(1-2\hat{s}_t) \\ &\quad -(\gamma(1+\lambda(\hat{s}_t)) - 1)\sigma_c\epsilon_{1,t+1} \\ &\quad + f_{n-1}(\tilde{Z}_{t+1}, \hat{s}_{t+1}, \hat{r}_t)\Big)\Big]\Big]. \qquad \text{(A123)} \end{aligned}$$

Here, $\epsilon_{1,t+1}$ denotes the first dimension of the shock ϵ_{t+1}.

C.5.2 Recursion for zero-coupon bond prices

We use $P^{\$}_{n,t}$ and $P_{n,t}$ to denote the prices of nominal and real n-period zero-coupon bonds. The strategy is to develop analytic expressions for one- and two-period bond prices. We then guess and verify recursively that the prices of real and nominal zero-coupon bonds with maturity $n \geq 2$ can be written in the following form:

$$\begin{aligned} P_{n,t} &= B_n(\tilde{Z}_t, \hat{s}_t, x_{t-1}), \qquad \text{(A124)} \\ P^{\$}_{n,t} &= exp(-n v^*_t) B^{\$}_n(\tilde{Z}_t, \hat{s}_t, x_{t-1}), \qquad \text{(A125)} \end{aligned}$$

where $B_n(\tilde{Z}_t, \hat{s}_t, x_{t-1})$ and $B^{\$}_n(\tilde{Z}_t, \hat{s}_t, x_{t-1})$ are functions of the state variables. As discussed in the main paper, we assume that the short-term nominal interest rate contains no risk premium, so the one-period log nominal interest rate equals $i_t = r_t + E_t\pi_{t+1}$. Taking account of the constants, one-period bond prices equal:

$$\begin{aligned} P^{\$}_{1,t} &= \exp(-Y_{3,t} - v^*_t - \bar{r}), \qquad \text{(A126)} \\ P_{1,t} &= \exp(-Y_{3,t} + \mathbb{E}_t Y_{2,t+1} - \bar{r}). \qquad \text{(A127)} \end{aligned}$$

We next solve for longer-term bond prices including risk premia. Substituting in (A126) into the bond-pricing recursion gives:

$$P^{\$}_{2,t} = \mathbb{E}_t\left[M_{t+1}P^{\$}_{1,t+1}\exp(-v^*_{t+1}-Y_{2,t+1})\right] \tag{A128}$$

$$= \mathbb{E}_t\left[M_{t+1}\exp(-Y_{3,t+1}-2v^*_{t+1}-Y_{2,t+1}-\bar{r})\right]. \tag{A129}$$

We can now verify that the two-period nominal bond price takes the form (A125):

$$B^{\$}_2(\tilde{Z}_t,\hat{s}_t,x_{t-1}) = \exp\left(E_t\left(m_{t+1}-Y_{3,t+1}-Y_{2,t+1}\right)-\bar{r}\right) \times\mathbb{E}_t\left[\exp\left(\left(-\gamma\left(\lambda(\hat{s}_t)+1\right)\Sigma_M-\underbrace{[(e_2+e_3)\Sigma+2e_4]}_{v_{\$}}\right)v_{t+1}\right)\right]. \tag{A130}$$

Here, we define the vector $v_{\$}$ to simplify notation. The random walk component of inflation v^*_t does not appear in (A130), because $B^{\$}_2$ is already scaled by $exp(-2v^*_t)$ by definition (A125). Taking logs, substituting out for $E_t m_{t+1}$, and using the definition for the sensitivity function $\lambda(\hat{s}_t)$, we get:

$$b^{\$}_2 = -e_3[I+B]A^{-1}\tilde{Z}_t+\frac{1}{2}v_{\$}\Sigma_v v_{\$}\prime +\gamma\left(\lambda(\hat{s}_t)+1\right)\Sigma_M\Sigma_v v'_{\$}-2\bar{r}. \tag{A131}$$

We similarly solve for two-period real bond prices in closed form:

$$P_{2,t} = \exp\left(E_t\left(m_{t+1}-Y_{3,t+1}+Y_{2,t+2}\right)-\bar{r}\right) \times\mathbb{E}_t\left[\exp\left((-\gamma(\lambda(\hat{s}_t)+1)\Sigma_M-\underbrace{(e_3-e_2B)\Sigma}_{v_r})v_{t+1}\right)\right] \tag{A132}$$

We define the vector v_r to simplify notation. Taking logs, substituting out for $E_t m_{t+1}$, and using the definition for $\lambda(\hat{s}_t)$ gives:

$$b_2(\tilde{Z}_t,\hat{s}_t,x_{t-1}) = -(e_3-e_2B)\left[I+B\right]A^{-1}\tilde{Z}_t+\frac{1}{2}v_r\Sigma_v v'_r+\gamma\left(\lambda(\hat{s}_t)+1\right)\Sigma_M\Sigma_v v'_r-2\bar{r}. \tag{A133}$$

For $n\geq 3$, we repeatedly substitute out for $E_t m_{t+1}$ to obtain the following recursion for real bond prices:

$$B_n(\tilde{Z}_t,\hat{s}_t,x_{t-1}) = \mathbb{E}_t\left[\exp\left(m_{t+1}+b_{n-1}(\tilde{Z}_{t+1},\hat{s}_{t+1},x_t)\right)\right]$$

$$= \mathbb{E}_t\left[\exp\left(-\bar{r}-(e_3-e_2B)A^{-1}\tilde{Z}_t-\frac{\gamma}{2}(1-\theta_0)(1-2\hat{s}_t)\right.\right.$$

$$\left.\left.-\gamma(1+\lambda(\hat{s}_t))\sigma_c\epsilon_{1,t+1}+b_{n-1}(\tilde{Z}_{t+1},\hat{s}_{t+1},x_t)\right)\right]. \tag{A134}$$

The recursion for nominal bond prices with $n \geq 3$ is similar. It is complicated by the fact that we need to integrate over long-term monetary policy shocks, which are not necessarily spanned by ϵ_{t+1}:

$$B_n^{\$}(\tilde{Z}_t, \hat{s}_t, x_{t-1}) \;=\; \mathbb{E}_t\left[\exp\left(m_{t+1} - Y_{2,t+1} - nv_{t+1}^{LT} + b_{n-1}^{\$}(\tilde{Z}_{t+1}, \hat{s}_{t+1}, x_t)\right)\right]. \quad \text{(A135)}$$

To reduce the number of dimensions along which we need to integrate numerically, we split v_{t+1}^{LT} into a component that is spanned by ϵ_{t+1} plus an orthogonal shock. This is useful because we can then use analytic expressions to integrate over the orthogonal component. We use the standard expression for conditional distributions of multivariate normal random variables. The distribution of v_{t+1}^{LT} conditional on ϵ_{t+1} is normal with:

$$v_{t+1}^{LT}\,|\epsilon_{t+1} \sim N\left(\underbrace{(A\Sigma\Sigma_v e_4')'}_{vec_*}\epsilon_{t+1}, \underbrace{(\sigma_{LT})^2 - (A\Sigma\Sigma_v e_4')'(A\Sigma\Sigma_v e_4')}_{\sigma_\perp^2}\right). \quad \text{(A136)}$$

We then write v_t^{LT} as the sum of two independent shocks:

$$v_{t+1}^{LT} \;=\; vec^*\epsilon_{t+1} + \epsilon_{t+1}^{\perp}, \quad \text{(A137)}$$

where $\epsilon_{t+1}^{\perp}$ is defined as

$$\epsilon_{t+1}^{\perp} \;:=\; v_{t+1}^{LT} - vec^*\epsilon_{t+1} \quad \text{(A138)}$$

We integrate analytically over $\epsilon_{t+1}^{\perp}$ in equation (A139):

$$\begin{aligned}
B_n^{\$}(\tilde{Z}_t, \hat{s}_t, x_{t-1}) &= \mathbb{E}_t\left[\exp\left(m_{t+1} - Y_{2,t+1} - nvec^*\epsilon_{t+1} + \frac{n^2}{2}(\sigma_\perp)^2 + b_{n-1}^{\$}(\tilde{Z}_{t+1}, \hat{s}_{t+1}, B^{\$}x_t)\right)\right], \\
&= \mathbb{E}_t\Bigg[\exp\Bigg(-\bar{r} - e_3A^{-1}\tilde{Z}_t - \frac{\gamma}{2}(1-\theta_0)(1-2\hat{s}_t) \\
&\quad -(\gamma(1+\lambda(\hat{s}_t))\sigma_c + \underbrace{e_2A^{-1}e_1'}_{vpi_1} + nvec^*e_1')\epsilon_{1,t+1} \\
&\quad -\left(\underbrace{e_2A^{-1}e_2'}_{vpi_2} + nvec^*e_2'\right)\epsilon_{2,t+1} \\
&\quad +\frac{n^2}{2}(\sigma_\perp)^2 + b_{n-1}^{\$}(\tilde{Z}_{t+1}, \hat{s}_{t+1}, x_t)\Bigg)\Bigg]. \quad \text{(A139)}
\end{aligned}$$

We define the vectors vpi_1 and vpi_2 as given above to avoid computing them repeatedly in our numerical algorithm.

C.5.3 Computing returns

The log return on the consumption claim equals:

$$r_{t+1}^c = \log\left(\frac{P_{t+1}^c + C_{t+1}}{P_t^c}\right), \tag{A140}$$

$$= \Delta c_{t+1} + \log\left(\frac{1 + \frac{P_{t+1}^c}{C_{t+1}}}{\frac{P_t^c}{C_t}}\right). \tag{A141}$$

Real and nominal log bond yields equal:

$$y_{n,t} = -\frac{1}{n} b_{n,t}, \tag{A142}$$

$$y_{n,t}^{\$} = -\frac{1}{n} b_{n,t}^{\$} + \pi_t^*. \tag{A143}$$

Real log bond returns equal:

$$r_{n,t+1} = b_{n-1,t+1} - b_{n,t}. \tag{A144}$$

Nominal log bond returns equal:

$$r_{n,t+1}^{\$} = b_{n-1,t+1}^{\$} - b_{n,t}^{\$} - (n-1)v_{t+1}^* + nv_t^*. \tag{A145}$$

Real and nominal bond log excess returns then equal:

$$xr_{n,t+1} = r_{n,t+1} - r_t, \tag{A146}$$

$$xr_{n,t+1}^{\$} = r_{n,t+1}^{\$} - i_t. \tag{A147}$$

C.5.4 Levered stock prices and returns

We note that the price of the levered equity claim is δP_t^c, so the price-dividend ratio equals:

$$\frac{P_t^\delta}{D_t^\delta} = \delta \frac{C_t}{D_t^\delta} \frac{P_t^c}{C_t}. \tag{A148}$$

Using the expression

$$D_{t+1}^\delta = P_{t+1}^c + C_{t+1} - (1-\delta) P_t^c \exp(r_t) - \delta P_t^c, \tag{A149}$$

and

$$P_t^\delta = \delta P_t^c \tag{A150}$$

gives the gross return on levered stocks:

$$\left(1+R^{\delta}_{t+1}\right) = \frac{D^{\delta}_{t+1}+P^{\delta}_{t+1}}{P^{\delta}_{t}}, \tag{A151}$$

$$= \frac{1}{\delta}\frac{P^{c}_{t+1}+C_{t+1}-(1-\delta)P^{c}_{t}exp(r_t)}{P^{c}_{t}}, \tag{A152}$$

$$= \frac{1}{\delta}\left(1+R^{c}_{t+1}\right)-\frac{1-\delta}{\delta}exp\left(r_t\right). \tag{A153}$$

Log stock excess returns then equal:

$$xr^{\delta}_{t+1} = r^{\delta}_{t+1}-r_t. \tag{A154}$$

To mimic firms' dividend smoothing in the data, we report simulated moments for the price of equities dividend by dividends smoothed over the past 64 quarters:

$$P^{\delta}_{t}/\left(\frac{1}{64}(D^{\delta}_{t}+D^{\delta}_{t-1}+...+D^{\delta}_{t-63})\right). \tag{A155}$$

C.6 Risk-premium decomposition

We use the superscript ^{rn} for risk-neutral, superscript ^{cf} for cash flow, and ^{rp} for risk premium. Risk-neutral valuations are expected cash flows discounted with the risk-neutral discount factor, that is consistent with equilibrium dynamics for the real interest rate:

$$M^{rn}_{t+1} = exp(-r_t). \tag{A156}$$

C.6.1 Risk-neutral zero-coupon bond prices

We use analogous recursions to solve for risk-neutral bond prices. One-period risk-neutral bond prices are given exactly as before by equations (A126) and (A127). For $n>1$, we guess and verify that the prices of real and nominal risk-neutral zero-coupon bonds with maturity n can be written in the following form

$$P^{rn}_{n,t} = B^{rn}_{n}(\tilde{Z}_t,\hat{s}_t,x_{t-1}), \tag{A157}$$

$$P^{\$,rn}_{n,t} = exp(-nv^{*}_{t})B^{\$,rn}_{n}(\tilde{Z}_t,\hat{s}_t,x_{t-1}). \tag{A158}$$

for some functions $B^{rn}_{n}(\tilde{Z}_t,\hat{s}_t,x_{t-1})$ and $B^{\$,rn}_{n}(\tilde{Z}_t,\hat{s}_t,x_{t-1})$.

We derive the two-period risk-neutral nominal bond price analytically:

$$P^{\$,rn}_{2,t} = exp(-r_t)\mathbb{E}_t\left[P^{\$,rn}_{1,t+1}\exp(-v^{*}_{t+1}-Y_{2,t+1})\right] \tag{A159}$$

$$= exp(-r_t)\mathbb{E}_t\left[\exp(-Y_{3,t+1}-2v^{*}_{t+1}-Y_{2,t+1}-\bar{r})\right]. \tag{A160}$$

We can hence verify that the two-period risk-neutral nominal bond price takes the form (A125)

$$b^{\$,rn}_{2} = -e_3\left[I+B\right]A^{-1}\tilde{Z}_t+\frac{1}{2}v_{\$}\Sigma_u v_{\$}\prime-2\bar{r} \tag{A161}$$

Here, the vector $v_\$$ is identical to the case with risk aversion. Comparing expressions (A161) and (A131) shows that they agree when $\gamma = 0$. We similarly solve for 2-period real bond prices in closed form:

$$\begin{aligned} P_{2,t}^{rn} &= \exp\left(-Y_{3,t} + \mathbb{E}_t Y_{2,t+1} - \bar{r}\right) \times \exp\left(\mathbb{E}_t\left(-Y_{3,t+1} + \mathbb{E}_{t+1} Y_{2,t+2} - \bar{r}\right)\right) \\ &\quad \times \mathbb{E}_t\left[\exp\left(-\underbrace{(e_3 - e_2 B)\Sigma}_{v_r} v_{t+1}\right)\right]. \end{aligned} \tag{A162}$$

The vector v_r is again identical to the case with risk aversion. Taking logs gives:

$$b_2^{rn}(\tilde{Z}_t, \hat{s}_t, x_{t-1}) = -(e_3 - e_2 B)\left[I + B\right] A^{-1} \tilde{Z}_t + \frac{1}{2} v_r \Sigma_u v_r' - 2\bar{r}. \tag{A163}$$

We note that the risk-neutral bond prices (A163) and bond prices with risk aversion (A133) are identical when the utility curvature parameter γ equals zero.

For $n \geq 3$ the n-period risk neutral real bond price B_n^{rn} satisfies the recursion:

$$B_n^{rn}(\tilde{Z}_t, \hat{s}_t, x_{t-1}) = \mathbb{E}_t\left[\exp\left(-\bar{r} - (e_3 - e_2 B) A^{-1} \tilde{Z}_t + b_{n-1}(\tilde{Z}_{t+1}, \hat{s}_{t+1}, x_t)\right)\right] \tag{A164}$$

We obtain a similar recursion for risk-neutral nominal bond prices:

$$B_n^{\$,rn}(\tilde{Z}_t, \hat{s}_t, x_{t-1}) = \mathbb{E}_t\left[\exp\left(Y_{3,t} + \mathbb{E}_t Y_{2,t+1} - \bar{r} - Y_{2,t+1} - n v_{t+1}^* + b_{n-1}^\$(\tilde{Z}_{t+1}, \hat{s}_{t+1}, x_t)\right)\right].$$

We again use the decomposition $v_{t+1}^* = vec^* \epsilon_{t+1} + \epsilon_{t+1}^\perp$ from Section C.5.2 to reduce the dimensionality of the numerical integration:

$$\begin{aligned} B_n^{\$,rn}(\tilde{Z}_t, \hat{s}_t, x_{t-1}) &= \mathbb{E}_t\left[\exp\left(-Y_{3,t} + \mathbb{E}_t Y_{2,t+1} - \bar{r} - Y_{2,t+1} - n \cdot vec^* \epsilon_{t+1} + \frac{n^2}{2}(\sigma^\perp)^2\right.\right. \\ &\quad \left.\left. + b_{n-1}^\$(\tilde{Z}_{t+1}, \hat{s}_{t+1}, x_t)\right)\right], \end{aligned} \tag{A165}$$

$$\begin{aligned} &= \mathbb{E}_t\left[\exp\left(-\bar{r} - e_3 A^{-1} \tilde{Z}_t - (\underbrace{e_2 A^{-1} e_1'}_{vpi_1} + n \cdot vec^* e_1')\epsilon_{1,t+1}\right.\right. \\ &\quad \left.\left. - \left(\underbrace{e_2 A^{-1} e_2'}_{vpi_2} + n \cdot vec^* e_2'\right)\epsilon_{2,t+1} + \frac{n^2}{2}(\sigma^\perp)^2 + b_{n-1}^\$(\tilde{Z}_{t+1}, \hat{s}_{t+1}, x_t)\right)\right]. \end{aligned} \tag{A166}$$

C.6.2 Risk-neutral zero-coupon consumption claims

Next, we derive recursive solutions for the risk-neutral prices of zero-coupon consumption claims. Let $P_{nt}^{c,rn}/C_t$ denote the risk-neutral price-dividend ratio of a zero-coupon claim on consumption at time $t+n$. The risk-neutral price-consumption ratio of a claim to the

entire stream of future consumption equals:

$$\frac{P_t^{c,rn}}{C_t} = \sum_{n=1}^{\infty} \frac{P_{nt}^{c,rn}}{C_t}. \tag{A167}$$

For $n \geq 1$, we guess and verify there exists a function $F_n^{rn}(\tilde{Z}_t, \hat{s}_t, x_{t-1})$, such that

$$\frac{P_{nt}^{c,rn}}{C_t} = F_n^{rn}\left(\tilde{Z}_t, \hat{s}_t, x_{t-1}\right). \tag{A168}$$

We start by deriving the analytic expression for F_1^{rn}. The one-period risk-neutral zero-coupon price-consumption ratio solves

$$\frac{P_{1,t}^{c,rn}}{C_t} = exp\left(-Y_{3,t} + \mathbb{E}_t Y_{2,t+1} - \bar{r}\right) \mathbb{E}_t\left[\frac{C_{t+1}}{C_t}\right] \tag{A169}$$

Using (26) to substitute for consumption growth, we can derive the following analytic expression for f_1^{rn}:

$$f_1^{rn}(\tilde{Z}_t, \hat{s}_t, x_{t-1}) = -(1-\rho^a)\left(e_3 - e_2 B\right) A^{-1}\tilde{Z}_t - \bar{r} + g + e_1[B - \phi I]A^{-1}\tilde{Z}_t + \frac{1}{2}\sigma_c^2. \tag{A170}$$

Next, we solve for f_n, $n \geq 2$ iteratively:

$$\frac{P_{nt}^{c,rn}}{C_t} = exp\left(-Y_{3,t} + \mathbb{E}_t Y_{2,t+1} - \bar{r}\right) \mathbb{E}_t\left[\frac{C_{t+1}}{C_t} F_{n-1}^{rn}\left(\tilde{Z}_{t+1}, \hat{s}_{t+1}, x_t\right)\right] \tag{A171}$$

This gives the following expression for f_n^{rn}:

$$\begin{aligned} f_n^{rn}(\tilde{Z}_t, \hat{s}_t, x_{t-1}) = \log\big[\mathbb{E}_t\big[\exp\big(&-(1-\rho^a)\left(Y_{3,t} + \mathbb{E}_t Y_{2,t+1}\right) - \bar{r} + g - \phi x_t + \mathbb{E}_t x_{t+1} + \sigma_c \epsilon_{1,t+1} \\ &+ f_{n-1}^{rn}(\tilde{Z}_{t+1}, \hat{s}_{t+1}, x_t)\big)\big]\big]. \end{aligned} \tag{A172}$$

Finally, we re-write $f_{n,t}^{rn}$ as an expectation involving $f_{n-1,t+1}^{rn}$, the state variables $\tilde{Z}_t$, and period $t+1$ shocks:

$$\begin{aligned} f_n^{rn}(\tilde{Z}_t, \hat{s}_t, x_{t-1}) = \log\Big[\mathbb{E}_t\Big[\exp\Big(&g + e_1[B - \phi I]A^{-1}\tilde{Z}_t - \bar{r} - (1-\rho^a)\left(e_3 - e_2 B\right) A^{-1}\tilde{Z}_t + \\ &+ \sigma_c \epsilon_{1,t+1} + f_{n-1}^{rn}(\tilde{Z}_{t+1}, \hat{s}_{t+1}, x_t)\Big)\Big]\Big]. \end{aligned} \tag{A173}$$

C.6.3 Risk-neutral returns

We plug risk-neutral price-consumption ratios and bond prices into equations (A141) through (A147). This gives risk-neutral returns on the consumption claim, risk-neutral log excess bond returns, and risk-neutral bond yields. We then substitute risk-neutral returns on the consumption claim into (A153)-(A154) to obtain risk-neutral log excess stock returns.

C.7 Modeling FOMC High-Frequency Asset Prices

In order to simulate high-frequency changes in stocks and bonds around FOMC announcements, we decompose the quarterly shock into a pre-FOMC and an FOMC component, which are assumed to be uncorrelated

$$v_t = v_t^{pre} + v_t^{FOMC}. \tag{A174}$$

We therefore effectively model FOMC dates as occurring always at the end of the quarter, because that is the only date when we compute asset prices. The variance-covariance matrix of shocks released prior to the FOMC announcement is

$$\Sigma_v^{pre} = \Sigma_v - diag\left([\sigma_x^{FOMC}, \sigma_\pi^{FOMC}, \sigma_{ST}^{FOMC}, \sigma_{LT}^{FOMC}]\right). \tag{A175}$$

We then split the rotated ϵ_t shock similarly according to

$$\epsilon_t^{pre} = A\Sigma v_t^{pre}, \tag{A176}$$
$$\epsilon_t^{FOMC} = A\Sigma v_t^{FOMC}. \tag{A177}$$

The aggregate dynamics and asset pricing solution are of course unchanged to before, because the distribution of quarterly fundamental shocks v_t is unchanged. But splitting it into two independent shocks allows us to differentiate asset prices before vs. after the FOMC shock v_t^{FOMC}.

We compute pre-FOMC asset prices very simply at the expected quarter t state vector before the FOMC shock is realized. The expected pre-FOMC state variables plus consumption are given by

$$\tilde{Z}_t^{pre} = \tilde{P}\tilde{Z}_{t-1} + \epsilon_t^{pre}, \tag{A178}$$
$$Y_t^{pre} = PY_{t-1} + A^{-1}\epsilon_t^{pre}, \tag{A179}$$
$$\hat{s}_t^{pre} = \theta_0\hat{s}_{t-1} + \theta_1 Y_{1,t-1} + \theta_2 Y_{1,t-2} + ...\lambda(\hat{s}_{t-1}, \bar{S})\sigma_c\epsilon_{1,t}^{pre}, \tag{A180}$$
$$c_t^{pre} = g + c_{t-1} + (Y_{1,t}^{pre} - \phi Y_{1,t-1}), \tag{A181}$$
$$v_t^{*,pre} = v_{t-1}^{*} + v_t^{LT,pre}. \tag{A182}$$

We compute pre-FOMC stock and bond prices by substituting the pre-FOMC state vector into the solutions from the asset pricing value function iterations:

$$\frac{P_t^{pre}}{C_t^{pre}} = F\left(\tilde{Z}_t^{pre}, \hat{s}_t^{pre}, x_{t-1}\right), \tag{A183}$$
$$P_{n,t}^{\$,pre} = exp\left(-nv_t^{*,pre}\right) B_n^{\$}\left(\tilde{Z}_t^{pre}, \hat{s}_t^{pre}, x_{t-1}\right), \tag{A184}$$
$$P_{n,t}^{pre} = B_n\left(\tilde{Z}_t^{pre}, \hat{s}_t^{pre}, x_{t-1}\right) \tag{A185}$$

The pre-FOMC nominal and real log bond yields are then given by

$$y_{n,t}^{\$,pre} = -n\log\left(P_{n,t}^{\$,pre}\right), \tag{A186}$$
$$y_{n,t}^{pre} = -n\log\left(P_{n,t}^{pre}\right). \tag{A187}$$

Pre-FOMC breakeven is computed as

$$breakeven_{n,t}^{pre} = y_{n,t}^{\$,pre} - y_{n,t}^{pre}. \tag{A188}$$

We then compute simulated changes in the short-term nominal interest rate, as well as long-term bond yields and breakeven around FOMC announcements

$$\Delta i_t^{FOMC} = (Y_{3,t} + v_t^*) - \left(Y_{3,t}^{pre} + v_t^{*,pre}\right), \tag{A189}$$

$$\Delta y_{n,t}^{\$,FOMC} = y_{n,t}^{\$} - y_{n,t}^{\$,pre}, \tag{A190}$$

$$\Delta y_{n,t}^{FOMC} = y_{n,t} - y_{n,t}^{pre}, \tag{A191}$$

$$\Delta breakeven_{n,t}^{FOMC} = breakeven_{n,t} - breakeven_{n,t}^{pre}. \tag{A192}$$

Stock returns around the FOMC date are computed assuming that no consumption takes place during the FOMC interval (equivalently, the FOMC intervals is infinitesimal), so

$$r_t^{c,FOMC} = \log\left(exp(c_t - c_t^{pre})\frac{\frac{P_t^c}{C_t}}{\frac{P_t^{c,pre}}{C_t^{pre}}}\right). \tag{A193}$$

The levered return around the FOMC date then is

$$r_t^{\delta,FOMC} = log((1/\delta)exp(r_t^{c,FOMC}) - ((1-\delta)/\delta)), \tag{A194}$$

which follows from using the standard formula for levered stock returns while setting the real interest rate and consumption to zero, because the FOMC interval is infinitesimal.

D Solving for Asset Prices numerically

We evaluate asset prices by iterating on a grid for the state vector as in Campbell, Pflueger, and Viceira (2020) building on Wachter (2005). Other numerical methodologies are faster, but their cost is that they cannot replicate the economic properties of Wachter (2005)'s numerical solution for Campbell-Cochrane. In unreported results, we verified that analytic linear approximations to the sensitivity function λ (e.g. Lopez, López-Salido, and Vazquez-Grande 2015), numerical higher-order perturbation methods using Dynare (Rudebusch and Swanson 2008), and global projection methods give solutions for Campbell-Cochrane that are economically very different from Wachter (2005)'s numerical solution.

Other approaches in the literature are also not appropriate for our problem. While Chen (2017) solves a model with habit and production using global projection and perturbation methods, his model features a linear sensitivity function and heteroskedastic consumption. By contrast, we have homoskedastic consumption and a highly nonlinear sensitivity function. Similarly, affine term structure models, such as Dai and Singleton (2000), generate affine relations between risk premia and state variables by assuming analytically convenient functional forms for the pricing kernel. In contrast to models that assume more convenient pricing kernels, our preferences are consistent with the stan-

dard log-linear New Keynesian consumption Euler equation and generate conditionally homoskedastic macroeconomic dynamics.

While iterating on a grid is significantly slower than perturbation or global projection methods, it is not prohibitively so. Our MATLAB algorithm for solving the asset pricing recursions (described in Section D.1) takes 94 seconds to run on a Lenovo X280 laptop with an i7-8650U CPU. Simulating the model (described in Section D.2) takes 35 seconds. The risk-neutral asset pricing recursions and simulating the risk-neutral stock returns take an additional 88 seconds and 37 seconds.

D.1 Implementing the asset pricing recursions

We implement the recursions in Sections C.5.1 and C.5.2 numerically through value function iteration on a grid. We solve for the functions f_n, b_n, and $b_n^\$$ using value function iteration along a five-dimensional state vector. We use a five-dimensional grid, with the first three dimensions corresponding to $\tilde{Z}_t$, the fourth dimension corresponding to $\hat{s}_t$, and the fifth dimension corresponding to x_{t-1}.

D.1.1 Grid

In this section, we use $\tilde{Z}, \hat{s}, x$ to denote the corresponding time-t variables. We use superscripts $^-$ to denote variables in the previous period and $^+$ to denote variables in the next period. We solve numerically for f_n, b_n, and $b_n^\$$ as functions of the vector of state variables $\left[\tilde{Z}, \hat{s}, x^-\right]$.

Our grid is densest along the $\hat{s}$ dimension to capture important non-linearities of asset prices with respect to the surplus consumption ratio. Following Wachter (2005), we choose a grid for the surplus consumption ratio that consists of an upper segment and a lower segment and covers a wide range of values for s_t. Let $S_{grid,1}$ denote a vector of 20 equally spaced points between 0 and S_{max} with S_{max} included and $s_{grid,2}$ a vector of 30 equally spaced points between $min\left(\log\left(S_{grid,1}\right)\right)$, and -50. The grid for $\hat{s}_t = s_t - \bar{s}$ then consists of the concatenation of $s_{grid,2} - \bar{s}$ and $\log\left(S_{grid,1}\right) - \bar{s}$.

We find that bond and stock prices are close to loglinear in $\tilde{Z}$ and $\hat{x}^-$, so coarser grids are sufficient along those dimensions of the state vector. In fact, the analytic expressions for f_1, b_2, and $b_2^\$$ show that one-period zero-coupon consumption claims and two-period bond prices are exactly log-linear in $\tilde{Z}$ and x^-. Numerical results indicate that this property translates to longer-period claims and f_n, b_n, and $b_n^\$$ are still approximately linear in $\tilde{Z}$ and x^- for general n. To speed up the value function iteration, we therefore use two grid points for each dimension of $\tilde{Z}$ and for x^-.

For $\tilde{Z}$, we use an equal-spaced three-dimensional grid. Let N denote the number of grid points along each dimension and m the width of the grid as a multiple of the unconditional standard deviation of $\tilde{Z}$. For each dimension of $\tilde{Z}$, we choose a grid of N equal-spaced points with the lowest point equal to $-m \times std(\tilde{Z})$ and the highest point equal to $m \times std(\tilde{Z})$. Here, the unconditional variance-covariance matrix of $\tilde{Z}$ is determined implicitly by the equation:

$$std(\tilde{Z}) \quad = \quad \sqrt{\tilde{B} Var\left(\tilde{Z}\right) \tilde{B}' + diag(1,1,1)}. \tag{A195}$$

For our baseline grid, we set $N = 2$ and $m = 2$.

For x^-, we consider an equal-spaced grid with $sizexm$ points ranging from $min\left(e_1 A\tilde{Z}_t : \tilde{Z} \in grid\right)$ to $max\left(e_1 A\tilde{Z} : \tilde{Z} \in grid\right)$. This choice of grid ensures that the grid for x^- covers the entire range of output gap values implied by the grid for $\tilde{Z}$. In our baseline evaluation, we set $sizexm = 2$.

With $N = 2$ grid points along each of the three dimensions of $\tilde{Z}$, 50 gridpoints for $\hat{s}$, and $sizexm = 2$ grid points for x^-, the combined grid has a total of $2^3 \cdot 50 \cdot 2 \cdot = 800$ points.

D.1.2 Numerical integration

Following Wachter (2005), we use Gauss-Legendre quadrature to evaluate the expectations (A123), (A134), and (A139) numerically. Gauss-Legendre quadrature is orders of magnitude faster than computing expectations by simulation. As in Wachter (2005), we evaluate infinite integrals over the density of standardized consumption shocks $(\epsilon_{1,t})$ using 40 integration node points and an integration domain ranging from -8 standard deviations to $+8$ standard deviations. To conserve speed and memory, we integrate over shocks orthogonal to surplus consumption $(\epsilon_{2,t})$ using a somewhat smaller number of integration node points, 15, but again an integration domain of ± 8 standard deviations. To evaluate bond and stock prices at points that are not on the grid, we use loglinear multi-linear interpolation and extrapolation.

For completeness, we recap the key features of Gauss-Legendre integration. Let $xGL_i,\ i = 1, ..., N_{GL}$ and $wGL_i = 1, ..., N_{GL}$ denote the Gauss-Legendre nodes and weights of N_{GL}th order. Gauss-Legendre quadrature then approximates a definite integral of any smooth function f on the interval $[-1, 1]$ by $\int_{-1}^{1} f(x)\, dx \approx \sum_{i=1}^{N_{GL}} wGL_i f(xGL_i)$. By change of variable, it is immediate that we can approximate the integral of a smooth function f on an interval $[-\bar{a}, \bar{a}]$ by

$$\int_{-\bar{a}}^{\bar{a}} f(x)\, dx \approx \sum_{i=1}^{N_{GL}} \underbrace{\bar{a} \times wGL_i}_{wGL_i^{\bar{a}}} f\left(\underbrace{\bar{a} \times xGL_i}_{xGL_i^{\bar{a}}}\right). \tag{A196}$$

Here, we use $xGL_i^{\bar{a}}$ and $wGL_i^{\bar{a}}$ to denote Gauss-Legendre node points and weights scaled to the interval $[-\bar{a}, \bar{a}]$.

We implement Gauss-Legendre quadrature to take expectations over ϵ_{t+1} as follows. Let N_1 denote the number of Gauss-Legendre nodes and $\bar{a}_1$ denote the integration domain for the shock $\epsilon_{1,t}$, that is perfectly correlated with output innovations. We set $xGL_{1,i} = xGL_i^{\bar{a}_1}$ and $wGL_{1,i} = wGL_i^{\bar{a}_1}$ for $i = 1, ..., N_1$, where the weights and nodes are as defined in equation (A196). Moreover, we set

$$pGL_{1,i} = \frac{1}{\sqrt{2\pi}} exp\left(-xGL_{1,i}^2\right) wGL_{1,i} / \sum_{i=1}^{N_1} \left(\frac{1}{\sqrt{2\pi}} exp\left(-xGL_{1,i}^2\right) wGL_{1,i}\right), \tag{A197}$$

and use the scaled weights $pGL_{1,i}$ for numerical integration. The scaling of (A197) ensures that the numerical expectation of a constant is evaluated to be the same constant (or intuitively that discretized probabilities sum to one).

We then evaluate numerically the expectation of any smooth function f of $\epsilon_{1,t}$ via:

$$E\left[f\left(\epsilon_{1,t}\right)\right] = \int_{-\infty}^{\infty} \frac{1}{\sqrt{2\pi}} exp\left(-\epsilon_1^2\right) f\left(\epsilon_1\right) d\epsilon_1, \tag{A198}$$

$$\approx \int_{-\bar{a}_1}^{\bar{a}_1} \frac{1}{\sqrt{2\pi}} exp\left(-\epsilon_1^2\right) f\left(\epsilon_1\right) d\epsilon_1, \tag{A199}$$

$$\approx \sum_{i=1}^{N_1} pGL_{1,i} f\left(xGL_{1,i}\right). \tag{A200}$$

Accuracy increases with $\bar{a}_1$ and N_1. We follow Wachter (2006) in setting $N_1 = 40$ and $\bar{a}_1 = 8$.

To take expectations over $\epsilon_{2,t}$ and $\epsilon_{3,t}$, we similarly use Gauss-Legendre quadrature with integration domain $\bar{a}_2 = 8$ and number of nodes $N_2 = 15$. We set $xGL_{2,i} = xGL_i^{\bar{a}_2}$ and $wGL_{2,i} = wGL_i^{\bar{a}_2}$ for $i = 1, ..., N_2$ and define the scaled weights:

$$pGL_{2,i} = \frac{1}{\sqrt{2\pi}} exp\left(-xGL_{2,i}^2\right) wGL_{2,i} / \sum_{i=1}^{N_2} \left(\frac{1}{\sqrt{2\pi}} exp\left(-xGL_{2,i}^2\right) wGL_{2,i}\right), \tag{A201}$$

The weights and nodes for $\epsilon_{3,t}$ are identical to those of $\epsilon_{2,t}$.

Since $\epsilon_{1,t}$, $\epsilon_{2,t}$, and $\epsilon_{3,t}$ are independent, we can evaluate the expectation of any smooth function $f\left(\epsilon_{1,t}, \epsilon_{2,t}, \epsilon_{2,t}\right)$ as

$$Ef\left(\epsilon_{1,t}, \epsilon_{2,t}, \epsilon_{3,t}\right) = \int_{-\infty}^{\infty} \frac{1}{\sqrt{2\pi}} exp\left(-\epsilon_1^2\right) \int_{-\infty}^{\infty} \frac{1}{\sqrt{2\pi}} exp\left(-\epsilon_2^2\right) \int_{-\infty}^{\infty} \frac{1}{\sqrt{2\pi}} exp\left(-\epsilon_3^2\right) f\left(\epsilon_1, \epsilon_2, \epsilon_3\right) d\epsilon_1 d\epsilon_2 d\epsilon_3$$

$$\approx \sum_{i=1}^{N_1} pGL_{1,i} \left[\sum_{j=1}^{N_2} pGL_{2,j} \left[\sum_{k=1}^{N_3} pGL_{3,k} f\left(xGL_{1,i}, xGL_{2,j}, xGL_{3,k}\right)\right]\right]. \tag{A202}$$

D.1.3 Recursive step

Let a superscript ^{num} denote the numerical counterparts to the analytic functions f_n, b_n, $b_n^{\$}$. We start by initializing $f_1^{num}\left(\tilde{Z}, \hat{s}, x^-\right)$, $b_2^{num}\left(\tilde{Z}, \hat{s}, x^-\right)$, and $b_2^{\$,num}\left(\tilde{Z}, \hat{s}, x^-\right)$ at each grid point according to the analytic expressions (A121), (A131) and (A133).

Next, we apply the recursive expressions (A123), (A134), and (A139) along the grid. Having computed f_{n-1}^{num} along the entire grid, we evaluate $f_n^{num}\left(\tilde{Z}, \hat{s}, x^-\right)$ at a grid point

$\left(\tilde{Z}, \hat{s}, x^{-}\right)$ as follows. We compute the expectation (A123) numerically as:

$$\begin{aligned} f_n^{num}(\tilde{Z}, \hat{s}, x^{-}) &= \log\left[\sum_{i=1}^{N_1} pGL_{1,i}\left[\sum_{j=1}^{N_2} pGL_{2,j}\left[\sum_{k=1}^{N_3} pGL_{3,k}\cdot\exp\left(g + e_1[B-\phi I]A^{-1}\tilde{Z}\right.\right.\right.\right. \\ &\quad -\bar{r} - (1-\rho^a)(e_3 - e_2 B)A^{-1}\tilde{Z} - \frac{\gamma}{2}(1-\theta_0)(1-2\hat{s}) \\ &\quad -(\gamma(1+\lambda(\hat{s}))-1)\sigma_c \times xGL_{1,i} \\ &\quad \left.\left.\left.\left. + f_{n-1}^{num}\left(\tilde{B}\tilde{Z} + \begin{bmatrix} xGL_{1,i} \\ xGL_{2,j} \\ xGL_{3,k} \end{bmatrix}, \theta_0\hat{s} + \theta_1 x + \theta_2 x^{-} + \lambda(\hat{s})\, xGL_{1,i}, x\right)\right]\right]\right], \end{aligned} \tag{A203}$$

where we evaluate x as a function of the state vector as

$$x = e_1 A^{-1}\tilde{Z}. \tag{A204}$$

To compute the right-hand-side of (A203), we need to evaluate f_{n-1}^{num} at points that are not on our grid. We interpolate f_{n-1}^{num} linearly (and hence F_{n-1}^{num} log-linearly). When the argument is outside the range of the grid, we extrapolate f_{n-1}^{num} linearly. It is clear from (A121) that linear inter- and extrapolation gives a good approximation of f_1. In fact, we can see that f_1 is exactly linear in $\tilde{Z}$, independent of x^{-}, and that it depends on $\lambda(\hat{s}) = \lambda_0\sqrt{1-2\hat{s}}$. We accommodate the fact that f_1 is not linear in $\hat{s}$ by choosing a much denser grid along the $\hat{s}$ dimension. We do not have analytic expressions for $f_n, n > 1$ (after all, that's why we need a numerical solution), but numerical solutions indicate that linear inter- and extrapolation gives good approximations for f_n with the chosen grid.

In terms of coding (A203), we face a trade-off between speed and readability of the code. We pre-allocate matrices outside loops and we code linear interpolation by hand (rather than using a pre-written interpolation routine) to conserve speed and memory. We also inline the linear interpolation steps (i.e. write them directly into the main function rather than calling a separate interpolation function). This speeds up the code substantially, while reducing its readability.

There are different methods to interpolate multidimensional functions. Specifically, we use multi-linear interpolation, corresponding to interpolating along each dimension one at a time. In order to enhance computational speed we do not rely on a pre-programmed interpolation routine, instead coding our own minimal interpolation routine. It is well-known that the result of multi-linear (or in the two-dimensional case bi-linear) interpolation does not depend on in which order one interpolates the different arguments. We find it convenient to interpolate $f_{n-1}^{num}\left(\tilde{Z}, \hat{s}, x^{-}\right)$ first along the x^{-} dimension, then along $\hat{s}$, then along $\tilde{Z}_1$, and finally along the $\tilde{Z}_2$ and $\tilde{Z}_3$ dimensions.

Finally, we evaluate the price-consumption ratio for the aggregate consumption stream by approximating it as the sum of the first 300 zero-coupon consumption claims:

$$F^{num}\left(\tilde{Z}_t, \hat{s}_t, x_{t-1}\right) = \sum_{n=1}^{300} exp\left(f_n^{num}(\tilde{Z}_t, \hat{s}_t, x_{t-1})\right). \tag{A205}$$

We iterate $b_n^{num}\left(\tilde{Z},\hat{s},x^-\right)$ and $b_n^{\$,num}\left(\tilde{Z},\hat{s},x^-\right)$ similarly according to:

$$\begin{aligned} b_n^{num}(\tilde{Z}_t,\hat{s}_t,x_{t-1}) &= \log\left[\sum_{i=1}^{N_1} pGL_{1,i}\left[\sum_{j=1}^{N_2} pGL_{2,j}\left[\sum_{k=1}^{N_3} pGL_{3,k}\right.\right.\right. \\ &\quad \cdot\exp\left(-\bar{r}-(e_3-e_2B)\,A^{-1}\tilde{Z}-\frac{\gamma}{2}(1-\theta_0)(1-2\hat{s})\right. \\ &\quad -\gamma\left(1+\lambda(\hat{s})\right)\sigma_c\times xGL_{1,i} \\ &\quad \left.\left.\left.\left.+b_{n-1}^{num}\left(\tilde{B}\tilde{Z}+\begin{bmatrix} xGL_{1,i}\\ xGL_{2,j}\\ xGL_{3,k}\end{bmatrix},\theta_0\hat{s}+\theta_1 x+\theta_2 x^-+\lambda\left(\hat{s}\right)xGL_{1,i},x\right)\right]\right]\right], \end{aligned} \tag{A206}$$

and

$$\begin{aligned} b_n^{\$,num}(\tilde{Z}_t,\hat{s}_t,x_{t-1}) &= \left[\sum_{i=1}^{N_1} pGL_{1,i}\left[\sum_{j=1}^{N_2} pGL_{2,j}\left[\sum_{k=1}^{N_3} pGL_{3,k}\right.\right.\right. \\ &\quad \cdot\exp\left(-\bar{r}-e_3A^{-1}\tilde{Z}-\frac{\gamma}{2}(1-\theta_0)(1-2\hat{s})\right. \\ &\quad -\left(\gamma\left(1+\lambda(\hat{s})\right)\sigma_c+vpi_1+n\cdot vec^*e_1'\right)\times xGL_{1,i} \\ &\quad -\left(vpi_2+n\cdot vec^*e_2'\right)xGL_{2,j}+\frac{n^2}{2}\left(\sigma^{\perp}\right)^2 \\ &\quad \left.\left.\left.\left.+b_{n-1}^{\$,num}\left(\tilde{B}\tilde{Z}+\begin{bmatrix} xGL_{1,i}\\ xGL_{2,j}\\ xGL_{3,k}\end{bmatrix},\theta_0\hat{s}+\theta_1 x+\theta_2 x^-+\lambda\left(\hat{s}\right)xGL_{1,i},x\right)\right]\right]\right], \end{aligned} \tag{A207}$$

(A208)

We again use multi-linear interpolation and extrapolation to evaluate $b_{n-1}^{\$,num}$ and b_{n-1}^{num} at points that are not on the grid. We similarly implement the recursions (A164), (A166), and (A173) numerically to obtain risk-neutral bond and consumption claim valuations $B_n^{rn,num}$, $B_n^{rn,\$,num}$, $G^{rn,num}$.

D.2 Simulating the Model

We simulate a draw of length T. Results in Tables 2 and Table 4 use $T = 10000$ and discard the first 100 simulation periods to ensure that the system has reached the stochastic steady-state. We report model moments averaged across 2 independent simulations.

We use superscript *sim* to denote simulated quantities. We use the MATLAB function mvnrnd to obtain independent draws $v_t^{sim}\sim N\left(0,\Sigma_v\right)$ for $t=1,2,...,T$. We then obtain the rotated shock according to $\epsilon_t^{sim}=Av_t^{sim}$ and $v_t^{LT,sim}=e_4v_t^{sim}$. We generate draws for $\tilde{Z}_t^{sim}, t=1,...,T$ by setting $\tilde{Z}_1^{sim}=0$ and then updating according to (A94). We obtain the simulated non-rotated state vector for $t=1,2,...,T$ through the relation $Y_t^{sim}=A^{-1}\tilde{Z}_t^{sim}$. We generate draws for the surplus consumption ratio by setting $\hat{s}_1^{sim}=0$ and $x_0^{sim}=0$ and then updating according to (A103). We generate the simulated random walk component of inflation $v_t^*, t=1,2,...,T$ by starting from $v_1^{*sim}=0$ and updating it according to equation (22) in the main paper. We initialize simulated log consumption

at $c_1^{sim} = 0$ and update it using (26). We then drop the first 100 simulation periods to allow the system to converge to the stochastic steady-state.

Having generated draws for the five state variables $\tilde{Z}^{sim}$, $\hat{s}^{sim}$, and x_{t-1}^{sim}, we obtain the simulated consumption-claim price-dividend ratio as $(P^c/C)_t^{sim} = F^{num}\left(\tilde{Z}_t^{sim}, \hat{s}_t^{sim}, x_{t-1}^{sim}\right)$, n-period real bond prices as
$P_{n,t}^{sim} = B_n^{num}\left(\tilde{Z}_t^{sim}, \hat{s}_t^{sim}, x_{t-1}^{sim}\right)$, and
$B_{n,t}^{\$,sim} = B_n^{\$,num}\left(\tilde{Z}_t^{sim}, \hat{s}_t^{sim}, x_{t-1}^{sim}\right)$. We obtain the corresponding risk-neutral valuation ratios by plugging into the risk-neutral asset pricing solutions:
$(P^c/C)_t^{rn,sim} = F^{rn,num}\left(\tilde{Z}_t^{sim}, \hat{s}_t^{sim}, x_{t-1}^{sim}\right)$,
$P_{n,t}^{rn,sim} = B_n^{rn,num}\left(\tilde{Z}_t^{sim}, \hat{s}_t^{sim}, x_{t-1}^{sim}\right)$, and
$B_{n,t}^{rn,\$,sim} = B_n^{rn,\$,num}\left(\tilde{Z}_t^{sim}, \hat{s}_t^{sim}, x_{t-1}^{sim}\right)$. We obtain nominal bond prices $P_{n,t}^{\$,sim}$ by combining $B_{n,t}^{\$,sim}$ and v_t^{*sim} according to (A125). We similarly obtain risk-neutral nominal bond prices $P_{n,t}^{rn,\$,sim}$ by combining $B_{n,t}^{rn,\$,sim}$ and v_t^{*sim} according to (A125).

To deal with the fact that $\tilde{Z}_t^{sim}$, $\hat{s}_t^{sim}$, x_{t-1}^{sim} are not usually on grid points we adopt a similar linear interpolation strategy as in the numerical evaluation of the asset pricing recursions described in Section D.1.3. We interpolate F^{num}, B_n^{num}, and $B_n^{\$,num}$ log-linearly. We simplify the interpolation strategy slightly compared to Section D.1.3. We use the MATLAB function griddedInterpolant, sacrificing some computational speed for simpler code. Even though rare events (and especially extremely negative realizations for $\hat{s}$) matter for the value function iteration in Section D.1.3, low-probability events have very little impact on the properties of simulated asset prices taking as given F^{num}, B^{num}, and $B^{\$,num}$. We therefore simplify the log-linear interpolation by truncating $\tilde{Z}_t^{sim}$, $\hat{s}_t^{sim}$, and x_{t-1}^{sim} at the maximum and minimum values covered by the grid.

Having generated $\left(\frac{P^c}{C}\right)_t^{sim}, t = 1, ..., T$, we compute log returns on the consumption claim $r_{t+1}^{c,sim}$ according to (A141). We obtain simulated price-dividend ratios for levered stocks by plugging into (A148). Finally, we obtain log bond yields and stock and bond excess returns as described in Section C.5.3. Risk-neutral bond and stock returns are computed by substituting $\left(\frac{P^c}{C}\right)^{rn,sim}$, $P_{n,t}^{rn,\$,sim}$, and $P_{n,t}^{rn,sim}$ into the same relations.

We simulate pre-FOMC asset prices as follows. We use the MATLAB function mvnrnd to generate independent draws for the FOMC shock
$v_t^{FOMC,sim} \sim N\left(0, diag\left(\left[0, 0, \left(\sigma_{ST}^{FOMC}\right)^2, \left(\sigma_{LT}^{FOMC}\right)^2\right]\right)\right)$, where $t = 1, ..., T$. Having drawn the FOMC shock $v_t^{FOMC,sim}$ we obtain the simulated pre-FOMC component of the overall quarterly simulated shock as

$$v_t^{pre,sim} = v_t^{sim} - v_t^{FOMC,sim}, \tag{A209}$$

$$\epsilon_t^{pre,sim} = A v_t^{pre,sim}. \tag{A210}$$

We then use the simulated values for $\tilde{Z}_{t-1}^{sim}$, Y_{t-1}^{sim}, c_{t-1}^{sim}, $\hat{s}_{t-1}^{sim}$, v_{t-1}^{*} and $\epsilon_t^{pre,sim}$ to compute the simulated pre-FOMC state vector according to equations (A178) through (A182). We then obtain pre-FOMC asset prices by substituting the simulated pre-FOMC state vector into equations (A183) through (A182). Simulated yield changes around FOMC news are then computed according to equations (A189) and (A192) and simulated FOMC stock returns are obtained according to equation (A194).

D.3 Parameter units

This subsection details the relation between parameter values in empirical (reported in the paper) and natural units (used for solving the code). We solve the model in natural units. However, it is most natural to report empirical moments and summary statistics in empirical units for interpretability.

For comparability with empirical moments, Table 1 reports model parameters in units that correspond to the output gap in annualized percent, and inflation and interest rates in annualized percent. As in Campbell, Pflueger, and Viceira (2020), we report the discount rate and the persistence of surplus consumption in annualized units. Concretely, Table 1 reports the following scaled parameters:

$$400 \times g, \tag{A211}$$
$$400 \times \bar{r}, \tag{A212}$$
$$\theta_0^4, \tag{A213}$$
$$\beta^4, \tag{A214}$$
$$4 \times \gamma^x \tag{A215}$$
$$100 \times \sigma_x, \tag{A216}$$
$$400 \times \sigma_\pi, \tag{A217}$$
$$400 \times \sigma_{ST}, \tag{A218}$$
$$400 \times \sigma_{LT}, \tag{A219}$$
$$\frac{1}{4} \times \psi, \tag{A220}$$
$$4 \times \kappa \tag{A221}$$

All other parameters reported in Table 1 do not need to be scaled.

E Details: Simulated Method of Moments

E.1 Reduced-Form Impulse Responses

This section describes how we estimate the macroeconomic impulse responses reported in Figure 2. We follow the procedure described below for both actual and simulated data, with the simulated data length matching the length of the empirical sample. Model impulse responses in Figures 2 are averaged over 100 simulations. In this section, we use subscripts IRF if variable names would otherwise be similar to different variables elsewhere in the paper.

To account for the unit root in inflation in the model, we estimate a vector error correction model of the form

$$Y_{IRF,t} = \Pi Y_{IRF,t-1} + \varepsilon_t \tag{A222}$$

where we define the vector for the VECM as:

$$Y_{IRF,t} = [x_{t-1}, \pi_t - \pi_{t-1}, i_t - \pi_t]. \tag{A223}$$

This definition of the VAR(1) vector guarantees that each of the variables is stationary when the data is simulated from our model since the unit root affects the short-term interest rate i_t only through its effect on inflation π_t.

The shocks ε_t are not orthogonal and we denote their estimated variance-covariance matrix by Σ_ε. Next, we rotate the innovations to be orthogonal. This means that we need to re-write (A222) in the form:

$$R^{-1} Y_{IRF,t} = \Pi_R Y_{IRF,t-1} + \eta_t \tag{A224}$$

where η_t is a vector of uncorrelated shocks, R is an invertible matrix, and $\Pi_R = R^{-1}\Pi$. We write the variance-covariance matrix of η_t as:

$$\Sigma_\eta = \mathbb{E}\eta_t'\eta_t = \begin{bmatrix} \sigma(\eta_1)^2 & 0 & 0 \\ 0 & \sigma(\eta_2)^2 & 0 \\ 0 & 0 & \sigma(\eta_3)^2 \end{bmatrix} \tag{A225}$$

We pick R^{-1} to be lower-diagonal with ones along the diagonal. Having estimated Π and Σ_ε we obtain R, Π_R, and Σ_η using Cholesky factorization.

We then construct impulse responses. We start with a unit standard deviation orthogonalized shock to output gap:

$$\eta_1 = [\sigma(\eta_1), 0, 0] \tag{A226}$$

which is equivalent to

$$\varepsilon_1 = R[\sigma(\eta_1), 0, 0]. \tag{A227}$$

The n-th response to a one standard deviation shock to the output gap then is computed as:

$$\Pi^{n-1}\varepsilon_1 = \Pi^{n-1} R[\sigma(\eta_1), 0, 0]. \tag{A228}$$

We can similarly compute the responses for the change in inflation $\pi_t - \pi_{t-1}$ and the difference between the nominal interest rate and inflation $i_t - \pi_t$. In order to then obtain the corresponding responses of inflation, we cumulate the responses of $\pi_t - \pi_{t-1}$ and finally add the response of inflation to that of $i_t - \pi_t$ to obtain the response of the short-term nominal interest rate.

E.2 Confidence intervals and objective function

We use a bootstrap method to compute confidence intervals for the empirical impulse responses shown in Figure 2 and for the variances of the impulse responses used in the SMM estimation. Let Π and Σ_ε denote the coefficient matrix and the variance-covariance matrix of shocks from estimating (A222) on actual data. We then generate bootstrapped data by simulating $Y^{boot}_{IRF,t}$ of identical sample length as the true data according to

$$Y^{boot}_{IRF,t} = \Pi Y^{boot}_{IRF,t-1} + \varepsilon^{boot}_t, \tag{A229}$$

where ε_t^{boot} are drawn as iid normal with mean zero and variance-covariance Σ_ε. On the bootstrapped data, we then apply the methodology for IRFs described in Section E.1. That is, we re-estimate (A222) on the bootstrapped data and use the resulting estimates to construct bootstrapped impulse response functions. We generate 1000 independent bootstrap samples. Figure 2 shows confidence intervals, such that 95% of the time the bootstrapped impulse responses are within the interval.

For our objective function, we define the empirical target moments as follows. $\hat{\Psi}$ is $[15 \times 1]$. It includes $15 = 6 \cdot 3 - 3$ impulse responses. We have 15 impulse response moments, because we have nine impulse responses at zero (shock period), one, two, four, eight, and twelve quarters each. However, three of the shock period impulse responses are zero by our choice of orthogonalization and we exclude them from the objective function.

Let $\hat{V}$ denote the bootstrapped variance-covariance matrix of $\hat{\Psi}^{boot} - \hat{\Psi}$. We then define the weighting matrix $\hat{W}$ for the SMM objective function as the diagonal matrix with the inverse variances for the 15 impulse response moments along the diagonal:

$$\hat{W} \quad = \quad diag(inv(\hat{V}_{1,1}), inv(\hat{V}_{2,2}), ..., inv(\hat{V}_{51,51})). \tag{A230}$$

The SMM objective function is then given by equation (39) in the main text.

E.3 Grid search

We minimize the objective function $J(\sigma)$ using a two-step grid search. To reduce the need to compute (computationally expensive) asset prices along the grid, we separate the parameters into $[\sigma_x, \sigma_\pi, \sigma_{ST}]$ and σ_{LT}. The first step of the grid search finds the parameter values for $[\sigma_x, \sigma_\pi, \sigma_{ST}]$ that minimize the objective function while holding the volatility of the long-term monetary policy shock constant at $\sigma_{LT} = 0.25$, which we have chosen to match roughly the volatility of changes in 10-on-10-year breakeven, which equals 0.26% in our empirical sample. In this first grid search step, we solve and simulate macroeconomic dynamics and reduced-form impulse responses (but not asset prices) over a grid for the first three volatility parameters. We choose an equally-spaced grid with 20 points between 0.01 and 1 for each of σ_x, σ_π, and σ_{ST}, so we evaluate the macroeconomic dynamics at a total of $20^3 = 8000$ gridpoints in this step. We discard parameter values in this step, where asset prices do not exist.

In a second step, we find the volatility of the long-term monetary policy shock σ_{LT} by minimizing the distance between the volatility of changes in 10-on-10 year breakeven in the model and in the data, while holding all other model parameters constant. This second step requires solving for asset prices at each grid point, and is hence substantially slower than the first step. We evaluate the model volatility of changes in 10-on-10-year breakeven inflation on an equally-spaced grid for σ_{LT} with 20 points between 0.01 and 1. Because it takes about 2 minutes to solve for macroeconomic dynamics and asset prices, this second step of the grid search takes about $2 \times 20 = 40$ minutes. We again discard parameter vectors where asset prices do not exist.

F Additional Model Results

F.1 Switching off model components

Table A1 shows that the model results described in Table 4 are robust to switching off individual model components. For instance, reducing the equilibrium volatility of Phillips curve, short-term monetary policy, or long-term monetary policy shocks leaves the relationship of stock returns and monetary policy surprises on FOMC dates unchanged. For the counterfactual exercises in columns (5) and (6) of Table A1 monetary policy shocks on FOMC dates are still non-zero, but they are unanticipated and out-of-equilibrium because the equilibrium volatility of monetary policy shocks set to zero.

The model results for high-frequency stocks and bonds around FOMC announcements are robust to switching off the link between expected growth and the short-term real rate by setting $\rho_a = 0$. Table A1, column (1) shows that the model regression coefficients are actually somewhat larger when we switch off this link, and that time-varying risk premia continue to represent about 50% of the overall stock response to monetary policy news. With $\rho^a = 0$, a surprise increase in the short-term monetary policy rate is not accompanied by higher growth expectations, so stocks fall even more than in our baseline calibration. The link between the short-term real rate and expected growth ($\rho^a > 0$) in our baseline calibration therefore helps, because it ensures that the stock return response to monetary policy shocks is not too large compared to the data, as in Nakamura and Steinsson (2018).

Switching off the habit shock in column (3) also increases the model slope coefficients around FOMC announcements, and continues to imply a substantial risk premium response, as in the baseline calibration. Intuitively, in the absence of independent habit shocks the consumption claim is conditionally perfectly correlated with surplus consumption, so stocks are even riskier for investors.

Table A1: Model Decomposition

	(1) Baseline	(2) $\rho^a = 0$	(3) $\sigma_x = 0$	(4) $\sigma_\pi = 0$	(5) $\sigma_{ST} = 0$	(6) $\sigma_{LT} = 0$
Panel A: Overall monetary policy shocks effect						
Slope(S&P 500 Return, Fed Funds)	-5.27	-11.38	-15.43	-5.15	-4.96	-5.20
Slope(S&P 500 Return, 10Y Breakeven)	5.89	11.54	17.00	5.74	5.54	5.81
Panel B: Monetary policy shocks effect on risk premia						
Slope(S&P 500 Risk Premium, Fed Funds)	-2.54	-7.71	-14.16	-2.49	-2.21	-2.46
Slope(S&P 500 Risk Premium, 10Y Breakeven)	2.7	7.57	15.34	2.64	2.35	2.63
Panel C: Bond Betas						
Real Bond-Stock Beta	0.03	0.07	0.17	0.02	-0.02	0.01
Breakeven-Stock Beta	-0.13	-0.16	-0.22	-0.13	-0.11	-0.04

Note: This table compares asset pricing moments while switching off individual model components. The real and breakeven stock betas are computed as in Table 2, and the asset price reactions around monetary policy dates are as in Table 4. Column (1) of Panel A repeats the model regression of Table 4, column (2). The remaining columns of Panel A report the corresponding model regression coefficients while switching off individual model components. Panel B reports regression estimates corresponding to Table 4, column (4), where the dependent variable is the risk premium component of equity returns. For all panels, column (1) repeats the baseline model results. Column (2) switches off predictable technology growth. Column (3) sets the demand shock to zero. Column (4) sets the Phillips curve shock to zero. Column (5) sets the short-term monetary policy shock to zero. Column (6) sets the long-term monetary policy shock to zero. For the counterfactual exercises in columns (5) and (6) of Table A1 monetary policy shocks on FOMC dates are still non-zero, but they are unanticipated and out-of-equilibrium because the equilibrium volatility of monetary policy shocks set to zero. All other parameters are held constant at the values listed in Table 1.

F.2 Model Real Bond Yields around FOMC Announcements

In this Appendix Section, we show that our model matches the comovement between the short-term nominal interest rate and long-term real bond yields around FOMC dates, which Nakamura and Steinsson (2018) and Hanson and Stein (2015) have documented.

Table A2: Data and Model Real Bond Yields around FOMC Announcements

	(1) Data	(2) Model	(3) Model ($\rho^a = 0$)
Slope(5Y Real Yield, Fed Funds)	0.42*	0.36	0.32
	(0.22)		
Risk Neutral		0.35	0.29
Slope(10Y Real Yield, Fed Funds)	0.28*	0.17	0.18
	(0.16)		
Risk Neutral		0.17	0.15

Note: This table compares the comovement of long-term real bond yields and short-term nominal interest rates around monetary policy announcements in the model and in the data. The table reports coefficient estimates from regressions of the form $\Delta^{FOMC} y_{n,t} = b_0 + b_1 \Delta^{FOMC} i_t + \varepsilon_t$, where $\Delta^{FOMC} y_{n,t}$ is either the change in the 10-year or 5-year real bond yield from the day before the FOMC announcement to the day after. We use zero-coupon TIPS yields from Gürkaynak, Sack, and Wright (2010). The surprise in the Federal Funds rate and the sample are as in Table 4. Model asset price changes around FOMC announcements are also as described in Table 4. Risk neutral rows show the slope coefficients when model long-term real bond yields are computed from the stochastic discount factor of a risk neutral investor taking macroeconomic dynamics as given.

Table A2 shows that our model matches the empirical relationship between long-term real yields and short-term nominal yields on FOMC days:

$$\Delta^{FOMC} y_{n,t} \quad = \quad b_0 + b_1 \Delta^{FOMC} i_t + \varepsilon_t, \tag{A231}$$

where $\Delta^{FOMC} y_{n,t}$ is the change in either the 10-year or the 5-year real bond yield and $\Delta^{FOMC} i_t$ is the change in the Federal Funds rate. Table A2, column (1) shows that long-term real bond (TIPS) yields indeed move with surprises in short-term interest rates in our sample, consistent with prior empirical results. In the data, a 25 bps surprise increase in the short-term nominal interest rate tends to be accompanied by a substantial 11 bps increase in the 5-year TIPS yield and a 7 bps increase in the 10-year TIPS yield.

Column (2) shows that the model replicates the positive empirical relationship between long-term real bond yields and short-term nominal yields on FOMC dates. In the model, a 25 bps point increase in short-term nominal yield is associated with a 9 bps increase in the 5-year real bond yield, and a 4 bps increase in the 10-year real bond yield, similarly to the data. Both of these coefficients are economically meaningful and within two standard deviations of the empirical estimates, though smaller than in the data.

One might expect that setting $\rho^a > 0$ (as in our baseline calibration) should lead to higher model regression coefficients in Table A2. The standard intuition in Nakamura

and Steinsson (2018) is that when monetary policy is perceived to follow the natural rate implied by expected growth, a surprise increase in the policy rate leads investors to update about expected growth going forward, thereby raising long-term real bond yields. Consistent with this intuition, column (3) shows that switching off the link between productivity growth and the real yields ($\rho^a = 0$) indeed weakens the link between short-term nominal and 5-year real bond yields. For the 10-year bond yields, setting $\rho^a = 0$ does not reduce the model slope coefficient of 10-year real bond yields onto the short-term policy rate around monetary policy announcements.

Looking at the slope coefficients for risk-neutral real bond yields provides an answer to this puzzling result. We compute risk-neutral real bond yields according to the expectations hypothesis, so they contain no risk premia. As expected, switching off the real rate - growth link ($\rho^a = 0$) weakens the slope coefficients of model risk-neutral real bond yields onto short-term policy rate surprises for both the 5-year and the 10-year real bond maturities. The role for risk premia in our model arises because whether real bond prices benefit from flight-to-safety is endogenous to the macroeconomic regime (including ρ^a). Table A1, Panel C shows that when investors do not learn about growth ($\rho^a = 0$) the real bond beta is positive, so real bonds are risky. Conversely, when investors learn about expected growth from interest rates ($\rho^a > 0$), the real bond beta is closer to zero and real bonds have greater hedging benefits for investors. Intuitively, when investors associate high interest rates with growth, negative real bond returns are associated with good macroeconomic news, driving down real bond betas and improving their risk profile for the representative agent. In turn, investors prefer to hold real bonds when investor risk aversion rises after a contractionary short-term monetary policy shock, dampening the increase in long-term real bond yields. This countervailing risk premium channel suggests that larger or more persistent changes in growth expectations may be required to explain any given empirical link between long-term real bond yields and short-term policy rates on FOMC dates.

Overall, we find that our model can replicate the empirical relationship between innovations in short-term nominal and long-term real bond yields around FOMC announcements, and endogenous flight-to-safety means that even greater variation in expected growth may be justified to explain the data.

F.3 Robustness Model FOMC Results

Table 4 and Figure 5 report the slope coefficients b_1 and b_2 from running the following regression on simulated model data

$$r_t^{\delta,FOMC} = b_0 + b_1 \Delta i_t^{FOMC} + b_2 \Delta breakeven_{n,t} + \varepsilon_t. \tag{A232}$$

We pick standard deviations for the ST and LT monetary policy shocks on FOMC days to match the empirical standard deviations of our respective proxies for those shocks: 4.3 bps and 3.3 bps. To make sure that our results on the relationship of monetary policy shocks and equity returns are not driven by the choice of those exact values, in Figure A1 we plot the estimates for b_1 and b_2 while varying $\sigma_{ST}^{FOMC}/\sigma_{LT}^{FOMC}$.

Figure A1: Model High-Frequency Regression Coefficients against Volatility of FOMC ST Monetary Policy Shock

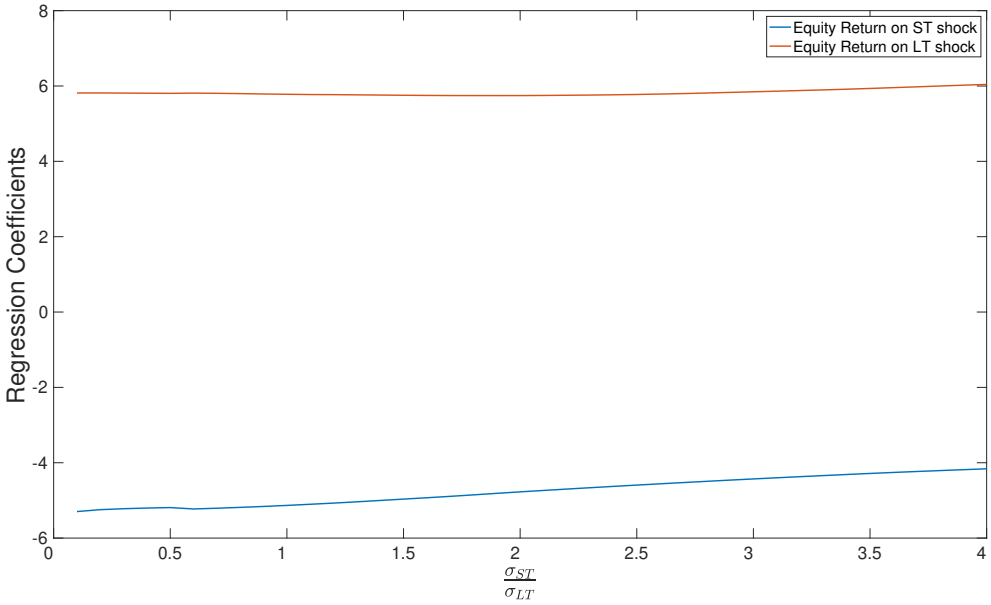

Note: This figure shows regression coefficients b_1 and b_2 from the model regression (A232), also shown in column (2) in Table 4 in the main paper. Each dot in the figure corresponds to a model simulation with a different value for the volatility of short-term monetary policy shocks realized on FOMC dates σ_{ST}^{FOMC}. We hold the volatility of the long-term monetary policy shock realized on FOMC dates constant at its baseline value of $\sigma_{LC}^{FOMC} = 3.3$ bps. We plot the model regression coefficients b_1 and b_2 on the y-axis against the ratio of the short-term to long-term monetary policy shocks realized on FOMC dates $\frac{\sigma_{ST}^{FOMC}}{\sigma_{FOMC}^{LT}}$ on the x-axis.

G Additional Empirical Results

Our model predicts that stock returns should be more sensitive to monetary policy news following a sequence of bad shocks, such as during a crisis. To verify that this prediction is in line with the data, in this section we tabulate the properties of stock returns in narrow windows around FOMC announcements during the depth of the financial crisis of 2008-09 (defined as October 2008 through December 2009).

In terms of summary statistics, we have 10 observations during this crisis period. The standard deviation of 1-hour stock returns is 1.04%, the standard deviation of Fed Funds rate innovations over the same time interval is 4.3 bps, and the standard deviation of breakeven changes on FOMC days is 3.4 bps. For comparison, our full sample has 146 FOMC date observations, with a standard deviation of 1-hour stock returns of 0.67% and virtually identical standard deviations for Federal Funds rate and breakeven surprises. During the crisis period, stock returns around FOMC announcements were hence about 50% more volatile, even though the proxies for monetary policy news were about equally as volatile as during the full sample.

Table A3 estimates the slope coefficients of stock returns onto Federal Funds rate surprises and breakeven changes around FOMC announcements for the crisis period, analogously to Table 3 columns (1) through (3). As predicted by theory, the slope coefficients are larger in magnitude during this period, which was characterized by a steep recession and high risk premia. Unfortunately, due to the small sample size, the standard errors are substantially larger than before, and we lose statistical significance.

Table A3: Empirical Equity Returns and Monetary Policy Surprises during 2008-09 Financial Crisis

	Dependent variable:		
	S&P 500 Return		
	(1)	(2)	(3)
FF Shock	−6.66		−4.23
	(4.85)		(6.46)
10Y Breakeven		10.26	8.22
		(8.81)	(10.38)
Constant	0.33	0.07	0.07
	(0.38)	(0.25)	(0.28)
Observations	10	10	10
R^2	0.08	0.09	0.14

Note: Regressions are analogous to Table 3 columns (1) through (3), except that this table uses the crisis subsample (October 2008 through December 2009).

APPENDIX REFERENCES

Campbell, John Y, and John H Cochrane, 1999, By force of habit, *Journal of Political Economy* 107, 205-251.

Campbell, John Y, Carolin Pflueger, and Luis M Viceira, 2020, Macroeconomic drivers of bond and equity risks, *Journal of Political Economy* 128, 3148–3185.

Cogley, Timothy, and Argia M. Sbordone, 2008, The time-varying volatility of macroeconomic fluctuations, *American Economic Review* 98, 2101–2126.

Greenwood, Jeremy, Zvi Hercowitz, and Gregory W Huffman, 1988, Investment, capacity utilization, and the real business cycle, *American Economic Review* pp. 402–417.

Hanson, Samuel G, and Jeremy C Stein, 2015, Monetary policy and long-term real rates, *Journal of Financial Economics* 115, 429–448.

Nakamura, Emi, and Jón Steinsson, 2018, High-frequency identification of monetary nonneutrality: the information effect, *Quarterly Journal of Economics* 133, 1283–1330.

Smets, Frank, and Rafael Wouters, 2007, Shocks and frictions in us business cycles: A Bayesian DSGE approach, *American Economic Review* pp. 586–606.

Wachter, Jessica A., 2005, Solving models with external habit, *Finance Research Letters* 2, 210–226.

Walsh, Carl E, 2017, *Monetary theory and policy* (MIT press).

Woodford, Michael, 2003, *Interest and Prices* (Princeton University Press)